Dissertation

The implication of natural killer cells and neutrophils in autoimmune disorders of the central nervous system.

zur Erlangung des akademischen Grades
D o c t o r r e r u m n a t u r a l i u m
(Dr. rer. nat.)

im Fach Biologie

eingereicht an der Lebenswissenschaftlichen Fakultät
der Humboldt-Universität zu Berlin

von

Dipl. Biochemikerin Laura Hertwig

Präsident der Humboldt-Universität zu Berlin
Prof. Dr. Jan-Hendrik Olbertz

Dekan der Lebenswissenschaftlichen Fakultät
Prof. Dr. Richard Lucius

Gutachter/innen: 1. Prof. Dr. Hans-Dieter Volk
2. Prof. Dr. med. Friedemann Paul
3. PD Dr. med. Olaf Hoffmann

Tag der Einreichung: 19.01.2016
Tag der mündlichen Prüfung: 01.06.2016

„Das Leben ist nicht das, was man gelebt hat, sondern das, woran man sich erinnert und wie man sich daran erinnert - um davon zu erzählen" (Gabriel García Márquez)

Abstract

The implication of natural killer (NK) cells and neutrophils in autoimmune disorders of the central nervous system (CNS) remains elusive, and therefore was investigated in a mouse model for multiple sclerosis (MS), experimental autoimmune encephalomyelitis (EAE), and in patients with MS and neuromyelitis optica (NMO), respectively.

In MS, a decreased frequency of circulating CX3CR1^{+}NK cells correlating with the patient disease activity has been reported. Therefore, the pattern of NK cell mobilization and the contribution of CX3CR1 to NK cell dynamics in response to neuroinflammatory insult were investigated in the EAE model. Here, NK cells similarly mobilized from the periphery and accumulated in the CNS in both wild-type (WT) and CX3CR1-deficient mice during EAE. However, in mice lacking CX3CR1 the infiltrated NK cells displayed an immature phenotype contrasting with the mature infiltrates in the WT counterparts, apparently contributing to EAE exacerbation in those animals since transfer of mature WT NK cells prior to immunization of CX3CR1-deficient mice exerted a protective effect. Together, these data suggest that the CX3CR1-mediated recruitment of mature CX3CR1^{+}NK cells limits EAE neuroinflammation.

Due to clinical similarities, the discrimination between MS and NMO is still challenging. In contrast to MS, neutrophil accumulations were found in CNS lesions and the cerebrospinal fluid (CSF) of NMO patients wherefore a comparative analysis of peripheral blood neutrophils in NMO and MS patients was performed. The results revealed an activated neutrophil phenotype in NMO and MS when compared to healthy individuals. In contrast, analysis of neutrophil migration, oxidative burst activity and degranulation showed a compromised neutrophil functionality in NMO compared to MS, which was not influenced by the treatment regime and clinical parameters of the patients. Thus, neutrophil functionality may represent a new diagnostic tool to discriminate between NMO and MS.

Keywords: CNS autoimmune diseases, multiple sclerosis, neuromyelitis optica, innate immunity, natural killer cells, neutrophils

Zusammenfassung

Die genaue Implikation natürlicher Killer(NK)-zellen und Neutrophile in Autoimmunerkrankungen des zentralen Nervensystems (ZNS) ist nach wie vor ungeklärt und wurde daher im Mausmodell der multiplen Sklerose (MS), der experimentellen Autoimmunenzephalomyelitis (EAE), sowie bei MS und Neuromyelitis optica (NMO) Patienten untersucht.

Bei MS Patienten konnte eine mit der Krankheitsaktivität korrelierende, reduzierte Zahl zirkulierender $CX3CR1^{+}$NK Zellen festgestellt werden. Daher wurden die NK Zell-Dynamiken und der Einfluss von CX3CR1 auf diese im EAE Mausmodell untersucht. Hierbei konnte in Wildtyp(WT) sowie auch CX3CR1-defizienten EAE Mäusen eine Rekrutierung peripherer NK Zellen in das ZNS beobachtet werden. Anders als bei WT EAE Mäusen wiesen die NK Zellen bei CX3CR1-defizienten Mäusen einen primär unreifen Phänotyp auf, der möglicherweise als ursächlich für die erhöhte Krankheitsaktivität dieser Tiere gemutmaßt werden kann. Der Transfer reifer NK Zellen vor Immunisierung CX3CR1-defizienter Tiere zeigte folglich protektive Effekte und lässt schlussfolgern, dass die CX3CR1-vermittelte Rekrutierung reifer NK Zellen die EAE Neuroinflammation limitiert.

Die Diskriminierung der MS von der klinisch ähnlichen NMO stellt nach wie vor eine Herausforderung dar. Neutrophile in ZNS-Läsionen und der Cerebrospinalflüssigkeit(CSF) können bei NMO, nicht aber MS Patienten nachgewiesen werden, weshalb Neutrophile aus dem Blut von NMO und MS Patienten hier vergleichend untersucht wurden. Die Neutrophile beider Patientengruppen wiesen einen aktivierten Phänotyp im Vergleich zu gesunden Kontrollen auf. Im Gegensatz dazu zeigte sich eine von Medikation und neurologischen Defiziten der Patienten unabhängige, kompromittierte Funktionalität der NMO verglichen mit MS Neutrophilen im Hinblick auf Migration, oxidativen Burst und Degranulierung. Die Neutrophilenfunktionalität könnte entsprechend potentiell als diagnostisches Diskriminierungskriterium zwischen der MS und der NMO dienen.

Schlagwörter: ZNS Autoimmunerkrankungen, Multiple sklerose, Neuromyelitis optica, angeborene Immunzellen, Natürliche Killerzellen, Neutrophile

Table of content

List of abbreviations

Abbreviation/ symbol	Full name
Δ	delta/ difference
%	percent
°C	degree Celsius
µg	microgram
µl	microliter
µM	micromole
µm	micrometer
18S rRNA	18 Svedberg ribosomal ribonucleic acid
7-AAD	7-aminoactinomycin
abs.	absolute
ADCC	antibody-dependent cellular cytotoxicity
APC (fluorophor)	allophycocyanin
APC (immunity)	antigen presenting cell
APRIL	proliferation-inducing ligand
AQP4	aquaporin 4
AUC	area under the curve
BAFF	B cell recruiting and activating factor
BBB	blood brain barrier
BM	bone marrow
BSA	bovine serum albumin
calcein-AM	calcein acetoxymethyl
cc	cubic centimeter
CCL	C-C chemokine ligand
CCR	C-C chemokine receptor
CD	cluster of differentiation
CD62L	L-selectin
CDCC	complement-dependent cytotoxicity
cDNA	complementary deoxyribonucleic acid
CFA	complete Freund's adjuvans
CLP	common lymphoid progenitor
CNS	central nervous system
CO_2	carbon dioxide
CSF	cerebrospinal fluid
C_t method	comparative threshold method
CX3CL	C-X3-C-chemokine ligand
CX3CL1	fractalkine
CX3CR	C-X3-C motif chemokine receptor
CX3CR1	fractalkine receptor
CXCL	C-X-C motif chemokine ligand
CXCR	C-X-C motif chemokine receptor
d	day
DNA	deoxyribonucleic acid

Abbreviation/ symbol	Full name
DC	dendritic cell
ddH_2O	double-distilled water
DHR 123	dihydrorhodamine 123
DMSO	dimethyl sulfoxide
DNAM-1	DNAX accessory molecule 1
DNase	deoxyribonuclease
dNTP	deoxynucleotid triphosphate
dsDNA	double-stranded DNA
E.coli	*Escherichia coli*
e.g.	exempli gratia
EAE	experimental autoimmune encephalomyelitis
EBV	Epstein-Barr virus
EDSS	expanded disability status scale
EDTA	ethylenediaminetetraacetic acid
ELISA	enzyme-linked immunosorbent assay
Eomes	eomesodermin
etc.	et cetera
EtOH	ethanol
Ets-1	avian erythroblastosis virus E26 oncogene homolog 1
FACS	fluorescence-activated cell sorting
FAM	6-carboxyfluorescein
FasL	tumor necrosis factor ligand superfamily, member 6
FasR	tumor necrosis factor receptor superfamily, member 6
Fc	fragment, crystallizable
FcR	Fc receptor
FCS	fetal calf serum
FEM	Research Institute for Experimental Medicine of the Charité
FITC	fluorescein isothiocyanate
fMLP	N-formyl-methionyl-leucyl-phenylalanine
fMLPR	N-formyl-methionyl-leucyl-phenylalanine receptor
FSC	forward scatter
g	standard gravity (9.80665 m/s^2)
G	Gauge
G-CSF	granulocyte-colony stimulating factor
GFP	green fluorescent protein
GM-CSF	granulocyte-macrophage colony-stimulating factor
H	hydrogen
H_2O	water
HC	healthy control
HEPES	4-(2-hydroxyethyl)-1-piperazineethanesulfonic acid
HLA	human leukocyte antigen
HSC	hematopoietic stem cell
Id-2	inhibitor of DNA binding 2, dominant negative helix-loop-helix protein
IFN	interferon

Abbreviation/ symbol	Full name
Ig	immunoglobulin
IL	interleukin
ILC	innate lymphoid cells
K	thousand
KCl	potassium chloride
kg	kilogram
KH_2PO_4	potassium dihydrogen orthophosphate
KIR	killer-cell immunoglobulin like receptor
KLGR1	killer cell lectin-like receptor G1
LaGeSo	Landesamt für Gesundheit und Soziales
LN	lymph nodes
MACS	magnetic cell sorting
max.	maximum
MBP	myelin basic protein
MedFl	median fluorescence
mg	milligram
MG	myasthenia gravis
MGB	minor groove binder
$MgCl_2$	magnesium chloride
MHC	major histocompatibility complex
min	minute
Mio.	million
ml	milliliter
mM	millimolar
mm	millimeter
MMP	matrix metalloproteinase
MOG	myelin oligodendrocyte glycoprotein
MPO	myeloperoxidase
MRI	magnetic resonance imaging
MS	multiple sclerosis
N	number
NH	sodium heparin
n.i.	non-immunized
Na_2HPO_4	sodium hydrogen phosphate
NaCl	sodium chloride
NADPH	nicotinamide adenine dinucleotide phosphate-oxidase
NaN_3	sodium azide
neg.	negative
NET	neutrophil extracellular trap
Nfil3	nuclear factor, interleukin 3 regulated
NK cell	natural killer cell
NKG2	killer cell lectin-like receptor subfamily K
NKp	natural killer cell p-related protein
nl	nanoliter
nM	nanomolar

Abbreviation/ symbol	Full name
nm	nanometer
NMO	neuromyelitis optica
NMOSD	NMO spectrum disorders
NO	nitric oxide
O_2•	oxygen radical
OBC	oxidative burst capacity
ODC	oligodendrocytes
p.i.	post immunization
PacBlue	pacific blue
PBS	phosphate buffered saline
PCR	polymerase chain reaction
PE	phycoerythrin
PE Cy7	phycoerythrin Cy7 conjugate
PerCP Cy5	peridinin-chlorophyll-protein complex: Cy5 conjugate
PFA	paraformaldehyde
pH	*potentia hydrogenii*
PLP	myelin proteolipid protein
PMA	phorbol 12-myristate 13-acetate
PMN	polymorphonuclear
PPMS	primary progressive MS
PRMS	progressive-relapsing MS
PTX	pertussis toxin
p-value	probability value
RA	rheumatoid arthritis
RNA	ribonucleic acid
RNase	ribonuclease
ROS	reactive oxygen species
rpm	revolutions per minute
RRMS	relapsing-remitting MS
rRNA	ribosomal RNA
RT	room temperature
rtPCR	real-time PCR
S	Svedberg
S1P5	sphingosine-1-phosphate receptor 5
SA	streptavidin
SD	standard deviation
sec	second
SEM	standard error of mean
SLE	systemic lupus erythematosus
SPMS	secondary-progressive MS
SS	Sjögren syndrome
SSC	sideward scatter
TAMRA	tetramethylrhodamine
Taq polymerase	*Thermus aquaticus* polymerase
T-bet	T-box transcription factor

Abbreviation/ symbol	Full name
TCR	T cell receptor
TGF	transforming growth factor
T_h cell	T helper cell
TLR	toll-like receptor
TNF	tumor necrosis factor
T_{reg} cell	regulatory T cell
Tris-HCl	trisamine hydrochloride
U	unit
VLA-4	α4 integrin very late antigen-4
w/v	weight per volume
WT	wild-type
x or *	mathematical sign for multiplication
/	mathematical sign for division

List of figures

List of tables

1. Introduction

1.1 Autoimmune disorders of the central nervous system (CNS)

Autoimmune diseases define a group of pathologies in which an abnormal immune response of the body results in the attack and destruction of self-structures. These responses can be systemic or restricted to specific organs and tissues. Immunologic malfunctions specifically directed against the central nervous system (CNS) are often characterized by local inflammations, neuronal demyelination and cell death resulting in diverse clinical symptoms from motoric to mental disabilities. Thereunder, multiple sclerosis (MS) represents the most prominent autoimmune disorder of the CNS affecting around 2.5 million people worldwide [16, 17]. In contrast, neuromyelitis optica (NMO) is a relatively new defined and rare but not less severe CNS demyelinating syndrome with a prevalence of 1 to 4 affections per 100 000 people worldwide [18] and sharing many similarities with MS.

1.1.1 Multiple sclerosis (MS)

Being a self-sustaining autoimmune disease that results in chronic immune attacks on the CNS, MS was first characterized in 1868 by the French physician Jean-Martin Charcot (1825-1893) [19]. Since then, an enormous progress in the investigation of the disease has been made to the present.

MS has a median prevalence of 30/100 000 people worldwide and around 150 000 people are affected in Germany only [17, 20]. The incidence of MS is higher in colder climates and the farther away from the equator with a ratio of women to men of approximately 2-3 to 1. Principally, MS can occur at any age whereby the most people are diagnosed between the age of 20 and 40 [21, 22] developing common symptoms such as fatigue, motoric disabilities, including muscles weakness and spasms, as well as impaired vision or disturbances in balance and coordination [21]. So far, it exist no cure for MS, but – to date – several disease-modifying medications (e.g. Copaxone, Avonex, Novantrone etc.) have been developed [23].

1.1.1.1 Etiology

MS is a multifactorial disease whose origin remains not fully understood, but is believed to arise from immunological dysfunction due to environmental trigger(s) in a genetically susceptible individual [17, 21].

A number of systematic genetic epidemiological and molecular genetic studies have provided important insights into the genetics of MS. These studies excluded a major gene locus to be the cause of MS but revealed a number of genes which predispose to the disease [17]. The earliest associations between MS and genetics were described in the 1970s and were found in the human leukocyte antigen (HLA; also termed as major histocompatibility complex, MHC) locus [24, 25]. Polymorphisms of these genes of the HLA, DR alpha *(*HLA-DRA) locus display a strong genetic risk factor in MS, presumably due to their role as antigen-presenting molecules to the disease associated pathogenic T cells.

In such genetically predisposed individuals diverse environmental factors have been proposed to represent a disease-triggering element. Risk factors such as industrial toxins, smoking or metal exposures are debated but a definite association with the disease could not be yielded so far [18, 21]. In contrast, vitamin D is an environmental factor which is believed to impact on MS. Low level of vitamin D are a common characteristic in MS patients correlating with patient's disease activity. Importantly, therapeutic approaches with high doses of vitamin D supplementation appeared to reduce relapses [26].
As well, infections due to bacteria or viruses, such as the Epstein-Barr virus (EBV) or measles, have also been proposed to play a role as triggering factors in MS [27], possibly through the mechanisms of "molecular mimicry" (cross-reactivity between CNS-derived self-antigens and foreign agents causes activation of autoreactive T cells) or the so-called "bystander activation" (non-specific inflammatory events occurring during infections cause the activation of autoreactive T cells) [28, 29].

Just recently, the microbiome and its putative role in the etiology of MS have acquired major attention. Some studies point towards an adverse composition of the gut flora in MS patients and it is speculated that the lack of specific gut bacteria-derived metabolites could be associated with the development of MS [30, 31].

Altogether, genetic predispositions in combination with heterogeneous environmental triggers may induce the MS-typical autoimmune response which is classically considered

as a response of autoreactive pathogenic cluster of differentiation (CD) 4^+ T cells to a CNS-antigen mediating demyelination and leading to the formation of acute inflammatory lesions, scar tissues, and sclerosis [16, 17].

This complex background of the disease is also reflected by different forms of disease courses (Figure 1): relapsing-remitting MS (RRMS), secondary-progressive MS (SPMS), primary progressive MS (PPMS), and progressive-relapsing MS (PRMS). RRMS is the most common form of MS accounting for around 85% of the patients. It is characterized by clearly defined attacks of worsening neurological function followed by periods of remission in which patients show clinical improvement or do not have any symptoms. It is estimated that more than half of these patients later develop secondary-progressive MS (SPMS). In these cases, after an initial period of relapsing-remitting MS, the disease begins to worsen steadily, with or without periods of remission. Approximately 10% of the MS patients are diagnosed with primary progressive MS (PPMS) which is characterized by continuous worsening of neurologic function from the onset of the disease with no periods of remission. Finally, progressive-relapsing MS (PRMS) represents the rarest form of MS affecting about 5% of patients. The disease course is characterized by a progressive worsening from the start with intermittent exacerbations present along the way [32].

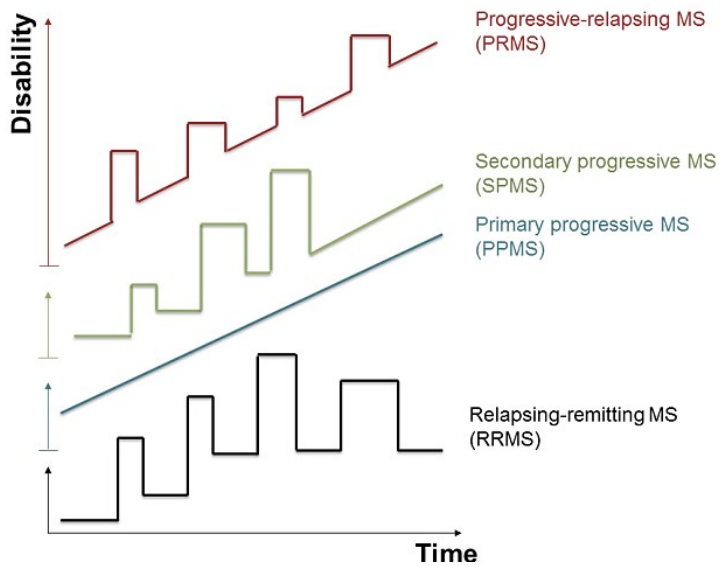

Figure 1. Clinical MS disease courses. Relapsing-remitting MS (black line) is the most common form of MS that later can develop into a secondary progressive MS (green line). Only few patients develop primary progressive MS (blue line) and even less patients are affected of progressive-relapsing MS (red line).

1.1.1.2 Immunopathogenesis

In MS patients, the heterogeneity of clinical manifestations correlates with the spatiotemporal occurrence and dissemination of inflammatory lesions within the CNS (Figure 2A). These inflammatory sites are characteristic for the disease and present at all disease stages but more pronounced during acute phases. They result from CNS infiltrating autoreactive immune cells which – after crossing the blood brain barrier (BBB) or the blood cerebrospinal fluid (CSF) barrier – promote inflammation, local activation and proliferation of micro- and astroglia (gliosis) and demyelination in the white and grey matter track ending in severe neuronal damages and losses (Figure 2B) [16].

So far, there are different immunological models regarding the development and progression of MS, but many aspects remain controversial, among others whether the disease is triggered inside the CNS or in the periphery. Assuming the latter, it is estimated that autoreactive T cells become activated at peripheral sites by CNS-derived antigen(s) such as myelin basic protein (MBP) or myelin oligodendrocyte glycoprotein (MOG) [33], by molecular mimicry or bystander activation [28, 29]. The CNS-intrinsic model suggests that events inside the CNS (e.g. inflammatory responses or infection) initiate the disease whereby the infiltration of lymphocytes and other immune cells takes place as a secondary process [16]. Commonly hypothesized by both paradigms and supported by histopathological data and results from experimental animal models, autoreactive T cells are believed to represent the key immune cell type in disease development. Early inflammatory lesions are dominated by $CD8^+$ T cells and macrophages, lower numbers of $CD4^+$ T cells as well as B cells and plasma cells. With the progression of the disease, microglia and astrocytes are chronically activated and predominantly diffuse T and B cell infiltrates can be detected [34, 35].

The principal events of immune dysregulation in MS are schematically represented in figure 2B involving both innate and adaptive immunity. Antigen presenting cells (APC) such as dendritic cells (DC) are speculated to be involved in the activation of autoreactive $CD4^+$ T cells in the periphery as well as in their differentiation through secretion of cytokines as for instance IL-12 (promotes differentiation of naïve $CD4^+$ T cell into IFN-γ producing T helper 1, T_h1, cells) or interleukin (IL)-23 (promotes differentiation of naïve $CD4^+$ T cell into IL-17-producing T helper 17, T_h17, cells) [35, 36]. In turn, these autoreactive helper T cells can produce matrix metalloproteinases and reactive oxygen species (ROS)

through which the BBB permeability could be increased [37, 38]. Once they have infiltrated the CNS their re-activation by local APCs in response to CNS antigens results in the secretion of pro-inflammatory cytokines and [interferon γ (IFN-γ), tumor necrosis factor α (TNF-α), interleukin (IL)-23, IL-8 etc.] activating CNS-resident cells (microglia, astrocytes), recruiting other immune cells (monocytes, natural killer (NK) cells etc.) and chronically orchestrating the formation of inflammatory lesions and demyelination [1, 16]. Importantly, T_h17 cells are also involved in the formation of ectopic lymphoid follicles in the CNS and therewith create a direct link to B cell pathology [39]. B cells themselves can act as APCs and recruit autoreactive T cells. Additionally, they have been found to be present, along with plasma cells and myelin-specific antibody, in MS plaques and areas of active demyelination, whereby antibody-mediated mechanisms can directly contribute to axonal demyelination [40]. Found in higher frequencies in inflammatory lesions than $CD4^+$ T cells, $CD8^+$ T cells represent another critical "player" in the MS disease pathogenesis [16, 34]. Whereas $CD4^+$ T cells are activated by APC-presented major histocompatibility complex (MHC) class II antigens, $CD8^+$ T cells recognize MHC class I antigens which are highly expressed within MS lesions, and also on neurons and glia [41, 42]. As well, granzyme B (as marker for cytotoxic activation)-expressing $CD8^+$ T cells could be found in close proximity to oligodendrocytes (ODC) and demyelinating axons supporting the common believe that $CD8^+$ T cells, in contrast to $CD4^+$ T cells, are able to directly lyse neurons. In line with this, their numbers are closely correlated with acute axonal damage in the brain and CSF [43, 44].

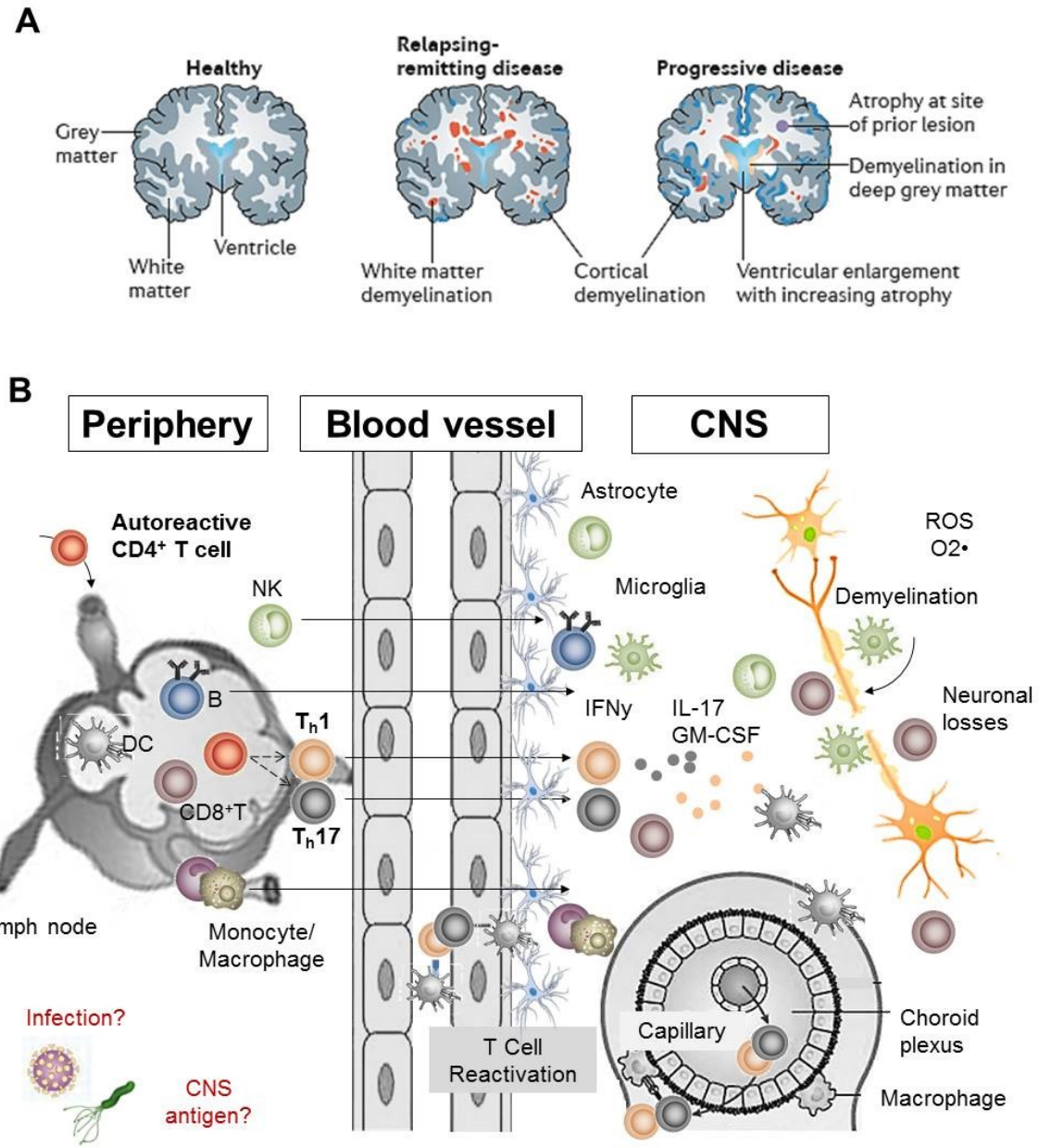

Figure 2. MS pathology and immunopathogenesis. A) Exemplary coronal brain views are shown for healthy individuals and MS in relapsing-remitting and progressive disease phase. MS pathology is characterized by demyelinated areas in the white and grey matter of the CNS. Consequently, continuous neuroaxonal loss leads to the atrophy of the brain accompanied by ventricular enlargement. B) Autoreactive T and B cells are activated in the periphery by CNS autoantigen presentation, molecular mimicry or bystander activation. Subsequently, $CD8^+$ T cells, differentiated $CD4^+$ T helper 1 (T_h1) and T_h17 cells, and B cells infiltrate the CNS by crossing the BBB or blood-CSF barrier, leading to inflammation, demyelination and tissue damage along with the recruitment of other (innate) immune cells such as NK cells, monocytes/macrophages or dendritic cells (DC). Hereby, soluble mediators and secreted pro-inflammatory cytokines (e.g. IFNy, IL-17, GM-CSF etc.) promote CNS inflammation and demyelination in the course of which CNS resident cells such as microglia and astrocytes are chronically activated as well. Abbreviations: BBB = blood brain barrier, CNS = central nervous system, DC = dendritic cell, GM-CSF = granulocyte macrophage colony stimulating factor, IFN-γ = interferon γ, IL = interleukin, NK cell = natural killer cell, O_2• = oxygen radical, ROS = reactive oxygen species, T_h cell = T helper cell. Figure 2A adapted from Dendrou et al. (2015); Figure 2B conceptually adapted and modified from Dendrou et al. (2015) [16].

1.1.1.3 Experimental autoimmune encephalomyelitis (EAE)

Experimental autoimmune encephalomyelitis (EAE) is the commonest model used to investigate MS. In this model, an immune response against myelin proteins/ peptides is generated in laboratory animals evoking an ascending paralysis that correlates with inflammatory lesions in the spinal cord, whereas – depending on the experimental design - the brain and optic nerves can also be affected [45, 46].

Since T. M. Rivers, D. H. Sprunt and G. P. Berry first published their observations on the induction of acute disseminated encephalomyelitis in monkeys in 1933 [47], the development and refinement of EAE has proceeded steadily. EAE can be induced in different species, such as rats, guinea pigs or monkeys, but over time, mice became the preferred animal for EAE research. This is presumably due to their genetic background (99% of the about 30,000 genes in mouse have direct counterparts in humans) and due to genetic advantageous resources as for instance transgenics or knockouts [48]. Classically, myelin proteins (or peptides) as the MBP, myelin proteolipid protein (PLP) or MOG, are used to induce EAE resulting in distinct disease forms with different disease characteristics with respect to both immunology and pathology. Likewise, these parameters are influenced by the genetic background of the mouse strain [45, 49, 50].

Most studies are presently performed on C57BL/6 mice immunized with MOG peptide (e.g. representing residues 35-55). Therefore, the MOG peptide is emulsified in complete Freund's adjuvant supplemented with *Mycobacterium tuberculosis.* Additionally, mice usually receive an injection of *Bordetella pertussis toxin* the day of immunization and repeated 48 hours later to support the breakdown of the BBB [48]. Approximately 10-12 days after immunization, mice develop a monophasic, chronic form of EAE without relapses in which they experience one acute paralytic disease exacerbation and then recover. Pathologically, this acute phase of neurological worsening is characterized by the activation of autoreactive $CD4^+$ T cells mediating CNS inflammation and demyelination, oligodendrocyte and neuronal death. By using a different mouse, e.g. the SJL/J strain, immunization with MBP or PLP emulsified in adjuvant induces the development and allows the investigation of a relapsing-remitting form of EAE disease, representative for the most common course of MS [49]. However, these models rather represent isolated immunological and histopathological aspects of the human MS; pathological events are largely restricted to the spinal cord in these models, whereas MS is predominantly a brain

disease showing prominent demyelination in the cortical brain regions [49, 51]. Therefore, several transgenic mouse models, as for example transgenic T cell receptor (TCR)-based animals characterized by spontaneous EAE development, have been generated so far. And even though their application is still not widely common due to several reasons (e.g. heterogeneous disease onset time and varying incidences), these mice allow deeper insights in the clinical and pathological disease complexity [52].

With exception of the spontaneous EAE models, EAE can generally be induced in two different ways. Active immunization is recommended if the initial phase of the immune response is of interest, in which an autoimmune response against the CNS is induced by activation of T cells [53]. Here, EAE induction with a myelin immunogen along with an adjuvant is performed directly and subcutaneously. In contrast, when interested in the effector phase in which activated T cells encounter and attack cells they take for pathogenic, EAE induction is rather performed passively, a process called adoptive transfer. Therefore, encephalitogenic $CD4^+$ T cells are generated in vitro and intravenously injected into the recipient mice [54].

1.1.2 Neuromyelitis optica (NMO)

Neuromyelitis optica (NMO), also known as Devic's disease, is an inflammatory CNS syndrome in which autoimmune attacks predominantly affect the optic nerves and the spinal cord [8, 9]. NMO was long believed to be a rare variant of MS, but is now considered a primarily anti-aquaporin-4 (AQP4) autoantibody-driven astrocytopathy with a pathogenesis that is distinct from MS [10, 11]. However, the pathogenic features that may help to differentiate these two diseases are so far limited. The discovery that only around 80% of the NMO patients are seropositive for the AQP4-immunoglobulin G (IgG), and further that a more restricted or more extensive CNS involvement – than optic neuritis and transversal myelitis – also may occur, prompted to the latest disease nomenclature defining the unifying term NMO spectrum disorders (NMOSD), which is stratified further by serologic testing (NMOSD with or without AQP4-IgG) [55].

1.1.2.1 Epidemiology and clinical features

In 1894, the French physician Eugène Devic first reported on a case of acute transverse myelitis and bilateral optic neuritis caused by extensive demyelination and necrosis in the

spinal cord and optic nerves of the patient. Initially considered a monophasic disease, studies revealed a relapsing-remitting disease course similar to MS in most of the patients. Therefore, and due to some other pathological similarities, it was long-standing controversial whether NMO is a variant of MS or not [56, 57]. In 2006, the revision of the diagnostic criteria for NMO distinguished NMO from MS as distinct disease entity [58]. The major discovery to which this distinction is affiliated was the finding of a NMO-IgG in the patient's sera. This disease-specific autoantibody was identified as anti-AQP4 autoantibody which induces astrocytic damage through binding to AQP4, the major water channel in the CNS, on astrocytic endfeet and simultaneously activating the complement [10, 59, 60].

The worldwide prevalence of NMO ranges from 1 to 4.4/100 000 [18]. However, it is estimated that the real number of NMO cases may be higher due to NMO patients misdiagnosed with MS (some studies reported 30-40% misdiagnosis) [61]. The median age of onset lies between 35-45 years [62]. Notably, the female ratio in NMO is very high (> 90%) with an approximate female to male ratio of 9:1 in seropositive patients and 2:1 in seronegative ones [11, 63]. Even though rare familial NMO cases have been reported, an inheritance pattern is not known so far. The majority of NMO cases are sporadic displaying a relapsing disease course (~80-90%) and, in contrast to MS, are more frequently associated with coexisting autoimmune diseases such as systemic lupus erythematosus (SLE), Sjögren syndrome (SS) or myasthenia gravis (MG) [57].

The clinical presentation is unpredictable in relapsing NMO and patients suffer from severe autoimmune attacks which are often more disabling than in MS with poor remission and fast accruement of irreversible neurological disabilities. According to the international consensus diagnostic criteria for NMOSD, core clinical characteristics include optic neuritis, acute myelitis, area postrema syndrome, acute brainstem syndrome, symptomatic narcolepsy or acute diencephalic clinical syndrome and symptomatic cerebral syndrome with NMOSD-typical brain lesions [55].

NMO-related deaths are often caused by severe ascending cervical myelitis or brainstem involvement resulting in respiratory failure. NMO is still incurable, but treatment options such as plasmapheresis or long-term immunosuppression (e.g. prednisolone, azathioprine, rituximab) to prevent relapses, to improve clinical symptoms and to restore neurological disabilities could be developed in the last years increasing NMO survival rates [8].

1.1.2.2 Immunopathogenesis

The precise etiology of NMO remains not fully understood. It is widespread hypothesized that anti-AQP4 enter the CNS, bind to astrocytic AQP4 water channels and therewith activate the classical cascade of the complement system. In turn, an inflammatory response is initiated recruiting granulocytes and macrophages from the periphery into the CNS and finally resulting in astrocytic and oligodendrocytic damage, demyelination, and neuronal loss, presumably through the mechanisms of complement-dependent cytotoxicity (CDCC) and antibody-dependent cellular cytotoxicity (ADCC) (Figure 3) [64].

Evidence for a crucial role of the pathogenic AQP4-IgG in the immunopathogenesis of NMO has been provided by several studies. For example, AQP4-IgG is highly specific for NMO and its serum levels correlate with the patient's disease activity [65, 66]. Consistently, treatment approaches targeting B cells have been shown to be the most effective and are associated with the decline of AQP4-IgG in serum [67, 68]. Moreover, the highest expression of AQP4 can be found in opticospinal tissues and apart from massive complement and granulocytic infiltrations, NMO lesions are characterized by their marked loss of astrocytic AQP4 and increased deposits of IgG and IgM [69-71]. Furthermore, AQP4-IgG has been shown to have complement-activating attributes [72].

However, it remains unclear which events initiate AQP4-IgG production, how these autoantibodies enter the CNS and by which mechanisms equivalent pathological events are initiated and promoted in the proportion of 10-20% AQP4 seronegative NMO patients. Speculations on these questions for example include the mechanisms of molecular mimicry, as for example the AQP4-specific T cell response has been shown to be increased in NMO and to display cross-reactivity to an intestinal bacteria-derived protein [73]. Another hypothesis involves circulating BBB permeabilizing factors, more precisely autoantibodies other than anti-AQP4 antibodies which may disrupt the BBB through upregulation of vascular endothelial growth factor in brain microvascular endothelial cells [74, 75].

Apart from AQP4-IgG, the involvement of other immunological player is strongly supported by experimental data even though their precise contribution and the molecular mechanisms behind need further investigations to understand the whole picture of NMO pathology. Especially macrophages, eosinophils and neutrophils, and potentially some T cell subsets appear to play a major role. All these cell subsets have been found to be

accumulated in acute NMO lesions [12, 76]. Additionally, AQP4-IgG can function on macrophages, neutrophils and eosinophils by binding to their Fc receptors. Analysis of the CSF revealed increased level of pro-inflammatory cytokines and factors in NMO patients. Thereunder the B cell recruiting and activating factor (BAFF), the proliferation-inducing ligand (APRIL), the C-X-C motif chemokine 13 (CXCL13) and IL-6 [77-79]. Interestingly, the latter has been shown to be increased in peripheral blood and is hypothesized to promote the maintenance of AQP4 antibody positive plasmablasts in NMO [80]. Moreover, IL-6 also induces the development and the maintaining of T_h17 cells, the producers of the cytokine IL-17, which has been found in increased amounts during acute attacks and – together with the chemokine IL-8 – is involved in the recruitment of neutrophils [81].

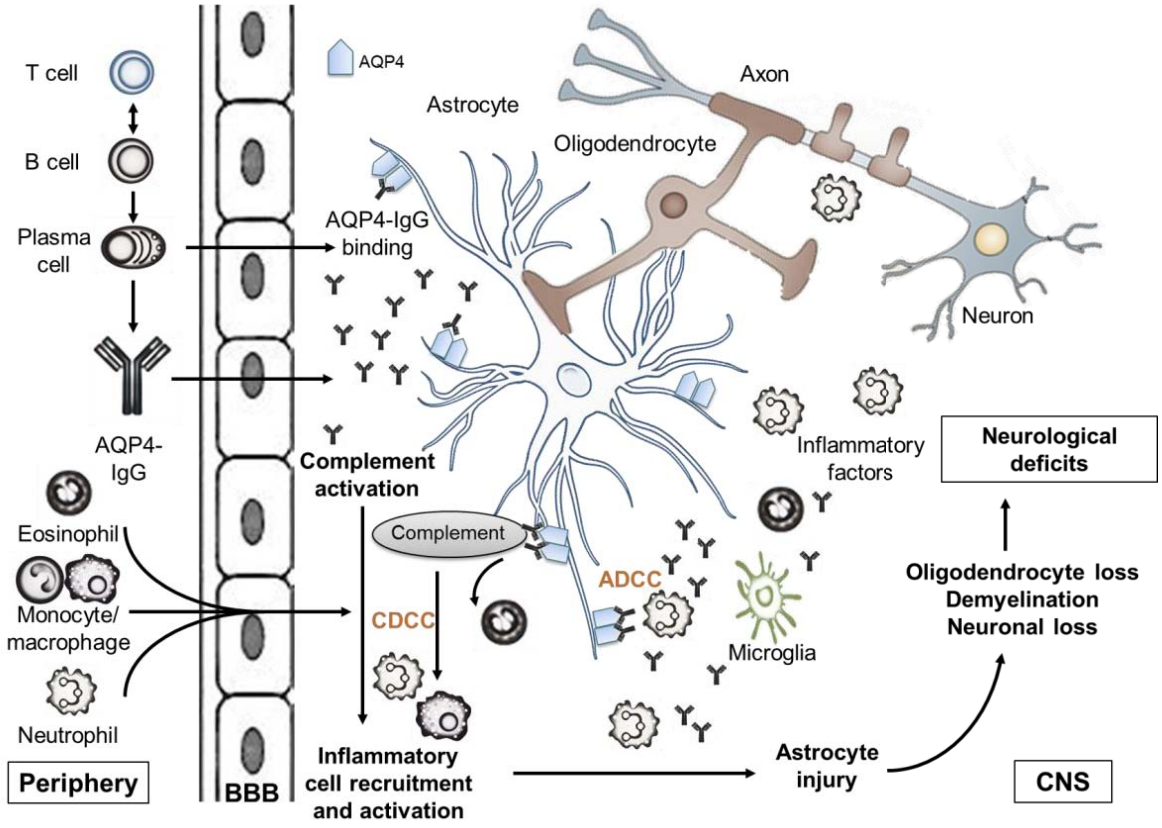

Figure 3. Current concept of NMO immunopathogenesis. Both AQP4-IgG and AQP4-IgG producing plasma cells infiltrate the CNS where AQP4-IgG bind to their epitope AQP4 on astrocytic endfeet. This binding induces the activation of the complement system and further the recruitment of peripheral immune cells, specifically granulocytes and macrophages. The resulting lesion formation through inflammation, oligodendrocyte injury, demyelination and neuronal loss are mediated by the mechanisms of CDCC and ADCC. Abbreviation: ADCC = antibody-dependent cellular cytotoxicity, AQP4-IgG = aquaporin 4 immunoglobulin G, BBB = blood brain barrier, CDCC = complement-dependent cytotoxicity, CNS = central nervous system. Figure conceptually adapted and modified from Papadopoulos et al. (2014) [64].

1.2 Innate leukocytes in autoimmunity

The innate immune system provides an immediate defense against invading pathogens and is composed of both components of the humoral and cellular immunity including anatomical barriers (e.g. skin), the complement system, antibodies and a number of myeloid and lymphoid cells which are granulocytes, mast cells, NK cells, γδ T cells, DCs and macrophages.

1.2.1 Natural killer (NK) cells

Natural killer (NK) cells are bone-marrow derived granular lymphocytes which are involved in the instant immune defense against microbial infections and malignancies. They were discovered in the early 1970s and first described as a lymphocyte subtype able to kill tumor and virally-infected cells by "natural" or spontaneous cytotoxicity without prior sensitization [82-84]. Today, NK cells are classified into the group 1 of innate lymphoid cells (ILC) [85] and known not only for their effector but also their immunoregulatory functions such as editing of DCs or modulating T_h responses [86, 87]. Moreover, even if they are traditionally considered as cells of the innate immune system, there is accumulating evidence that NK cells combine hallmarks of innate and also adaptive immunity by acting unspecific against foreign antigens first but being able to develop long-lived memory of these antigens thereafter as it is known for B and T lymphocytes [88, 89].

1.2.1.1 NK cell homeostasis

NK cells develop from hematopoietic stem cell (HSC)-derived common lymphoid progenitors (CLP) in the bone marrow. Alternatively, recent studies suggest that NK cells also can develop in lymph nodes, thymus and the liver [90]. Several transcription, soluble and membrane factors have been identified to be involved the generation of NK cells as for example the transcription factors inhibitor of DNA binding 2 (Id-2), avian erythroblastosis virus E26 oncogene homolog 1 (Ets-1) or interleukin 3 regulated nuclear factor (Nfil3) and the hematopoietic growth factor IL-7 [91-94]. Phenotypic and functional NK cell maturation is predominantly regulated by the T-box transcription factor (T-bet) and eomesodermin (Eomes) [95] as well as the interleukins IL-12, IL-15 and IL-18 and the transforming growth factor (TGF)-β, in- and outside the bone marrow [87, 96].

Once NK cells – that have gained phenotypical and functional competence – are released from the bone marrow, a process positively regulated by the bioreactive lipid sphingosine-1-phosphate receptor 5 (S1P5), they reside in various lymphoid and non-lymphoid organs during basal homeostasis, predominantly in blood, spleen, liver, lung, but can also be found for example in lymph nodes, thymus or uterus at lower frequencies [97, 98]. Roughly, 0.1-0.4 NK cells/ ml are continuously present in circulation in human corresponding to up to 15% of the circulating lymphocyte population [99]. However, NK cell traffic between circulation and other organs remains not fully characterized even though many chemokines [e.g. CC-chemokine ligands (CCL) 3-5 and 19, CXC-chemokine ligands (CXCL) 12, CX3C-chemokine ligand (CX3CL) 1], chemokine receptors [e.g. CC-chemokine receptors (CCR) 1, 5, 7, CXC-chemokine receptors (CXCR) 3, 4, 6, and CX3C-chemokine receptor 1 (CX3CR1)] and adhesion molecules [e.g. α2 integrin, α4 integrin and DNAX accessory molecule 1 (DNAM1)] have already been shown to be implicated in NK cell localization [97, 100], which appears to be tightly regulated during NK cell development and homeostasis in mice and humans.

At steady-state, the majority of peripheral NK cells is localized to the red pulp of the spleen and the sinusoidal regions of the liver [101]. During viral infection, this homeostasis is disturbed. NK cells become activated, proliferate robustly and clonal-like expansions have been described in spleen and liver where the NK cells infiltrate the white pulp and parenchyma, respectively, further leading to their recruitment into lymphoid/ non-lymphoid tissues near the infected foci [102, 103].

1.2.1.2 NK cell receptors and acquisition of function

The recognition of non-self and "altered self" cells and therewith NK cell function are based on a system of numerous receptors whose engagement decides on quality and intensity of the NK cell response. This system is composed of two types of receptors which are of either inhibitory or activating nature [104].

According to the "missing-self hypothesis", NK cells use inhibitory receptors to fathom the presence or absence of self-molecules – i.e. MHC class I molecules – which are constitutively expressed on healthy self-cells but not or at very low levels on susceptible target cells [105]. This capacity is enabled by previous "NK cell licensing" during which NK

cells are educated by detecting host MHC class I molecules and further adapt to their environment through "priming" by cytokines (e.g. IL-12, IL-15 and IL-18) [106]. Thereafter, the integration of inhibitory and activating receptor signaling with surrounding cells in circulation maintains a dynamic balance regulating NK cell activation and therewith determining NK cell function i.e. killing target cells and/ or the production of cytokines within the scope of immunomodulation [107, 108].

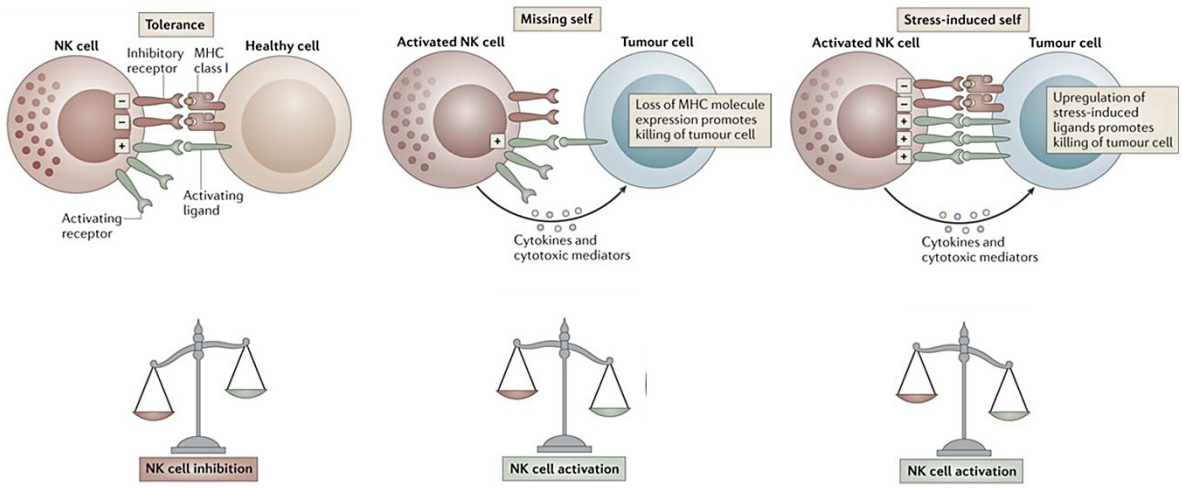

Figure 4. NK cell activation. The integration of inhibitory and activating receptors dictates the activation of NK cells. Ligation of inhibitory receptors to MHC class I on a healthy cell results in NK cell tolerance (left) whereas the NK cell becomes activated to kill a target cell as soon as MHC class I molecules are absent as for example on tumor cells (middle) or present at reduced levels (as it is typical for stressed cells) together with an overwhelming ligation of activating receptors. (Adapted and modified in arrangement from Vivier et al., 2012 [105])

Within a high number and diversity in both human and mouse, prominent inhibitory receptors are most of the killer-cell immunoglobulin like receptors (KIRs) representing the main receptors for MCH class I molecule recognition, the co-inhibitory receptor killer-cell lectin like receptor G1 (KLRG1) or the killer cell lectin-like receptor subfamily K, member A (NKG2A). The receptor Ly49 exists in both inhibitory and activating isoforms and typical activating receptors are CD16 (FcγIIIA), the natural killer cell p46-related protein (NKp46), NKG2C and –D or DNAM1 [107].

As soon as the ligation and signaling of activating receptors overcomes the one of inhibitory receptors, NK cells deploy their killing activity inducing target cell apoptosis either by sectreting cytolytic granule (e.g. release of granzymes and perforins) or by ligating so-called death ligands on the target cell surface forming death ligand/ receptor

signaling complexes (e.g. apoptosis antigen 1 receptor and ligand FasR/ FasL) [109]. Another mechanism of action used by NK cells is the antibody-dependent cellular cytotoxicity (ADCC). Here, antibodies which have bound to target antigens are recognized by CD16 (FcγRIII) receptors on the NK cell surface inducing the release of cytotoxic granules to kill the respective target cell [110].

1.2.1.3 NK cell subtypes and migration to target organs

Classically, human NK cells are subdivided according to their expression of the neural cell adhesion molecule CD56 into $CD56^{bright}$ and $CD56^{dim}$ NK cells (Figure 5). Approximately 90% of the peripheral NK cells in circulation are $CD56^{dim}$ NK cells whereas $CD56^{bright}$ NK cells are more abundant in secondary lymphoid tissues (e.g. lymph nodes, tonsils) [101, 111]. This distribution is related to several phenotypic differences. For example, $CD56^{bright}$ NK cells but not $CD56^{dim}$ NK cells express high levels of the chemokine receptor CCR7 and the adhesion molecule CD62L which are both involved in the homing to secondary lymphoid tissues pointing towards distinct trafficking patterns of these NK cell subsets during the immune response [112]. Moreover, NK cell effector function depends on the NK cell phenotype. Cytokine receptors for cytokines such as IL-1, IL-10, IL-12, IL-15 or IL-18 are constitutively expressed on all NK cell subsets, but show the highest expression on $CD56^{bright}$ NK cells. Therefore, $CD56^{bright}$ NK cells are designated as regulatory NK cells producing high amounts of immunoregulatory cytokines (e.g. IFN-γ, TNF-β, GM-CSF, IL-10 or IL-13) [113-117]. The IL-2 receptor is also highly expressed on this $CD56^{bright}$ population explaining their high proliferative capacity [118]. In contrast, $CD56^{bright}$ NK cells do not express CD16 [119] and only low levels of KIRs [120], all important for target recognition and effector function whereas these receptors are strongly expressed on $CD56^{dim}$ NK cells wherefore they are termed cytotoxic NK cells [99, 121].

Mouse NK cells share some phenotypic similarities with human NK cells (predominantly regarding cytokine receptors and some KIRs) but there are also several differences. Since murine NK cells do not express CD56, they are conventionally subdivided according to the maturation markers CD27 and CD11b (Figure 5) [122, 123]. Furthermore, depending on the mouse strain, murine NK cells constitutively express the activating receptors NK1.1 and/ or NKp46 but lack NKp30 which is present in human. In line with this, all mouse but not human NK cell subsets display cytotoxic effector functions. As well, mouse NK cells differ

in the expression of chemokine receptors and adhesion molecules from their human counterparts (e.g. CD62L is constitutively expressed on murine NK cells) suggesting distinct tissue distributions and unique trafficking patterns during immune responses [100, 122, 123].

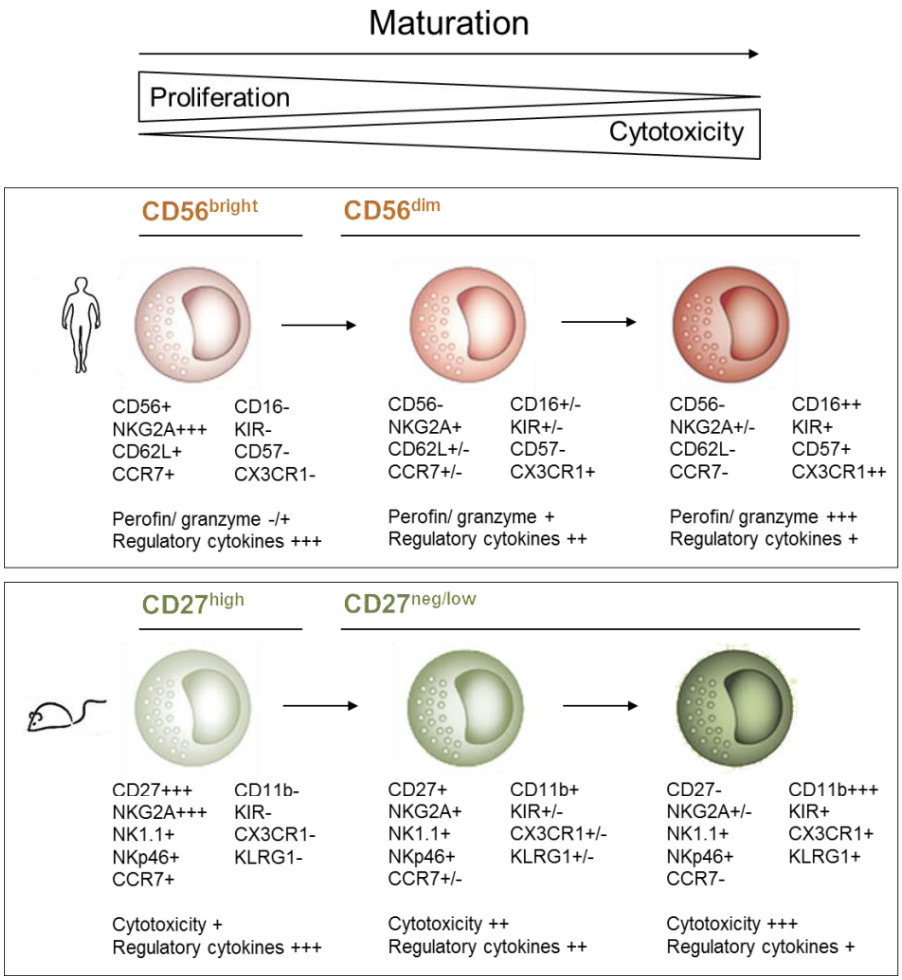

Figure 5. NK cell subsets in human and mouse. Human NK cells are classically defined as CD56^{bright} and CD56^{dim} NK cells phenotypically – and therewith also functionally – differing in their expression profiles of activating and inhibitory receptors, cytokine and chemokine receptors as well as adhesion molecules. Murine NK cells are subdivided according to their expression levels of CD27 and CD11b and share some phenotypical and functional similarities with human NK cell subsets. Main differences between human and mouse NK cells can be found in the expression of chemokine receptors and adhesion molecules.

The homing of NK cells to target organs is determined by their NK cell chemokine receptor and adhesion molecule expression profile as well as organ-specific determinants. Whereas data on human NK cell trafficking and recirculation are difficult to obtain, many studies in mice have been performed under healthy and various pathological conditions. As described in section 1.2.1.1., the majority of NK cells are located in liver and spleen during basal homeostasis [101]. While the chemokine receptors CCR1-3, 5 and CXCR6 were shown

to be involved for the NK cell recruitment into the liver [100], several receptors have been discussed (e.g. CCR5, CXCR3) but no precise receptor has been identified so far to be responsible for the NK cell homing into the spleen, wherefore it is speculated if NK cells might simply be pushed into the spleen by the blood flow [124]. NK cell homing to the lung, skin and gut involves the ligation of diverse chemokine receptors such as CCR2, CXCR3, CX3CR1 (lung) or CCR5, CXCR3, CXCR1 and CCR6 (skin). CXCR4 is required for the NK cell migration into the uterus and CCR5 and CXCR3 might participate to their trafficking into the pancreas. NK cells have further been reported to infiltrate the CNS through ligation of the chemokines CX3CL1, CXCL10 and CCL2 [101].

A comparison of these findings with the phenotypes of the defined NK cell subsets reveals that homing and recirculation at steady-state and under inflammatory conditions appear to be NK cell subset specific and to depend on the organ-specific microenvironments.

1.2.1.4 NK cells in autoimmunity

Apart from their role in the early hots defense and the shaping of innate and adaptive immune responses, NK cells have also been implicated in the initiation and/ or maintenance of autoimmune diseases [125]. In hemophagocytic lymphohistiocytosis, a failure of the cytolytic NK cell function in immunoregulation is reported [126]. Such an impaired NK cell function has also been described in several other autoimmune disorders. Decreased peripheral NK cell numbers or impaired NK cell cytotoxic activity were observed in patients with MS, systemic lupus erythematosus (SLE), rheumatoid arthritis (RA) or type 1 diabetes mellitus [127].

In RA, NK cell infiltrations were found in the synovial fluid of the affected joints displaying a predominantly $CD56^{bright}$ phenotype with decreased expression of KIRs and CD16b. These NK cells were further shown to produce highly increased levels of the pro-inflammatory cytokines IFN-γ and TNF-α resulting in a dysregulated immunoregulation at the inflammatory sites. In contrast, $CD56^{bright}$ NK cell numbers in peripheral blood of RA patients are decreased [127]. However, animal studies showed that NK cell depletion results in an earlier disease onset and increased generation of T_h17 cells and neutrophil recruitment to the inflamed joints [127, 128]. Therefore, it remains conflicting whether NK cells have disease controlling or rather disease enhancing effects in RA.

Several deficits in peripheral NK cells have also been reported in SLE patients correlating with their clinical manifestations. Circulating NK cells are decreased in numbers and display low cytotoxicity [127]. However, apart from these findings, the implication of NK cells in the SLE disease development remains not fully understood yet.

The contribution of NK cells to autoimmune neuroinflammation remains controversial. In MS, several studies presented evidence for a decreased number of NK cells in peripheral blood, an enrichment of $CD56^{bright}$ NK cells in the CSF and a spatiotemporal correlation between NK cell cytotoxic activity and diseases relapses [2, 3, 5, 129]. These evidences for deficient NK cell activity in MS patients suggest that NK cells may have a protective, disease-limiting role in neuroinflammation [6, 130-133]. However, data from the EAE animal model are contradictory reporting both a protective [134] as well as a pathogenic [135] role for NK cells in disease pathogenesis. Due to the hererogeneity and versatility of NK cells with respect to their phenotype, function and organ distribution [101, 112, 122, 136], one could hypothesize that while a certain subtype may contribute to pathology, another subset may be protective in the appropriate environment [137]. In this context , our group previously showed a reduced gene expression of CX3CR1 – the receptor for the chemokine CX3CL1 (fractalkine) – exclusively on NK cells but no other immune cells in MS patients, and a correlation of the frequency of circulating CX3CR1-expressing NK cells with disease activity [6]. We also found that the expression of CX3CR1 serves to discriminate fully mature from immature human NK cells [138]. Thus, diminished levels of CX3CR1-expressing NK cells may be associated with a decreased frequency of mature NK cells in MS. Consistently, mice deficient for CX3CR1, develop a more severe EAE associated with a reduced recruitment of NK cells into the inflamed CNS [7]. This suggests that CX3CR1-expression may be related to the migration or effector function of “protective” NK cells.

1.2.2 Neutrophils

Neutrophils are the most abundant leukocytes in circulation playing a crucial role in the first line of immunological defense against bacterial and fungal infections. They have first been described by P. Ehrlich in 1880 as cells characterized by a “polymorphous nucleus” retaining neutral dyes wherefore he named them “neutrophils”. Due to their unique lobulated nucleus, neutrophils are also often designated as polymorphonucelear leukocytes (PMNs). Like the developmentally related basophils and eosinophils,

neutrophils belong to the granulocytes-family of white blood cells which are characterized by a storage of granules with antimicrobial functions [139].

1.2.2.1 Neutrophil homeostasis

Neutrophils only have a relatively short circulating half-life of 6-8 hours and are produced in the bone marrow at a basal rate of 5-10 x 10^{10} cells per day. Since these effector cells possess highly destructive capacities, neutrophil homeostasis is critically regulated to prevent the damage of healthy tissues by preserving an equilibrium between granulopoiesis (genesis of neutrophils), bone marrow storage and release, margination (prolonged organ-specific transit) and clearance [140].

In the bone marrow, granulopoiesis is primarily shaped by the granulocyte colony stimulating factor (G-CSF) which stimulates neutrophil production, proliferation and release into circulation [141, 142]. The latter is further regulated by the chemokine receptor CXCR4 [143] and the α_4 integrin very late antigen-4 (VLA-4) [144] whose absence and expression are important for the release and retention of neutrophils, respectively. Once released from the bone marrow, one distinguishes between a circulating pool and a marginated pool of neutrophils, i.e. neutrophils which are temporarily stored in specific organs (termed as prolonged transit) but can quickly be recovered into circulation [140]. Both neutrophil pools approximately cover 50% of the bone marrow released neutrophils under healthy conditions. The marginated neutrophils can predominantly be found in the liver, spleen and bone marrow where, in the absence of infection or injury, apoptotic neutrophils are cleared by macrophages. This clearance, in turn, leads to G-CSF generation and therewith stimulation of granulopoiesis in the bone marrow to maintain neutrophil homeostasis [140].

Under systemic stress or inflammation, neutrophilia is induced in the circulation. Here, the release of multiple pro-inflammatory mediators (e.g. TNF-α, IL-1β, IL-17 or IL-8) results in the priming of resting neutrophils and their subsequent recruitment to the sites of infection or inflammation. At these sites, neutrophils become fully activated by encountering infectious or host-derived inflammatory signals (e.g. N-formylmethionyl-leucyl-phenylalanine, fMLP, or other pathogenic particles), deploy their antimicrobial

arsenal and finally undergo apoptosis, necrosis or are lost following trans-epithelial migration [139, 145].

1.2.2.2 Mechanisms of pathogen killing

Neutrophils possess various mechanisms of action to effectively clear infections or resolve inflammation. A summary of them is shown is figure 6.

Once neutrophils have been primed, they are guided through chemotactic signals to the site of infection or inflammation where they leave the circulation, cross endothelium and enter the inflammatory site. Here, neutrophils can use different mechanisms to combat pathogens. These primarily include degranulation, oxidative burst, phagocytosis and NETosis [146].

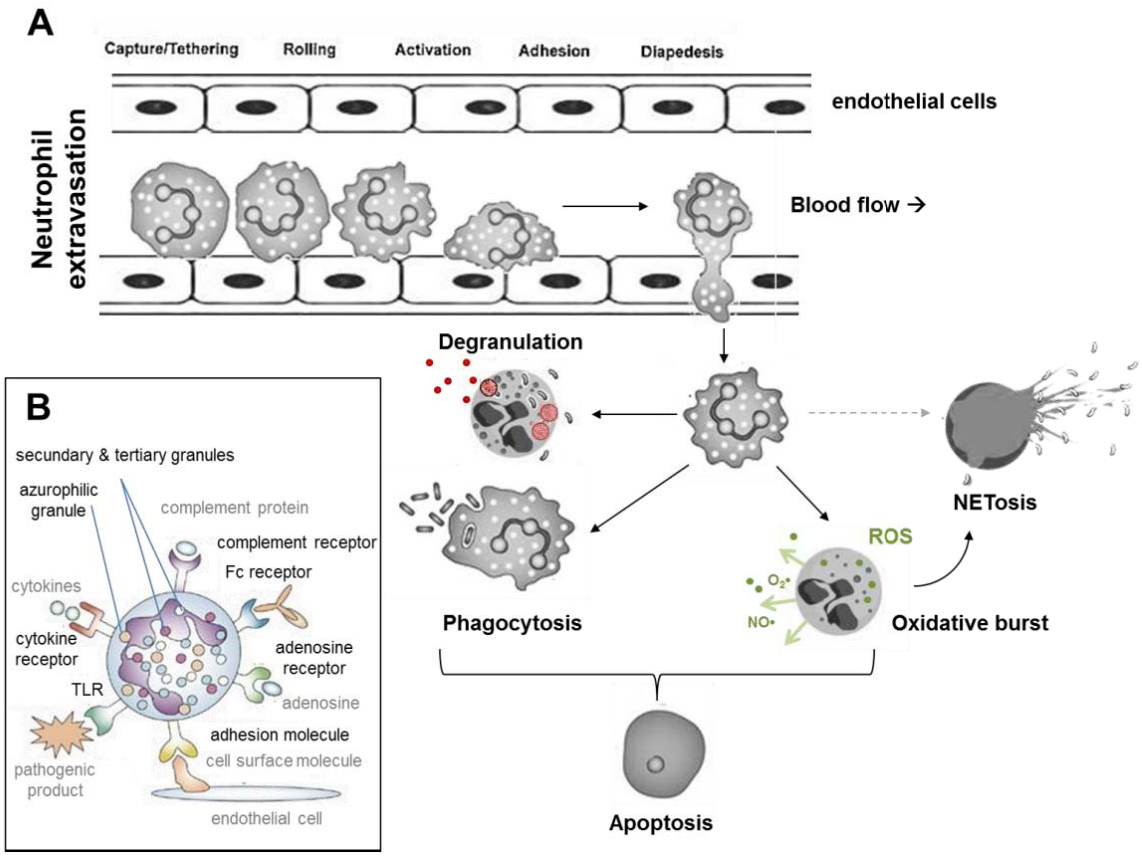

Figure 6. Neutrophil mechanisms of action. A) Subsequent to extravasation into sites of infection or inflammation, neutrophils deploy their antimicrobial arsenal by initiating degranulation, oxidative burst, phagocytosis and/ or NETosis. With the exception of "NETotic" neutrophils, neutrophils undergo apoptosis after the clearance process and are ingested by macrophages. Cellular components (neutrophil cells) were adapted and modified from Kolaczkowska and Kubes (2013) [145]. B) Schematic representation of important surface receptors and molecules through which neutrophil operate in the course of antimicrobial defense. Abbreviations: ROS = reactive oxygen species, TLR = toll-like receptor. Figure 2B adapted from Eyles et al. (2006) [147].

Degranulation involves the release of antimicrobial peptides and enzymes to fight an infection/ inflammation. These molecules are stored in specific organelles – the granules – which fuse with the plasma membrane (or phagosome during pathogen uptake) upon neutrophil activation causing extracellular release (or intracellularly into the phagosome) of contents [146]. There are three different types of neutrophil granules. Azurophilic granules represent the most prominent granules in neutrophils. They contain cationic molecules (e.g. myeloperoxidase (MPO), PMN elastase, defensins, cathepsin G) which interact with the negatively charged membrane components of pathogens resulting in membrane permeabilization and further inhibition of DNA/ RNA synthesis. Moreover, neutrophils possess specific granules (e.g. lysozyme, lactoferrin), gelatinase granules [e.g. gelatinase, matrix metalloproteinases (MMP) 8, 9 and 25] and secretory vesicles that predominantly contain adhesion and chemotactic receptors important for neutrophil recruitment during inflammation [139].

In the course of antimicrobial defense, neutrophils increase their production of reactive oxygen species (ROS) directly after their activation in a process called oxidative burst (or respiratory burst). These ROS are highly aggressive molecules that can modify and damage cells by oxidation of DNA/ RNA, proteins and lipids [139]. Their production is initiated by the nicotinamide adenine dinucleotide phosphate-oxidase (NADPH) oxidase complex after its assemblage on the plasma and/ or phagosomal membrane. In the first step, oxygen is reduced to superoxide which then gives rise to various ROS in the course of a reactive oxygen cascade (e.g. hyperoxide, hydroxyl radical, hydrogen peroxide or nitric oxide) [139, 148].

For the removal of pathogens and cell debris, neutrophils use the mechanism of phagocytosis [149]. This process involves the receptor-mediated internalization of pathogenic particles. Phagocytosis can occur directly through the recognition of particles by pattern-recognition receptors (e.g. Toll-like receptors, TLRs), or indirectly after particle opsonization and recognition through neutrophilic Fc or complement receptors [139] (Figure 6B). After particle engulfment, internal granules containing hydrolytic enzymes, and also NADPH oxidase subunits to further induce/ amplify killing mechanisms like the oxidative burst, fuse to the phagocytic vacuole and deliver their antimicrobial molecules into the lumen of the phagosome [139, 149].

Distinct from apoptosis, neutrophil extracellular trap (NET)-osis is a relatively new discovered, programmed cell death mechanism by which neutrophils can kill pathogens [150]. This mechanism allows to expose pathogens to high concentrations of antimicrobials – NETs – released by the neutrophils. NETs are composed of decondensed chromatin DNA associated with histones, granular proteins, and a few cytoplasmic proteins [150-153] and formation of these pro-inflammatory structures seems to depend on the generation of ROS by the NADPH oxidase complex [154]. However, the whole mechanism of NET formation is not completely understood yet.

1.2.2.3 Neutrophils in autoimmunity

Neutrophils are highly relevant for the protection against bacterial and fungal infections as well as against intracellular pathogens such as viruses. Moreover, they are important regulators of not only the innate but also the adaptive immune responses shaping them at various levels [155]. However, due to their plethora of highly toxic, antimicrobial weapons, neutrophils also can have self-detrimental effects when improperly regulated. Apart from commonly known neutrophil disorders (e.g. severe congenital neutropenia or chronic granulomatous disease), several studies indicate that neutrophils are involved in different pathological autoimmune disorders such as type 1 diabetes mellitus or SLE. Here they display abnormalities in phenotype and function and are suggested to play a central role in both the initiation and the effector phase of the diseases [156, 157].

In SLE, neutropenia, an impaired neutrophil phagocytic capacity and alterations in the oxidative metabolism have been reported. Most importantly, anti-double-stranded (ds) DNA antibody-containing immune complexes have been found to be crucial pathogenic features of this autoimmune disease and NETs have been proposed to be the source of these complexes. Consistently, NETosis levels in the periphery as well as in tissues were shown to correlate with circulating anti-dsDNA titers. As well, enzymatic NET degradation by DNase I was found to be impaired in approximately one-third of SLE cases correlating with increased levels of antinuclear and anti-NET antibodies and with higher prevalence of lupus nephritis. Moreover, this aberrant formation and simultaneously impaired clearance of NETs were shown to activate the complement and plasmacytoid dendritic cells leading to disease exacerbation and endothelial dysfunctions [156, 157].

Considering autoimmune disorders of the CNS, peripheral neutrophils have been shown to display a primed phenotype and further to show increased degranulation and respiratory burst activity in RRMS. Moreover, serum levels of NETs were found to be increased in these patients [158]. Studies performed in the EAE mouse model further highlighted that neutrophils appear to play a crucial role in the preclinical disease phase by CXCL2 chemokine induced and IL-17 mediated neutrophil recruitment to the CNS contributing to the disruption of the BBB and formation of inflammatory lesions [159-161]. In addition, neutrophils were suggested to participate in the processes of demyelination and axonal degeneration. In the acute but not remission phase of EAE, neutrophils were observed in increased numbers in the CNS providing local factors for the maturation of professional APCs which, in turn, (re-)stimulate myelin-specific T cells and therewith promote progression and reactivation of inflammatory responses [162]. In line with these data, it was reported that the effector phase of EAE mice treated with anti-granulocytes antibodies could be inhibited [163].

In contrast to MS, NMO lesions are characterized by extensive complement deposits and neutrophil infiltrates [12, 13, 164, 165]. Moreover, neutrophil counts and levels of neutrophil-related cytokines such as IL-8 or G-CSF were shown to be increased in the CSF of NMO patients during acute relapses [14, 15, 166]. In NMO mice, which were generated by intracerebral injection of serum IgG from NMO patients together with human complement, increased severity of NMO lesions could be observed when neutrophilia was induced by G-CSF injection(s). In contrast, depletion of neutrophils led to a significant reduction of neuroinflammation and demyelination, indicating a direct involvement of neutrophils in NMO lesion formation. However, the precise implication of neutrophils in CNS autoimmune disorders such as NMO and MS remains not fully understood and needs further investigations [167].

2. Aim and purpose

The present thesis work includes two projects aiming to investigate the role of innate immune cell types, precisely NK cells and neutrophils, in autoimmune diseases of the CNS.

(1) Implication of NK cells and the contribution of the chemokine receptor CX3CR1 to NK cell dynamics in the EAE mouse model

The expression of the chemokine receptor CX3CR1 serves to discriminate fully mature from immature human NK cells [138]. Both, gene and protein expression of CX3CR1 have been shown to be reduced in NK cells of MS patients and MS flares appear to correlate with the frequency of circulating CX3CR1-positive NK cells [6]. Moreover CX3CR1-deficient mice develop a more severe EAE disease course than their WT counterparts, apparently associated with an impaired recruitment of NK cells into the inflamed CNS [7]. These findings suggest that CX3CR1 is involved in the recruitment or effector function of "protective" NK cells, but it remains unclear whether a particular NK cell subtype confers protection, how and where protective NK cells exert their function and how they are mobilized during the course of neuroinflammation. Therefore, the follwing aspects were aimed to be worked on:

- How are NK cells distributed during EAE-related neuroinflammation?
- How does the expression of CX3CR1 affect NK cell dynamics in EAE mice?
- Is CX3CR1 important for NK cell recruitment into the CNS?
- Do NK cells exert a protective or rather detrimental effect in EAE?
- Are different NK cells subsets responsible for this protection or neuronal damage?

(2) Phenotypic and functional characterization of neutrophils in NMO and MS

Serum AQP4-IgG represents the most important marker for NMO diagnosis [10, 59]. However, up to 20% of NMO patients are seronegative [55] for AQP4-IgG or become seronegative during the disease course elucidating the need for additional prognostic and diagnostic marker. In this context, neutrophils or neutrophil-derived molecular components could display potential targets since extensive neutrophil deposits are characteristic for

NMO lesions and neutrophil counts and levels of neutrophil-related cytokines such as IL-8 or G-CSF were further shown to be increased in the CSF of NMO patients during acute relapses [14, 15, 166]. Therefore, it was investigated if activity and/ or phenotype of peripheral blood-derived neutrophils may help to better diagnose NMO and help with the distinction from other conditions such as MS by considering the following questions:

- Does neutrophil phenotype differ between NMO and MS patients compared to healthy controls (HC)?
- Are neutrophil effector functions intact in NMO and MS when compared to HC with respect to migration, ROS production, degranulation and phagocytosis?
- Do neutrophil phenotypic and functional characteristics correlate with clinical parameters of NMO and/ or MS patients?
- Does medical treatment of the patients affect the neutrophil phenotype and functionality in NMO or MS?

3. Materials and methods

3.1 Laboratory materials

3.1.1 Devices

Device	Company
ABI PRISM 7000 Sequence Detection System	Applied Biosystems, Darmstadt, Germany
Balance, Kern EW 820-2NM	Kern&Sohn GmbH, Balingen, Germany
Benchtop Centrifuge	NeoLab, Heidelberg, Germany
Cell Incubator	Binder GmbH, Tuttlingen, Germany
Eppendorf Centrifuge 5417R	Eppendorf AG, Hamburg, Germany
Eppendorf Centrifuge 5810R	Eppendorf AG, Hamburg, Germany
Eppendorf MasterCycler Gradient	Eppendorf AG, Hamburg, Germany
Eppendorf Thermomixer Compact	Eppendorf AG, Hamburg, Germany
FACSCanto™	BD Pharmingen™, Heidelberg, Germany
GFL WaterBath	GFL, Burgwedel, Germany
GlomaxMulti Detection System	Promega, Mannheim, Germany
HeraCell Incubator	Heraeus, Hanau, Germany
Laminar flow hood HeraSafe	Heraeus, Hanau, Germany
Liquid nitrogen tank	Messer, Bad Soden, Germany
LSR FortessaTM	BD Pharmingen™, Heidelberg, Germany
Magnetic stirrer	MLW RH3, Germany
Megafuge 1.0	Thermo Fisher Scientific, Waltham, USA
NanoDrop™	NanoDrop Technologies Inc., Delaware, USA
Neubauer counting chamber	Brand GmbH & Co KG, Wertheim, Deutschland
pH Meter	Schott Instruments GmbH, Mainz, Germany
PIPETMAN® Multichannel	Gilson Inc., Middleton, USA
Pipettes (10 µl, 20 µl, 200 µl and 1000 µl)	Eppendorf AG, Hamburg, Germany
Pipetus®	Hirschmann Laborgeräte, Eberstadt, Germany
PrimoVert Inverted Microscope	Zeiss, Oberkochen, Germany
Rotamax 120 Orbital Shaker	Heidolph Instruments GmbH & Co. KG, Schwabach, Germany
Timer	Eppendorf AG, Hamburg, Germany
Transferpette® Multichannel Pipette	BrandTech® Scientific, Essex, USA
Vacuum Pump	KNF Neuberger, Inc., Trenton, USA
Vortex Genie 2	Scientific Industries Inc., Bohemia, New York, USA
Wallac Victor2 1420 Multilabel Spectrofluorimeter	Perkin Elmer, Waltham, USA

3.1.2 General consumables and materials

Consumable/ material	Company
BD Falcon Conical Tubes (15 and 50 ml)	BD Bioscience™, Heidelberg, Germany
BD Falcon Pipets and Pipetters	BD Bioscience™, Heidelberg, Germany
BD Falcon™ Round-Bottom Tubes (5 ml) (for FACS)	BD Bioscience™, Heidelberg, Germany
BD Vacutainer® Blood Collection Tubes	BD Pharmingen™, Heidelberg, Germany
BD Vacutainer® Eclipse™ Blood Collection Needle	BD Pharmingen™, Heidelberg, Germany
BD Vacutainer® One-Use Holder	BD Pharmingen™, Heidelberg, Germany
BD Vacutainer® Push Button Blood Collection Set	BD Pharmingen™, Heidelberg, Germany
BD Vacutainer® Safety-Lok™ Blood Collection Set	BD Pharmingen™, Heidelberg, Germany
Biosphere® Tips (all sizes)	Sarstedt AG & Co, Nümbrecht, Germany
Blood lancets	Feather Safety Razor Co., Ltd., Osaka, Japan
Cell strainer (100 and 70 µm)	BD Bioscience™, Heidelberg, Germany
Corning® 96-well microtiter plates	Sigma-Aldrich, Schnelldorf, Germany
Corning® Plastic Culture Dishes, Petri Style	Sigma-Aldrich, Schnelldorf, Germany
Dumont Medical dissection instruments (forceps, scissors etc.)	Fine Science Tools GmbH, Heidelberg, Germany
Eppendorf tubes (0,5 ml, 1,5 ml, 2 ml)	Eppendorf AG, Hamburg, Germany
FORTUNA® OPTIMA® glass syringes	Poulten & Graf GmbH, Wertheim, Germany
Hemacytometer Cover Glasses	VWR International, Radnor, USA
Nunc® Cooling & Cryogenics	Sigma-Aldrich, Schnelldorf, Germany
LS-Columns	Miltenyi Biotec, Bergisch Gladbach, Germany
Magnetic stirring staffs	Handelskontor Freitag, Minden, Germany
Mr. Frosty™ Freezing container	Thermo Fisher Scientific Inc., Waltham, Germany
Parafilm	American Can Company, Greenwich, USA
Pipettes	Eppendorf AG, Hamburg, Germany
Reaction vessels (glassware)	Schott AG and DURAN Group GmbH (Mainz, Germany) and VWR International (Radnor, USA)
Reaction vessels (plasticware)	Vitlab (Großostheim, Germany) and Kartell Labware (Noviglio, Italy)
Safety-Multifly® 21G 200 mm	Sarstedt AG & Co, Nümbrecht, Germany
S-Monovette® 1.6ml K3 EDTA	Sarstedt AG & Co, Nümbrecht, Germany
S-Monovette® 7.5ml NH (Heparin)	Sarstedt AG & Co, Nümbrecht, Germany
S-Monovette® 7.5ml Z (Serum)	Sarstedt AG & Co, Nümbrecht, Germany
Storage racks	TPP (Trasadingen, Switzerland) and Brand GmbH & Co KG (Wertheim, Deutschland)
Syringes and cannula	BD Medical™, Heidelberg, Germany
Tourniquets for venipuncture	Medka Medizinprodukte
TrueCount™ Tubes	BD Bioscience™, Heidelberg, Germany

3.1.3 Buffers, solutions and cell culture media

Buffer/ solution	Compounds	Company
Phosphate buffered saline (PBS)	137,0 mM NaCl	Merck Millipore KGaA, Darmstadt, Germany
	2,7 mM KCl	Carl Roth GmbH + Co. KG, Karlsruhe, Germany
	1,5 mM KH_2PO_4	Merck Millipore KGaA, Darmstadt, Germany
	8,1 mM Na_2HPO_4	Sigma-Aldrich, Schnelldorf, Germany
	pH 7,2	
Cell culture medium (mouse)	RPMI-1640	Seromed Biochrom GmbH, Berlin, Germany *
	10% Fetal calf serum (FCS)	Sigma-Aldrich, Schnelldorf, Germany
	50 µM β-mercaptoethanol	Sigma-Aldrich, Schnelldorf, Germany
	100 U/ ml penicillin	Seromed Biochrom GmbH, Berlin, Germany *
	100 µg/ ml streptomycin	Seromed Biochrom GmbH, Berlin, Germany *
Cell culture wash medium (mouse)	RPMI-1640	Seromed Biochrom GmbH, Berlin, Germany *
	15% FCS	Sigma-Aldrich, Schnelldorf, Germany
	100 U/ ml penicillin	Seromed Biochrom GmbH, Berlin, Germany *
	100 µg/ ml streptomycin	Seromed Biochrom GmbH, Berlin, Germany *
Cell fixing solution	4% paraformaldehyde (PFA)	Merck Millipore KGaA, Darmstadt, Germany
	PBS	
Complete growth medium	RPMI-1640	Seromed Biochrom GmbH, Berlin, Germany *
	10% Fetal calf serum (FCS)	Sigma-Aldrich, Schnelldorf, Germany
	1% HEPES	Gibco®, Thermo Fisher Scientific Inc., Waltham, Germany
	2 mM L-glutamine	Sigma-Aldrich, Schnelldorf, Germany
	100 U/ ml penicillin	Seromed Biochrom GmbH, Berlin, Germany *
	100 µg/ ml streptomycin	Seromed Biochrom GmbH, Berlin, Germany *
Defrosting medium	RPMI-1640	Seromed Biochrom GmbH, Berlin, Germany *
	5% HEPES	Gibco®, Thermo Fisher Scientific Inc., Waltham, Germany
	10% FCS	Sigma-Aldrich, Schnelldorf, Germany
	1% penicillin-streptomyin	Seromed Biochrom GmbH, Berlin, Germany *
Dimethyl sulfoxide (DMSO) medium solution	RPMI-1640	Seromed Biochrom GmbH, Berlin, Germany *
	1% HEPES	Gibco®, Thermo Fisher Scientific Inc., Waltham, Germany
	20% DMSO	Sigma-Aldrich, Schnelldorf, Germany
Erythrocyte lysis buffer	10 mM Tris-HCl (Trizma® hydrochloride HCL, pH 8,0)	Sigma-Aldrich, Schnelldorf, Germany
	320 mM sucrose	Sigma-Aldrich, Schnelldorf, Germany

Buffer/ solution	Compounds	Company
	5 mM magnesium chloride ($MgCl_2$)	Sigma-Aldrich, Schnelldorf, Germany
	1% Triton X-100	Sigma-Aldrich, Schnelldorf, Germany
FACS-buffer	1% (w/v) bovine serum albumin (BSA)	SERVA Electrophoresis GmbH, Germany
	0,5% sodium azide (NaN_3)	Sigma-Aldrich, Schnelldorf, Germany
	PBS	
FCS-Medium	RPMI-1640	Seromed Biochrom GmbH, Berlin, Germany *
	5% HEPES	Gibco®, Thermo Fisher Scientific Inc., Waltham, Germany
	10% FCS	Sigma-Aldrich, Schnelldorf, Germany
	1% L-glutamin	Sigma-Aldrich, Schnelldorf, Germany
	1% penicillin-streptomycin	Seromed Biochrom GmbH, Berlin, Germany *
Freezing medium	RPMI-1640	Seromed Biochrom GmbH, Berlin, Germany *
	5% HEPES	Gibco®, Thermo Fisher Scientific Inc., Waltham, Germany
	20% FCS	Sigma-Aldrich, Schnelldorf, Germany
	10% DMSO	Sigma-Aldrich, Schnelldorf, Germany
MACS buffer	2 mM EDTA	Sigma-Aldrich, Schnelldorf, Germany
	0,5% BSA	SERVA Electrophoresis GmbH, Germany
	PBS	
Trypan blue solution	0,4% (w/v) trypan blue	Sigma-Aldrich, Schnelldorf, Germany
	PBS	

* now division of Merck Millipore KGaA, Darmstadt, Germany

Buffers and solutions within the scope of commercially available kits ready for use (ELISAs, Migratest™, Phagotest™, RNA isolation etc.) were prepared with the provided reagents according to the manufacturer's instructions.

3.1.4 Other chemicals and reagents

Chemical/ reagent	Company
BD Lysis buffer	BD Bioscience™, Heidelberg, Germany
Calcein-acetoxymethyl (AM)-ester	MoBiTec, Göttingen, Deutschland
Complete Freund's Adjuvans (CFA)	Difco Laboratories, Detroit, USA
Double-distilled (dd) H_2O	Gibco®, Thermo Fisher Scientific Inc., Waltham, Germany
Dihydrorhodamine (DHR) 123	Sigma-Aldrich, Schnelldorf, Germany
Deoxyribonuclease (DNase)	Sigma-Aldrich, Schnelldorf, Germany
Ethanol (EtOH)	Merck Millipore KGaA, Darmstadt, Germany

Chemical/ reagent	Company
Fc block mouse and human	BD Pharmingen™, Heidelberg, Germany
Histopaque®	Sigma-Aldrich, Schnelldorf, Germany
Ionomycin	Sigma-Aldrich, Schnelldorf, Germany
Isopropanol	J. T. Baker Chemicals, Deventer, Netherlands
Ketamine	Actavis GmbH & Co. KG, Munich, Germany
Mycobacterium tuberculosis H37 RA	Difco Microbiology, Lawrence, USA
Myelin oligodendrocyte glycoprotein 35-55 (MOG_{35-55}) (Y R S P F S R V V H L Y R N G), purity > 95 %	Pepceuticals Ltd., Leicester, UK
N-formyl-methionyl-leucyl-phenylalanine (fMLP)	Sigma-Aldrich, Schnelldorf, Germany
Phosphate buffered saline (PBS)	Gibco®, Thermo Fisher Scientific Inc., Waltham, Germany
peqGOLD Trifast™	peqLAB Biotechnologie GmbH, Erlangen, Germany
Percoll®	Sigma-Aldrich, Schnelldorf, Germany
Pertussis-toxin (PTX)	Sigma-Aldrich, Schnelldorf, Germany
Phorbol-12-myristate-13-acetate (PMA)	Sigma-Aldrich, Schnelldorf, Germany
qPCR™ Mastermix Plus	Eurogentec, Seraing, Belgium
Triton X-100	Sigma-Aldrich, Schnelldorf, Germany
TrueCount™ Tubes	BD Bioscience™, Heidelberg, Germany
Xylazine	Bayer Vital GmbH, Leverkrusen, Germany

3.1.5 Kits

Kit	Company
E.Z.N.A.® Total RNA Kit 1	Omega, Bio-Tek, Norcross, USA
Human G-CSF ELISA	R&D Systems, Abingdon, UK
Human IL-8 ELISA	Invitrogen, Darmstadt, Germany
Human MPO ELISA	Biolegend, London, UK
Human PMN Elastase ELISA	eBioscience, Frankfurt am Main, Germany
Migratest™	Glycotope, Berlin, Germany
Mouse NK Cell Isolation Kit II	Miltenyi Biotec, Bergisch Gladbach, Germany
Phagotest™	Glycotope, Berlin, Germany
RNeasy® Mini Kit (QIAGEN, Germany)	QIAGEN, Hilden, Germany

3.1.6 Antibodies

Antibody	Host/isotype	Conjugate	Clone	Company	Dilution
anti-human					
CD16	mouse IgG1, k	Bio	MEM-154	Antikörper Online, Aachen, Germany	1:500
CD43	mouse IgG1, k	PE	1G10	BD Pharmingen™, Heidelberg, Germany	1:100
CD46	mouse IgG1, k	PE	8E2	eBioscience, San Diego, CA	1:500
CD55	mouse IgG1, k	PE	143-30	eBioscience, San Diego, CA	1:20
CD59	mouse IgG2a, k	PE	p282 (H19)	Biolegend, London, UK	1:10
CD62L	mouse IgG1, k	PE	DREG-56	eBioscience, San Diego, USA	1:100

Antibody	Host/isotype	Conjugate	Clone	Company	Dilution
anti-human					
CD63	mouse IgG1, k	PE	H5C6	BD Pharmingen™, Heidelberg, Germany	1:20
CXCR1	mouse IgG2b, k	PE	5A12	BD Pharmingen™, Heidelberg, Germany	1:20
fMLPR	mouse IgG1, k	PE	5F1	BD Pharmingen™, Heidelberg, Germany	1:5
TLR2	mouse IgG2a, k	PE	TL2.1	eBioscience, San Diego, USA	1:10
SA	mouse IgG2b, k	PacBlue	-	eBioscience, San Diego, USA	1:600
isotype controls:					
IgG1 K	mouse	PE	MOPC-21	BD Pharmingen™, Heidelberg, Germany	1:1 - 1:100
IgG2a K	mouse	PE	G155-178	BD Pharmingen™, Heidelberg, Germany	1:1
IgG2b K	mouse	PE	eBM2a	eBioscience, San Diego, USA	1:1 - 1:10
anti-mouse					
CD3	hamster IgG_2, k	PacBlue	500A2	BD Pharmingen™, Heidelberg, Germany	1:500
CD4	rat IgG2a, k	Per CP	RM4-5	BD Pharmingen™, Heidelberg, Germany	1:100
CD8	rat IgG2a, k	PE	53-6.7	BD Pharmingen™, Heidelberg, Germany	1:100
CD11b	rat IgG2b, k	PE	M1/70	BD Pharmingen™, Heidelberg, Germany	1:600
CD27	hamster IgG	PE Cy7	LG.7F9	eBioscience, San Diego, USA	1:50
CD45	rat IgG2b, k	FITC	30-F11	eBioscience, San Diego, USA	1:20
CD45.1	mouse IgG2a, k	PerCP Cy5.5	A20	eBioscience, San Diego, USA	1:10
CD45.2	rat IgG2b, k	APC Cy7	104	Biolegend, San Diego, USA	1:10
CX3CR1	polyclonal goat IgG	FITC	polyclonal	R&D Systems, Minneapolis, USA	1:20
CX3CR1	mouse IgG2a, k	PerCP Cy5	SA011F11	Biolegend, San Diego, USA	1:50
GFP	rat IgG2a, k	Biotin	5F12.4	eBioscience, San Diego, USA	1:50
NK1.1	mouse IgG2a, k	APC	PK136	Miltenyi Biotec, Bergisch Gladbach, Germany	1:50
SA	-	PE Cy5	-	BD Pharmingen™, Heidelberg, Germany	1:50

3.1.7 Primers

Name	Primer	Sequence 5' → 3'
mouse-18S	Forward	TTC GAA CGT CTG CCC TAT CAA
	Reverse	TCC CCG TCA CCC ATG GT
	Probe	CGA TGG TAG TCG CCG TGC CTA CCA
mouse-IL10	Forward	TCG GCC AGA GCC ACA TG
	Reverse	AGG TAA AAC TGG ATC ATT TCC GAT A
mouse-IL10	Probe	TGC AGG ACT TTA AGG GTT ACT TGG GTT GC
mouse-IL13	Forward	AGC CTG TGG CCT GGT CC
	Reverse	TCA AGA AGA AAT GTG CTC AAG CTG
	Probe	CAC AGG GCA ACT GAG GCA GGC A
mouse-GM-CSF	Forward	GCC ATC AAA GAA GCC CTG AA
	Reverse	GCG GGT CTG CAC ACA TGT TA
	Probe	ACA TGC CTG TCA CAT TGA ATG AAG AAG TAG AAG
mouse-IFN-γ	Forward	CAG CAA CAG CAA GGC GAA A
	Reverse	CTG GAC CTG TGG GTT GTT GAC
	Probe	AGG ATG CAT TCA TGA GTA TTG CCA AGT TTG A
mouse-TNF-α	Forward	CCA AAT GGC CTC CCT CTC AT
	Reverse	TCC TCC ACT TGG TGG TTT GC

Name	Primer	Sequence 5' → 3'
mouse-TNF-α	Probe*	CTC ACA CTC AGA TCA T

All probes were bought from Eurofins MWG GmbH, Germany.

*Probe for m-TNF-α is labelled with minor groove binder (MGB); all other probes are 6-carboxyfluorescein (FAM)- and tetramethylrhodamine (TAMRA) labelled.

3.1.8 Software programs

Software	Company
BD FACSDIVA^{Tm}	BD Bioscience^{TM}, Heidelberg, Germany
EndNote X7	EndNote Inc., Thomson Reuters, New York, USA
FlowJo 7.5	FlowJo Enterprise, Ashland, USA
Microsoft Office 2013	Microsoft Corporation, Redmond, USA
Primer Express® 2.0	Applied Biosystems, New York, USA
Prism 5.01	GraphPad, San Diego, USA

3.2 Animals

WT C57BL/6 mice were received from the Research Institute for Experimental Medicine (FEM) of the Charite (Berlin, Germany). Breeding of homozygote and heterozygote CX3CR1 deficient (CX3CR1$^{GFP/GFP}$) mice was conducted at the FEM under specific pathogen-free conditions. All animal experiments were approved by the regional animal study committee of Berlin (LAGeSo) and performed in accordance to national guidelines.

3.3 Patients

Two independent cohorts of HC and patients were recruited at the Clinical and Experimental MS Research Center, Charité – University Medicine Berlin. The first cohort included 10 HC, 12 MS and 12 NMO patients. 12 HC, 10 MS as well as 10 NMO patients participated in the second cohort. All study participants signed a written informed consent and the study was approved by the local ethics committee. MS and NMO patients were all in a remission state and were neurologically stable for at least one month. NMO diagnosis followed the revised criteria for NMO in 2006 [58] and 2007 [168]. 17 out of the 22 NMO patients were seropositive for AQP4-IgG (Euroimmun, Lübeck, Germany). All MS patients

included were RRMS patients and diagnosis was performed according to the 2010 revised McDonald criteria [169]. The Kurtzke Expanded Disability Status Scale (EDSS) [170] was used to evaluate neurological disability. Untreated patients were treatment-free at least for three months prior to recruitment. 22 Gender-matched volunteers without acute/ chronic infections or autoimmune diseases were included as healthy controls (HC). Demographic and clinical characteristics of all study participants are listed in table 1.

Table 1. Patient demographic and clinical characteristics [171].

Group	N	Female:Male ratio	Mean age ± SD	Treatment (N)	N seropositive for AQP4	Median EDSS (score - range)
HC	22	18:4	39 ± 10.5	-	-	-
NMO	22	19:3	42 ± 12.5	Untreated (6)	6/6	3.7 (1 – 7.5)
				Azathioprin (7)	3/7	
				Rituximab (7)	7/7	
				(Methyl)Prednisolone (1)	1/1	
				Glatiramer acetate (1)	0/1	
MS	22	18:4	43 ± 12.1	Untreated (9)	-	2.6 (0 – 5.5)
				Beta-Interferon (4)		
				Fingolimod (2)		
				Boswellic acid (2)		
				Glatiramer acetate (1)		
				Diazoxide (2)		
				Dimethyl fumarate (2)		

3.4 Cell-biological methods

3.4.1 Isolation of immune cells

3.4.1.1 Isolation of lymphocytes from murine peripheral blood

Murine peripheral blood was collected in 2 ml Eppendorf tubes containing 0.5 ml of 2 mM EDTA. Erythrocytes were eliminated by adding 10 ml erythrocyte lysis buffer per 1 ml blood for 10 minutes (min) at room temperature (RT) and subsequent centrifugation for 5 min at 550 x g and RT. Thereafter, the cell pellet was washed once in 10 ml mouse wash medium and centrifuged for 5 min at 550 x g and RT. The supernatant was discarded and lymphocyte cells were resuspended in 2 ml mouse medium and kept at 4°C until use.

3.4.1.2 Isolation of lymphocytes from murine lymph nodes and spleen

Spleens and lymph nodes were mashed using 100 µm cell strainers placed onto 50 ml falcon tubes. After mashing, cell strainers were washed twice and cell suspensions were filled up to 50 ml, both with mouse wash medium. Subsequent to centrifugation (5 min, 550 x g, RT), cell pellets were resuspended and incubated in 10 ml erythrocyte lysis buffer plus 5 ml mouse medium for 10 min at RT. Falcon tubes were centrifuged (5 min at 550 x g, RT) and pellets were washed twice with 30 ml mouse wash medium (5 min at 550 x g, RT). Lymphocyte cell pellets were finally resuspended in 2 ml (lymph nodes) or 10 ml (spleen) mouse medium and kept at 4°C until use.

3.4.1.3 Isolation of lymphocytes from murine CNS

Mouse brain and spinal cord were mashed together in mouse medium using a 70 µm cell strainer placed into a 55 mm petri dish. The cell strainer was washed with mouse medium until the cell strainer cleaned up. The cell suspension was transferred into a 15 ml falcon tube and filled up to 15 ml with mouse medium. After centrifugation for 10 min at 400 x g and 4°C, the supernatant was aspirated und the pellet was vortexed before adding 6 ml of 37% Percoll solution (tempered to RT). The mixture was spun down (20 min at 2800 x g, RT) and the Percoll solution as well as myelin components were aspirated up to a left-over of 500 µl. 6 ml mouse wash medium were added and the cell suspension was centrifuged 10 min at 400 x g and 4°C. The washing step was repeated using 10 ml mouse wash medium. After centrifugation, the pellet was resuspended in 1 ml mouse medium and stored at 4°C until use.

3.4.2 Serum separation from venous human blood

After venipuncture, serum separator tubes were sit for 30 min at RT (until clot-formation) and subsequently centrifuged at 2000 revolutions per minute (rpm) for 10 min at RT. Serum phase was transferred into cryo-tubes and stored at -80°C until use.

3.4.3 Cell freezing and thawing

Always 1-5 x 10^6 cells were taken up in 0.5 ml freezing medium and mixed with 0.5 ml of freshly prepared 20% DMSO medium solution. The cell suspension was transferred into a cryo-tube and stored in a Mr. Frosty™ freezing container at -80°C overnight. The next day,

the sample was transferred into a liquid nitrogen tank. All working steps were performed on ice.

To defrost frozen cells, cryo-tubes were taken out from the liquid nitrogen storage and placed as fast as possible into a 37°C water bath. Cells were quickly thawed by gently swirling the vial in the 37°C water bath until there was just a small bit of ice left in the vial. Under the laminar flow hood, pre-warmed complete growth medium was added dropwise, the cell suspension was transferred into a 15 ml falcon tube, filled up to 15 ml with pre-warmed medium and centrifuged (on average 10 min at 300 x g, RT, depending on the actual cell type). The supernatant was discarded and the cell pellet was resuspended in an appropriate volume of complete growth medium (1-10 ml) for further cell culturing or functional assays.

3.4.4 Cell culture

All experiments involving cell culturing were performed under sterile conditions in a laminar flow hood. Cells were cultured in respective aseptic incubators with 37°C and 5% CO_2. Before use, dissection instruments were boiled for 5 min followed by a short flaming and sterilization with 70% EtOH. Single-use consumables and materials were sterilized with 70% EtOH. All materials and waste were autoclaved at 120°C and 1 bar after use.

3.4.4.1 Cell culturing of murine NK cells with PMA and ionomycin

NK cells were negatively selected from splenocytes of unmanipulated WT or CX3CR1$^{GFP/GFP}$ mice using the NK Isolation kit II according to the manufacturer's instructions (see 3.6.2.). Purity of NK cells was verified by flow cytometry (see 3.6.1.) and was consistently >85%. Thereafter, NK cells were diluted in mouse medium to a concentration of 2 x 10^6 cells/ ml and stimulated with 100 µg/ ml phorbol 12-myristate 13-acetate (PMA) and 1 µg/ ml ionomycin for 4h at 37°C. After stimulation, NK cells were washed twice with PBS (5 min, 550 x g, RT).

3.4.4.2 Cell culturing of murine YAC-1 lymphoma cells

Frozen murine YAC-1 lymphoma cells were defrosted as described in section 3.4.3. and long-term cultured in complete growth medium. Passages of the cells were performed twice per week diluting the cells 1:2 in fresh medium. Cells generally showed a viability of >80%.

3.4.5 Determination of cell numbers and viability

3.4.5.1 Detection of absolute cell numbers

Neutrophil cell counting was performed by Labor Berlin – Charité Vivantes GmbH.

Absolute numbers of NK cells were evaluated using TrueCount™ Tubes according to the manufacturer's instructions. Therefore, one unit beads was diluted in 1 ml fluorescence-activated cell sorting (FACS) buffer and 100 µl of this solution were added to each sample before measuring it at the flow cytometer. Absolute numbers were calculated according to the formula:

$$\frac{\text{counting beads (total)} * \text{NK cells (acquired)}}{\text{counting beads (acquired)}}$$

3.4.5.2 Trypan blue staining

To determine the number of cells in a suspension, a sample of cells was diluted 1:10 in trypan blue solution. 10 µl of the dilution was then transferred into a Neubauer counting chamber and cells in the 16 fields of one quadrant (n) were counted manually under a light microscope. Death cells were excluded by their blue coloration which they classically show through uptake of the trypan blue dye. The total number of cells in suspension was finally calculated by the following formula:

Total number of cells in suspension =

n x dilution (trypan blue) x volume of total cell suspension (ml) x 10^4 (Neubauer-factor)

3.4.6 NK cell cytotoxicity measurement: Calcein-acetyoxymethyl release assay

NK cell cytotoxicity was determined using the calcein-acetyoxymethyl release assay (in collaboration with Dr. Isabell Hamann, former PhD-student and postdoctoral researcher in the group of PD Dr. Carmen Infante Duarte). Therefore, NK effector cells were prepared as described in section 5.4.4.1. whereby PMA/ ionomycin stimulation was only applied for the positive control. YAC-1 target cells (see 3.4.4.2.) were harvested, washed 3 times with 10 ml PBS (5 min, 550 x g, RT) and incubated with 15 µM calcein-AM (30 min at 37°C). After 3 times washing with complete growth medium, cell were adjusted to 4 x 10^5 cells/ ml for the cytotoxicity assay. 100 µl of target cells and 100 µl of various effector cell dilutions were placed into a flat bottom 96-well microtiter plate (effector: target cell ratios ranging from 40:1 to 5:1) and incubated for 4 h at 37°C in 5% CO_2. 40 µl of each supernatant were harvested, diluted in 60 µl of complete medium and placed into a fresh flat-bottom plate. Samples were measured in quadruplicate using a Wallac Victor2 1420 Multilabel spectrofluorimeter (excitation filter: 485 nm; emission filter: 535 nm).

Specific lysis (percentage of calcein-AM release) was calculated according to the formula:

$$\text{Specific lysis} = \frac{(\text{test release} - \text{spontaneous release})}{(\text{maximum release} - \text{spontaneous release})} * 100$$

The spontaneous release corresponds to the calcein-AM released from target cells in complete medium alone. The maximum release conforms to calcein-AM released from target cells lysed in complete medium containing 1.8% Triton X-100.

3.4.7 Neutrophil functional assays

3.4.7.1 Oxidative burst assay

Whole blood samples (100 µl) were stimulated for 15 min at 37°C with and without 100 nM of the chemoattractant fMLP. Thereafter, 10 µM of cell-permeable fluorogenic dihydrorhodamine 123 (DHR 123) were added for 5 min at 37°C. Erythrocytes were lysed with BD lysing buffer (1 ml lysis buffer per 100 µl blood) for 10 min at RT and the oxidative burst capacity (OBC) was analyzed by flow cytometry subsequently. Granulocytes were gated as described in section 3.6.1. and FlowJo 7.5 was used to evaluate

the mean fluorescence of rhodamine 123 resulting from oxidation of DHR 123 by neutrophil-derived reactive oxygen species (ROS).

3.4.7.2 Migration assay

Neutrophil chemotactic function was quantified with Migratest™. Per individual tested, leukocyte-rich plasma from 2 ml heparinized whole blood was isolated by spontaneous sedimentation (40 min, RT) and 2 x 100 µl of this leukocyte-rich phase were then placed into cell culture inserts, preloaded in two wells of a 24-well dish. Chemotaxis was conducted for 30 min at 37°C towards a gradient of fMLP peptide in Migratest™ incubation buffer (5 µl of 10 µM fMLP per 1 ml buffer) in comparison to a control without fMLP gradient (Migratest™ incubation buffer only). Both supernatants and flow-throughs were collected and placed on ice. 20 µl counting beads and 20 µl DNA vitality staining dye were added for 10 min and samples were measured at the flow cytometer.

3.4.7.3 Phagocytosis assay

Neutrophil phagocytosis was assessed using the commercially available Phagotest™. In this assay, 100 µl heparinized whole blood were incubated with 20 µl opsonized FITC-labelled *E.coli*-bacteria for 10 min at 37°C, a negative control sample remained on ice. Phagocytosis was stopped by adding 100 µl ice-cold Phagotest™ quenching solution and samples were washed twice with 3 ml Phagotest™ wash solution for 5 min at 250 x g and 4°C. Thereafter, erythrocytes were lysed with 2 ml Phagotest™ lysing solution for 20 min at RT, centrifuged for 5 min at 250 x g and 4°C and washed again. 200 µl DNA vitality staining dye were added to each sample just prior to the analysis by flow cytometry.

3.5 Molecular-biological methods

Molecular-biological methods were performed in collaboration with Dr. Isabell Hamann, former PhD-student and postdoctoral researcher in the group of PD Dr. Carmen Infante Duarte.

3.5.1 Isolation of lymphocyte RNA and reverse transcription

Lymphocyte ribonucleic acid (RNA) was isolated using the RNeasy® Mini Kit or the E.Z.N.A.® Total RNA Kit 1. Total RNA was then reversely transcribed to complentary deoxyribonucleic acid (cDNA) with random hexamers using the TaqMan Reverse Transcription Reagents, according to the manufacturer's instructions.

Splenic lymphocytes were prepared as described in 5.4.1.2. excluding resuspension of the obtained cell pellet in mouse medium. Instead, cell pellet was resuspended in kit-provided lysis buffer for not only disrupting cell walls but further inactivating RNases. The cell suspension was thereafter homogenized manually by passing the lysate at least 5 times through a blunt 20-gauge (G) needle fitted to an RNase-free syringe. Next, 70% EtOH was added, mixed by pipetting and placed into a collection tube for centrifugation (15-60 sec, 10 000 rpm, RT) during which RNA was bound in the column. Flow-through was discarded and the column was washed 2-3 times with RNA washing buffer (15-60 sec, 10 000 rpm, RT). The column was transferred into a new 1.5 ml centrifuge tube and RNA was eluted by adding RNase-free water (centrifugation for 1 min at maximum speed, RT). RNA concentration and purity was measured in a NanoDrop spectrophotometer at 260 nm and 280 nm. Only RNA samples with a purity ratio 260/ 280nm between 1.8 and 2.0 were used for reverse transcription. RNA samples were kept on ice when used directly or were stored at -80° until use.

For the RNA quantification of target genes, quantitative real-time polymerase chain reaction (PCR) was performed. Therefore, RNA was reversely transcribed into complementary DNA (cDNA) first, using retrovirus-associated enzymes named reverse transcriptases. These enzymes use RNA templates and short random hexamer primers complementary to the 3' end of the RNA to direct the synthesis of first strand cDNA. All working steps were performed on ice. Tables 2 and 3 list pipetting schema and program for reverse transcription, respectively, using a thermocycler.

Table 2. Pipetting schema for reverse transcription.

Reagent	Volume (µl)
Buffer (10x)	2
$MgCl_2$ (25 mM)	4.4
dNTPs (10 mM)	4
Random Hexamer (50 µM)	1
RNase Inhibitor (20 U/µl)	0.4
Reverse Transcriptase (50 U/µl)	0,5
RNA	X
H_2O	ad 20

Table 3. Reverse transcription program.

	Temperature	Duration	Cycles
Annealing	25°C	10 min	1 x
Reverse Transcription	48°C	30 min	1 x
Enzyme activation	95°C	5 min	1 x
Cooling period	4°C	30 min	1 x

3.5.2 Quantitative real-time PCR

Quantitative real-time PCR allows the determination and quantification of the expression of a target gene. The method combines specific oligonucleotide probes, which hybridize to the target sequence, and the 5' exonuclease activity of the *Taq* DNA polymerase. This enzyme cleaves the oligonucleotide probes during the PCR process, thereby generating a detectable signal. Precisely, the oligonucleotide probes are labeled at their 5' end with the fluorescent reporter dye 6-carboxyfluorescein (FAM) and with the quencher tetramethylrhodamine (TAMRA) at their 3' end whereby detection of the probe's fluorescence is prevented by the close proximity of the reporter to the quencher. The 5' to 3' exonuclease activity of the *Taq* polymerase breaks down this proximity allowing unquenched emission of fluorescence being directly proportional to the amount of gene product in each single PCR cycle, and thus enabling the retroactive/ retrograde quantification of the initial target gene expression [172].

Quantitative real-time PCR was performed on an ABI Prism 7000 Sequence Detection System. Primers and probes are listed in section 3.1.7. 18S rRNA, used as the endogenous reference, was constantly expressed across all of the samples analysed, which were run in duplicates. Results obtained by real-time PCR were quantified using the comparative

threshold method ($\Delta\Delta C_t$) [173, 174] and target gene expression was normalized to the endogenous reference for each sample.

All working steps were performed on ice in 96-well microtiter plates. Pipetting layout and PCR cycle programm are listed in Table 4 and 5 below.

Table 4. Pipetting layout for quantitative real-time PCR.

Reagent	Volume (µl)
PCR-Mastermix (2x)	12.5
Forward-Primer (10 µM)	1
Reverse-Primer (10 µM)	1
Oligonucleotide probe (5 µM)	1
H_2O	4.5
cDNA	5
Total volume	25

Table 5. Quantitative real-time PCR cycle program.

	Temperature	Duration	Cycles
Activation of Uracil-DNA glycosylase	50°C	2 min	1 x
Activation of Taq-polymerase	95°C	10 min	1 x
Strand-denaturation	95°C	15 s	40 - 45 x
Primer annealing and elongation	60°C	1 min	

3.6 Immunological methods

3.6.1 Flow cytometry

Flow cytometry represents a biotechnological, laser-based method which allows the multiparametric analysis of cells and particles in solution. Hereby, physical, chemical and/ or biological characteristics of the target cells or particles such as morphology and size, DNA/ RNA content, intra-/ extracellular cytokines, proliferation, apoptosis etc. are determined by channeling the suspension though a micro-cuvette (flow cell) ensuring the screening of each single cell/ particle by a laser-filter-system (optic system). The resulting light signals, dependent on the cell/ particle's specific properties (size, granularity, internal complexity) or previous fluorescent labelling, are converted into electrical signals (optical-to-electronic coupling system), amplified and the cell/ particle's characteristics can be derived using respective software programs [175, 176].

For the analysis of extracellular surface markers by flow cytometry, 10^6 cells per staining (prepared as described in the sections 3.4.1-3) were centrifuged for 5 min at 550 x g and 4°C and the cell pellet was incubated subsequently for 15 min at 4°C with mouse Fc block (diluted 1:50 in FACS buffer) to block unspecific binding sites. Thereafter, primary fluorescent-labelled antibody (or a mixture of such primary antibodies) diluted in FACS buffer was directly added to the cells and incubated for 30 min at 4°C in the dark. Cells were washed with 1 ml FACS buffer (5 min at 550 x g, 4°C). In case that biotinylated primary antibodies were used, cells were incubated with a respective fluorescent-labelled secondary antibody diluted in FACS buffer for another 20 min at 4°C in the dark (all primary and secondary antibodies used are listed in section 3.1.6.). The washing step was repeated and after resuspension in 100-200 µl FACS buffer, cells were measured in the flow cytometer. If measurements were not instantly possible, cells were washed in 1 ml PBS and incubated in cell fixing solution (PBS + 2% PFA) for 20 min at RT. Cells were washed twice with PBS, resuspended in 100-200 µl FACS buffer and kept at 4°C in the dark until measurement.

Using BD FACS DIVA^{TM} for initial analysis directly at the flow cytometer and FlowJo 7.5 for detailed data analysis, lymphocytes were identified by their characteristic size and granularity in the sideward to forward scatter graph. NK cells were distinguished from other lymphocytes by their lack of CD3 and expression of NK1.1. NK cells were further sub-classified according to the expression of the maturation markers CD11b and CD27 in pre-mature ($CD11b^{-}CD27^{-}$), immature ($CD11b^{neg/low}CD27^{+}$), mature ($CD11b^{+}CD27^{+}$) and fully differentiated NK cells ($CD11b^{high}CD27^{-}$). Granulocytes were identified by their characteristic size and granularity in the sideward to forward scatter graph. Neutrophils were distinguished from eosinophils by their lower autofluorescence in the FITC- and PE-channel and by expression of CD16b. Median fluorescence intensity (MedFl) was determined to assess surface marker expression, and data were normalized using the formula:

$$\frac{\text{MedFl (Marker)} * 100}{\text{MedFl (respective isotype control)}}$$

3.6.2 Magnetic cell sorting (MACS) of murine NK cells

For NK cell isolation and purification from target organs, the NK Cell Isolation Kit II was used according to the manufacturer's instructions. In summary, the kit is based on magnetic cell sorting (MACS) negatively selecting NK cells from a cell suspension by depleting non-target cells which are labelled with a cocktail of biotin-conjugated monoclonal antibodies and anti-biotin monoclonal antibodies conjugated to magnetic micro-breads. Therefore, organ extracted cells were first resuspended in MACS buffer (40 µl buffer/ 10^7 cells) and incubated for 5 min at 4°C with a NK cell biotin-antibody cocktail (10 µl/ 10^7 cells). Cells were washed in 2 ml MACS buffer per 10^7 cells and centrifuged at 4°C and 300 x g for 10 min. 80 µl buffer per 10^7 cells and 20 µl anti-biotin micro-beads were added and incubated for another 10 min at 4°C. The cell suspension was subsequently applied onto a MACS column (at a max 2 x 10^9 cells per column) equilibrated beforehand with 3 ml MACS buffer and placed in the magnetic field of a respective MACS separator. The flow-through containing the enriched NK cells was collected and the column was washed with additional 3 ml of MACS buffer to collect remaining NK cells. A sample of 100 µl before and after MACS separation was saved to verify the NK cell purity by flow cytometry (see 3.6.1.).

3.6.3 Enzyme-linked immunosorbent assay (ELISA)

Concentrations of cytokines and soluble factors in human serum or cell culture medium were determined by enzyme-linked immunosorbent assay (ELISA). All ELISAs used were conventional sandwich-ELISAs and were commercially acquired. ELISAs were performed according to the specific manufacturer's instructions. Generally, 100-200 µl of the required standard and sample diluents were applied into the 96-well ELISA plate, already pre-coated with a target-specific capture antibody. The plate was covered with an adhesive film and incubated at RT for 1-2 h on a microplate shaker (200 rpm). After incubation, the adhesive film was removed and wells were washed with 200-400 µl kit-provided wash buffer (3-4 times). 100-200 µl substrate conjugate (corresponding to a target specific, enzyme-conjugated antibody) were added per well, the plate was covered with adhesive film and incubated for 1 h at RT and 200 rpm. Washing steps were repeated and 100-200 µl substrate solution (corresponding to a solution of a chromophore which becomes enzymatically converted into a colored product) were added in each well for 20-30 min at

RT and in the dark. Enzymatic reaction was stopped by adding 50 µl stop solution per well. ELISA plates were read at 450 nm in the Glomax Multi Detection plate reader.

3.6.4 Degranulation assay

Conventional sandwich ELISAs (section 3.6.3.) were performed to evaluate serum levels of neutrophil MPO and PMN elastase. Assays were conducted as indicated in the manufacturer's instructions, and ELISA plates were read at 450 nm in the Glomax Multi Detection plate reader. The expression of CD63 on the outer cell membrane due to azurophilic granules exocytosis [177] was analyzed by surface staining for flow cytometry (section 3.6.1.) using PE-conjugated human monoclonal anti-CD63 (listed in section 3.1.6.).

3.7 *In vivo* methods

3.7.1 Induction and assessment of an active experimental autoimmune encephalomyelitis (EAE)

To induce active EAE, C57/BL6 WT or CX3CR1$^{GFP/GFP}$ mice were immunized subcutaneously with 250 µg myelin oligodendrocyte glycoprotein peptide 35-55 (MOG_{35-55}) emulsified in complete Freund's adjuvant containing 800 µg *Mycobacterium tuberculosis* H37Ra. *Pertussis toxin* (PTX, 200 ng) was injected intraperitoneally the day of immunization and repeated 48 hours later. Mice were weighed and examined daily for EAE symptoms and scored as follows: 0, no signs of neurologic disease; 1, lack of tail tone; 2, abnormal gait, hind-limb weakness; 2.5, partial hind-limb paralysis; 3, complete hind-limb paralysis; 3.5, ascending paralysis; 4, tetraplegia; and 5, moribund or death. Mice were sacrificed when they reached a score of > 3.0. To determine the cumulative disease activity, the area under the curve (AUC) from the clinical score plot for each individual mouse was calculated using GraphPad Prism 5.01.

3.7.2 Transfer of NK cells prior to EAE induction

WT and CX3CR1$^{GFP/GFP}$ mice were killed by cervical dislocation to collect the spleens. Splenocytes were isolated as described in section 3.4.1.2. and purified NK cells were obtained using negative cell separation (MACS NK Cell Isolation Kit II, section 3.6.2.).

One day prior to EAE immunization, 0.5-1 x 10^6 WT or CX3CR1$^{GFP/GFP}$ NK cells or 200 µl PBS as control were injected intravenously into CX3CR1$^{GFP/GFP}$ recipient mice. Active EAE was induced as described above.

3.7.3 Mouse perfusion

Mice were lethally anaesthetized with a mixture of ketamine (415 mg/ kg) and xylazine (9.7 mg/ kg). As soon as reflexes between the toes were not present any longer, the peritoneum was opened and the aorta was cut above the diaphragm. Blood was collected in 2 ml tubes prepared with 0.5 ml 2 mM EDTA, inverted twice and kept at RT until use. The needle of a 25-G butterfly was adjusted on a 12-cc syringe that has been filled with PBS was carefully inserted into the left ventricle of the heart. Correct placement of the needle was confirmed by minimal resistance and dark red blood beginning to flow from the right atrium. The animal was then perfused with the entire 12 cc syringe of PBS (20 ml). Thereafter, organs of interest were taken out into 1.5 ml tubes prepared with 1 ml mouse wash medium and kept on ice until use.

3.8 Statistics

GraphPad Prism 5.01 was used for all statistical analyses.

Statistical analysis of animal experiments and resulting data

Two-tailed, non-parametric Mann-Whitney test was used for all two-group comparisons. EAE clinical scores were analysed using the non-parametric Mann-Whitney test for two-grop comparisons or the Kruskal-Wallis test (with Dunn's post-hoc test) for three-group comparisons. EAE onset curves were analysed using the log-rank (Mantel-Cox) test.

Statistical analysis of patient data

Non-parametric Kruskal-Wallis test (with the Dunn's post-hoc-test) was used for multiple-group comparisons. Since the multiple comparisons analysis of each cohort separately only revealed similar trends but did not achieve similar significant values – due to the limitations in sample size – the final analysis was performed in the combined cohort of 22

HC, 22 NMO and 22 MS patients. For correlation analyses the non-parametric Spearman test was applied.

For all statistical analyses, probability (p)-values < 0.05 were considered significant (* $p < 0.05$, ** $p < 0.01$, *** $p < 0.001$). Data and statistics includes in text passages are indicated as means ± SEM. Figures show bars or dots indicating mean ± SEM.

4. Results

4.1 NK cell mobilization and contribution of CX3CR1 to NK cell dynamics during EAE neuroinflammation

Data from our research group previously emphasized the role of NK cells in the pathogenesis of MS and further highlighted an involvement of the chemokine receptor CX3CR1 on NK cells in MS. Reduced expression of this receptor on circulating NK cells and a correlation between CX3CR1-positive NK cells and the patient's disease activity were found. Precisely, patients in stable, non-acute disease phase exhibited significantly low levels of $CX3CR1^+$ NK cells in contrast to patients suffering from acute relapses [6] whose frequencies resembled more to those in HC. Moreover, expression of CX3CR1 on NK cells in human could be related to the NK cell maturation status und therewith to NK cell cytotoxicity [138] which has been shown to be impaired in MS in numerous studies [2-5, 129]. In addition, EAE mouse data suggested that the recruitment of NK cells into the inflamed CNS depends on CX3CR1 [7]. However, the implication of NK cells and NK cell subtypes as well as the precise contribution of CX3CR1 on NK cells in MS/ EAE remain not fully understood and therefore have been further investigated in extended animal experiments in the present work.

4.1.1 Decline of NK cells in the periphery and migration into the CNS in WT EAE mice

To examine NK cell dynamics *in vivo* during neuroinflammation, NK cell frequencies were longitudinally monitored in peripheral blood of C57BL/6 WT mice during the course of EAE disease (Figure 7C). Here, frequencies of peripheral blood NK cells were found to decrease directly after the peak of disease (day 16) reaching a minimum 20 days after immunization [from 5.01 ± 1.43 % (day 0) to 2.67 ± 0.95% (day 20)].

This observation may point to a neuroinflammation-related mobilization of NK cells wherefore the distribution of NK cells in the CNS and the immune tissues spleen and lymph nodes was investigated next in non-immunized (n.i.) mice, at disease onset (day 10), and at time of the observed decrease of NK cells in blood (day 20) in C57BL/6 WT (Figure 7D). It could be observed that already at day 10 post immunization (p.i.), NK cells

infiltrated into the CNS [413.6 ± 83.8 cells (day 0) to 831.0 ± 302.5 cells (day 10)] and decreased in lymph nodes [7695.0 ± 827.3 cells/ million (Mio.) (day 0) to 5189.0 ± 469.1 cells/ Mio. (day 10)] and spleen [28820.0 ± 1731.0 cells/ Mio. (day 0) to 9385.0 ± 1173.0 cells/ Mio. (day 10)]. At day 20, increased numbers of NK cells were found in the CNS (701.9 ± 235.6 cells) associated with a significant decrease of the number of circulating NK cells in blood [11395.0 ± 2108.0 cells/ Mio. (day 0) to 2133.0 ± 826.3 cells/ Mio. (day 20)] and to a lower extend also in lymph nodes (4396.0 ± 275.4 cells/ Mio.).

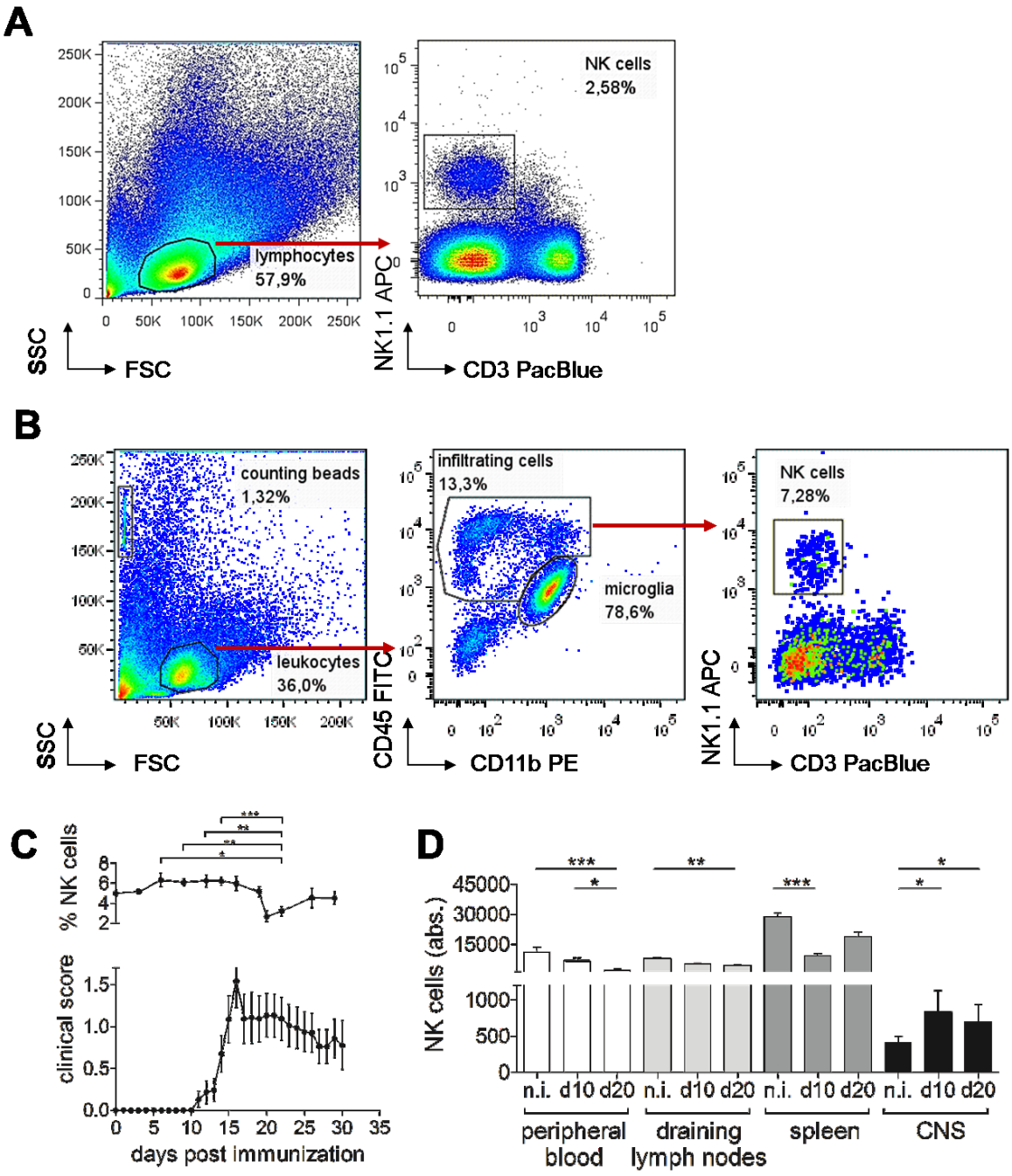

Figure 7. NK cell dynamics in WT EAE mice. C57/BL6 mice (n = 24) were immunized with MOG_{33-35} and scored daily. A) General gating strategy for the analysis of NK cells by flow cytometry in C) peripheral blood, lymph nodes, spleen and B) CNS by selecting the $CD3^{-}$ $NK1.1^{+}$ cells from the lymphocyte and infiltrating cell population, respectively. C) Peripheral blood was taken every other day to analyse NK cell frequencies by flow cytometry. Clinical EAE disease course (lower graph) and corresponding NK cell frequencies (upper graph) are shown. D) Transversal monitoring of absolute NK cell counts in peripheral blood, lymph nodes, spleen and CNS assessed by flow cytometry at day 0 [non-immunized (n.i.) mice, n = 10], day 10 (n = 5) and day 20 (n = 10) after MOG_{35-55} immunization. NK cell numbers in blood, lymph nodes and spleen are indicated as cells/ Mio., NK cell numbers in the CNS are indicated as absolute numbers. One-way ANOVA was used for statistical analyses. Data are presented as mean ± SEM. * $P < 0.05$, ** $p < 0.01$, *** $p < 0.001$. (Hertwig et al., Eur J Immunol, in revision)

4.1.2 Similar NK cell migration patterns in CX3CR1-deficient mice compared to WT mice during EAE

To assess the contribution of the chemokine receptor CX3CR1 to NK cell dynamics during neuroinflammation, EAE was induced in CX3CR1-deficient mice (precisely $CX3CR1^{GFP/GFP}$ mice) and NK cell migration patterns were monitored as described in 4.1.1. and figure 7. Huang et al. (2006) previously reported a more severe EAE course in CX3CR1-deficient animals, apparently associated with a diminished migration of NK cells into the inflamed CNS [7]. These observations could experimentally be confirmed (Figure 8).

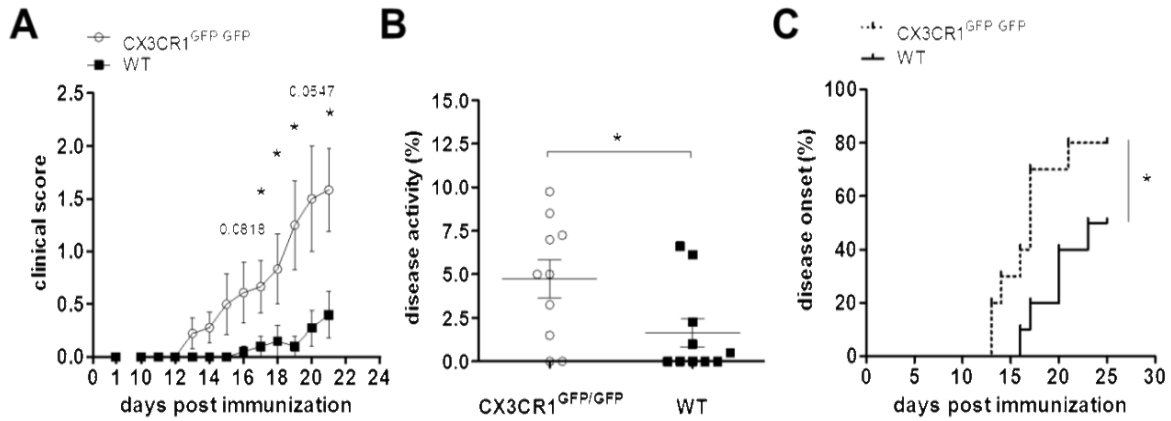

Figure 8: Comparison of the clinical parameters of CX3CR1-deficient and WT EAE mice. EAE was induced in CX3CR1-deficient ($CX3CR1^{GFP/GFP}$) and WT mice with MOG_{33-35} and mice were scored daily. A) Clinical EAE disease scores are shown as mean ± SEM. B) Disease activities with horizontal lines as mean ± SEM were evaluated by calculating the area under the curve (AUC) of the clinical disease course of each single mouse. C) EAE disease onset. * $P < 0.05$, ** $p < 0.01$, *** $p < 0.001$.

Although EAE disease was generally very mild in both mice types, CX3CR1-deficient mice were more susceptible to EAE than WT mice, showing a significant increase in the disease severity (Figure 8A), a higher disease activity (4.7 ± 1.1% in CX3CR1-deficient mice versus 1.7 ± 0.8% in WT mice) and earlier disease onset (Figure 8B and C). The clinical EAE data are summarized in Table 6.

Table 6. Clinical disease data of CX3CR1-deficient and WT EAE mice*.

Group	N	Incidence	Mean disease onset ± SD	Mean maximum clinical score ± SD
$CX3CR1^{GFP/GFP}$	10	8 / 10	16.0 ± 2.7	1.9 ± 0.6
WT	10	6 / 10	18.4 ± 2.6	1.4 ± 0.7

* Hertwig et al., Eur J Immunol, in revision

The analysis of NK cell numbers in blood, spleen, draining lymph nodes and the CNS at day 20 p.i. revealed an increase of the NK cell fraction in the CNS of CX3CR1-deficient mice from day 0 to day 20 p.i. (168.3 ± 35.2 cells to 773.5 ± 279.1 cells) (Figure 9A) as it has previously been observed in WT EAE mice (Figure 7C and D). However, no differences were observed in the peripheral blood. Additionally, NK cell numbers were diminished in the spleen at day 10 after immunization [24540.0 ± 407.3 cells/ Mio. (day 0) to 7496.0 ± 505.5 cells/ Mio. (day 10)], whereas an only low reduction was observed in the draining lymph nodes [3735.0 ± 633.4 cells/ Mio. (day 0) to 1905.0 ± 484.7 cells/ Mio. (day 20)] (Figure 9A).

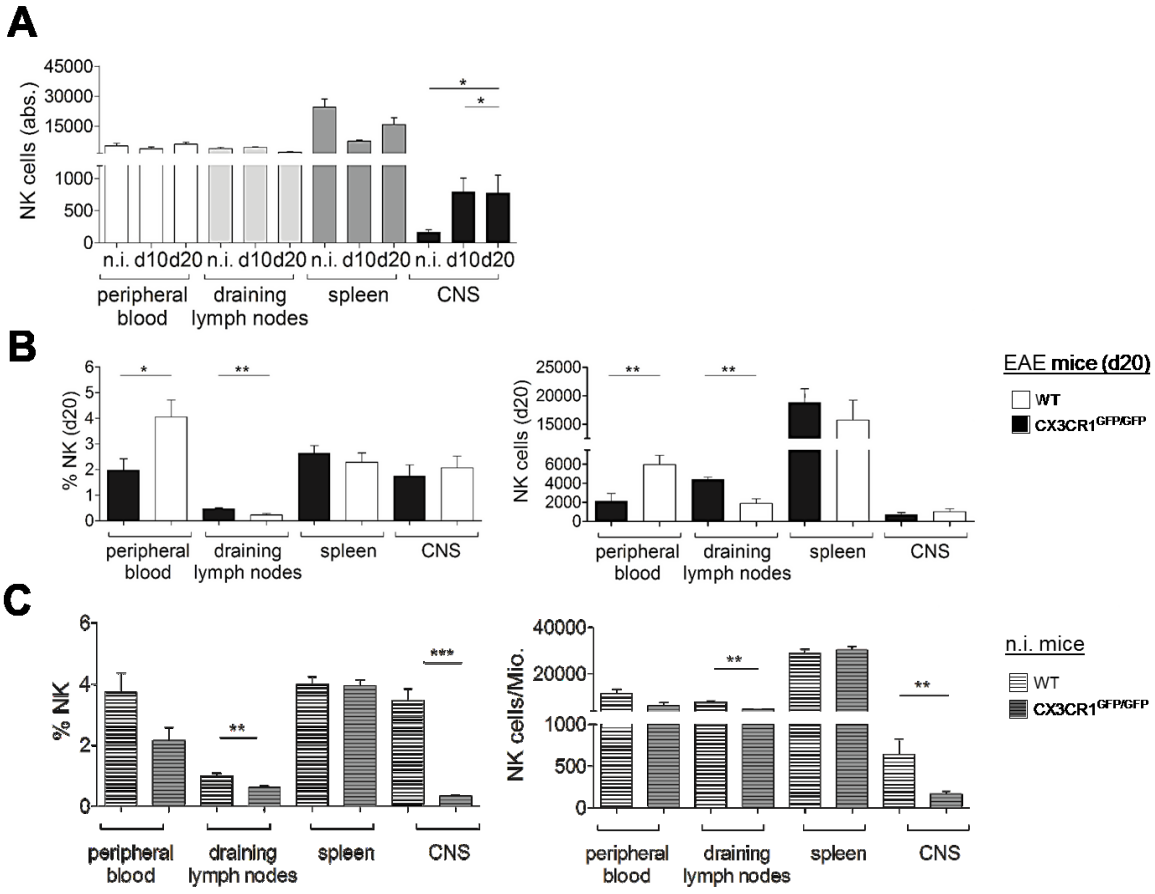

Figure 9. Tissue distribution of NK cells in healthy and EAE CX3CR1-deficient and WT mice. EAE was induced in WT and CX3CR1-deficient mice. A) CX3CR1$^{GFP/GFP}$ mice were sacrificed at day 0 (n.i., healthy controls; n = 10), day 10 (n = 5) and day 20 (established EAE, n = 10). Flow cytometry was performed to analyse NK cell numbers in blood, lymph nodes, spleen and the CNS. NK cell numbers in blood, lymph nodes and spleen are indicated as cells/ Mio., NK cell numbers in the CNS are indicated as absolute numbers. B) Absolute NK cell counts and frequencies from EAE WT (n = 10) and CX3CR1$^{GFP/GFP}$ (n = 8) mice were compared at day 20 p.i.. C) in n.i. healthy mice (WT: n = 10 and CX3CR1$^{GFP/GFP}$: n = 10). NK cell numbers and frequencies are shown as mean ± SEM. * P < 0.05, ** p < 0.01, *** p < 0.001. (Hertwig et al., Eur J Immunol, in revision)

Comparing the NK cell numbers and frequencies between WT and CX3CR1-deficient mice at day 20 p.i., no differences between both mice types were found in the spleen and CNS [Figure 9B, showing the NK cell frequencies (left) and absolute numbers (right)]. However, NK cell numbers and frequencies in blood were significantly higher in CX3CR1-deficient (4.1 ± 0.7% ~ 5985.0 ± 957.7 cells/ Mio.) compared to WT mice (1.9 ± 0.4% ~ 2133.0 ± 826.3 cells/ Mio.), but lower in the draining lymph nodes (0.2 ± 0.1% ~ 1905.0 ± 484.7 cells/ Mio. versus 0.5 ± 0.03% ~ 4396.0 ± 275.4 cells/ Mio., respectively) (Figure 9B). The latter observation was true for n.i. mice too (Figure 9C). In contrast to day 20 p.i., both frequency and absolute numbers of NK cells were extremely reduced in the CNS of n.i. CX3CR1-deficient mice (0.3 ± 0.03% ~ 168.3 ± 35.2 cells) compared to WT animals (3.7 ± 0.4% ~ 413.6 ± 83.8 cells) (Figure 9C). No significant differences in number or frequencies were detected in peripheral blood and spleen.

4.1.3 CX3CR1-deficient NK cells do not exhibit intrinsic deficits

Our group previously reported that human NK cell cytokine expression, activation status, maturation, cytotoxic activity, and proliferative responses [138] are influenced by the expression of CX3CR1. For this reason, the general cytotoxic activity and the cytokine profile from spleen-derived NK cells of unmanipulated WT and CX3CR1-deficient mice using calcein-acetyoxymethyl release assay and quantitative real-time PCR, respectively, were examined to exclude that CX3CR1-deficient NK cells may have intrinsic deficits in their functionality that could influence the experimental data. Here, the cytotoxicity assay revealed the same NK-cell-effector-/YAC-1-target-cell ratio-dependent lysis capacity of CX3CR1-deficient NK cells compared to WT NK cells (Figure 10A). As well, $CX3CR1^{+/+}$ and CX3CR1-deficient murine NK cells expressed similar levels of the effector cytokines IFN-gamma, GM-CSF, TNF-alpha, IL-10 and IL-13 (Figure 10B).

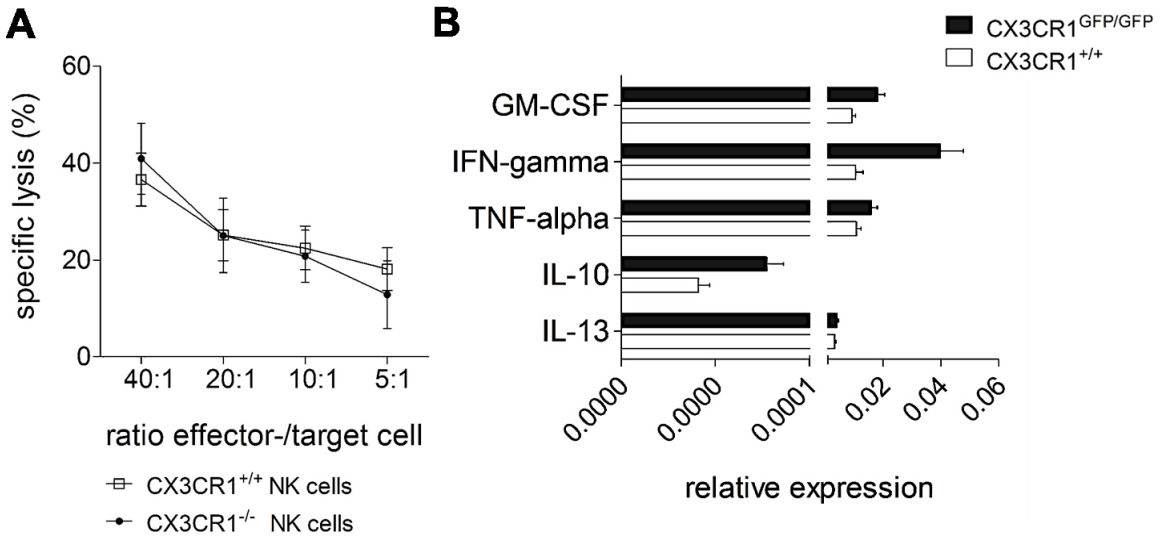

Figure 10. Functional properties of splenic WT and CX3CR1-deficient NK cells. WT and CX3CR1$^{GFP/GFP}$ NK cells were analysed for their cytotoxic activity and cytokine profiles. A) Cytotoxicity measurement of CX3CR1$^{+/+}$ (n = 5) compared to CX3CR1$^{GFP/GFP}$ (n = 7) NK cells at different effector (NK cells) to target (YAC-1 cells) cell ratios, using calcein-acetyoxymethyl release assay. B) Relative expression of pro- and anti-inflammatory cytokines in CX3CR1$^{+/+}$ (n = 10) and CX3CR1$^{GFP/GFP}$ (n = 10) NK cells assessed by quantitative real-time PCR. (Data were generated in collaboration with Dr. I. Hamann; Hertwig et al., Eur J Immunol, in revision).

In addition to the testing of funcionality, NK cell maturation phenotypes were compared by flow cytometry. The lack of CX3CR1 did not influenced the NK cell maturation according to the expression of the conventional maturation marker CD11b and CD27. All different CD3$^-$NK1.1$^+$ NK cell fractions of the i.e. immature (CD11b$^{neg/low}$ CD27$^+$), mature (CD11b$^+$ CD27$^+$) and terminal differentiated NK cells (CD11b^{high} CD27$^-$) (Figure 11, right panels) were present in peripheral blood (Figure 11A) and spleen (Figure 11B) of CX3CR1-deficient mice. Moreover, it could be observed that the fractions of fully differentiated cells were even larger in CX3CR1-deficient mice than in WT (36.7 ± 3.4% compared to 23.9 ± 3.5% cells in blood and 50.9 ± 2.3% compared to 34.7 ± 1.4% cells in spleen), while the fractions of immature and early mature cells were smaller (19.8 ± 2.4% compared to 29.1 ± 2.2% early mature cells in blood; 15.3 ± 1.0% compared to 24.8 ± 0.8% immature cells and 22.4 ± 1.8% compared to 32.4 ± 0.8% early mature cells in spleen).

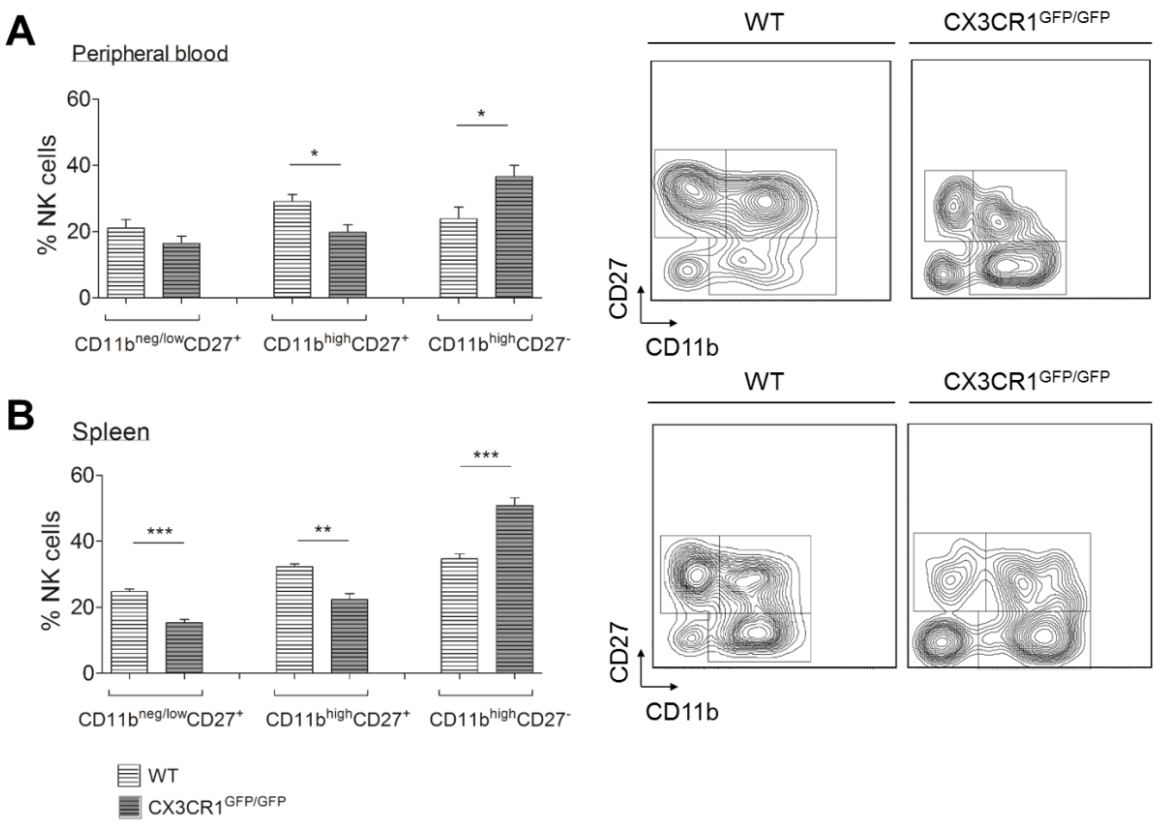

Figure 11. NK cell subsets in blood and spleen of n.i. WT and CX3CR1-deficient mice. NK cells subsets were defined according to the expression of CD27 and CD11b in immature $CD3^-$ $NK1.1^+$ $CD11b^{neg/low}$ $CD27^+$, mature NK cells as $CD3^-$ $NK1.1^+$ $CD11b^+$ $CD27^+$ and fully differentiated NK cells as $CD3^-$ $NK1.1^+$ $CD11b^{high}$ $CD27^-$. Frequencies of the different NK cell subsets are shown as mean ± SEM in A) peripheral blood and B) spleen of WT (n = 10) and CX3CR1-deficient (n = 10) mice. * $P < 0.05$, ** $p < 0.01$, *** $p < 0.001$. Representative flow cytometry contour plots illustrating the different NK cell subsets in WT and CX3CR1-deficient ($CX3CR1^{GFP/GFP}$) mice are shown alongside. (Hertwig et al., Eur J Immunol, in revision).

4.1.4 Impaired recruitment of mature NK cells into the inflamed CNS in CX3CR1-deficient EAE mice

Since CX3CR1 appeared to not be involved in the overall migration of NK cells in EAE, it was next investigated whether CX3CR1 may rather be involved in the recruitment of a particular NK cell subtype into the inflamed CNS, as has been postulated for human NK cells [137, 178].

In n.i. healthy WT animals, CX3CR1 was found to be predominantly expressed on pre-mature/ tolerant $CD11b^-CD27^-$ (NK cells with predominantly inhibitory signals) and fully differentiated mature $CD11b^+$ $CD27^-$ NK cells (Figure 12). Thus, it could be speculated that the lack of CX3CR1 may affect circulation of these distinct fractions during EAE.

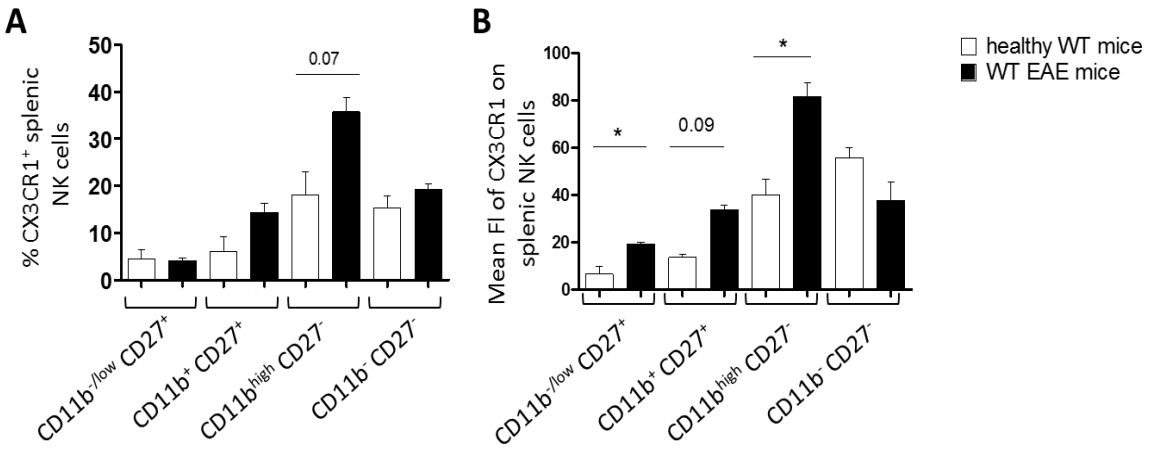

Figure 12. **CX3CR1 expression on splenic NK cells.** According to their maturational status, splenic NK cell subsets from healthy and immunized WT mice were analyzed for their expression of CX3CR1 (n = 10 and n = 5, respectively). Mean fluorescence intensities (right graph) and percentages of CX3CR1-positive cells (left graph) within the immature ($CD11b^{neg/low}$ $CD27^{+}$), mature ($CD11b^{+}$ $CD27^{+}$), terminally differentiated ($CD11b^{high}$ $CD27^{-}$) and pre-mature (tolerant, $CD11b^{-}$ $CD27^{-}$) NK cell populations are shown as bars ± SEM. * $P < 0.05$, ** $p < 0.01$, *** $p < 0.001$.

To verify this hypothesis, NK cells were isolated from peripheral blood, lymph nodes, spleen and the CNS of WT and CX3CR1 deficient mice with EAE at day 20 p.i. and analysed by flow cytometry to asses their maturation phenotype. The proportions of mature $CD11b^{high}$ $CD27^{+}$ and fully differentiated $CD11b^{high}$ $CD27^{-}$ NK cells were significantly reduced in the CNS of CX3CR1-deficient mice (14.2 ± 2.9% compared to 25.5 ± 2.9% mature cells and 9.7 ± 4.9% compared to 15.2 ± 3.7% fully differentiated cells), but increased in spleen when compared to WT mice (54.5 ± 2.5% compared to 43.1 ± 4.5% fully differentiated cells) (Figure 13A). These shifts in the mature versus immature NK cell fractions observed under CX3CR1-deficiency in spleen and CNS were also reflected in a diminished (spleen) and elevated (CNS) immature to mature NK cell ratio compared to WT animals (1.1 ± 0.2 compared to 2.3 ± 0.5 in spleen and 5.1 ± 0.9 compared to 2.5 ± 0.4 in the CNS) (Figure 13B, right graph). In comparison, immature to mature NK cell ratios were not significantly different between healthy n.i. WT and CX3CR1-deficient mice (Figure 13B, left graph).

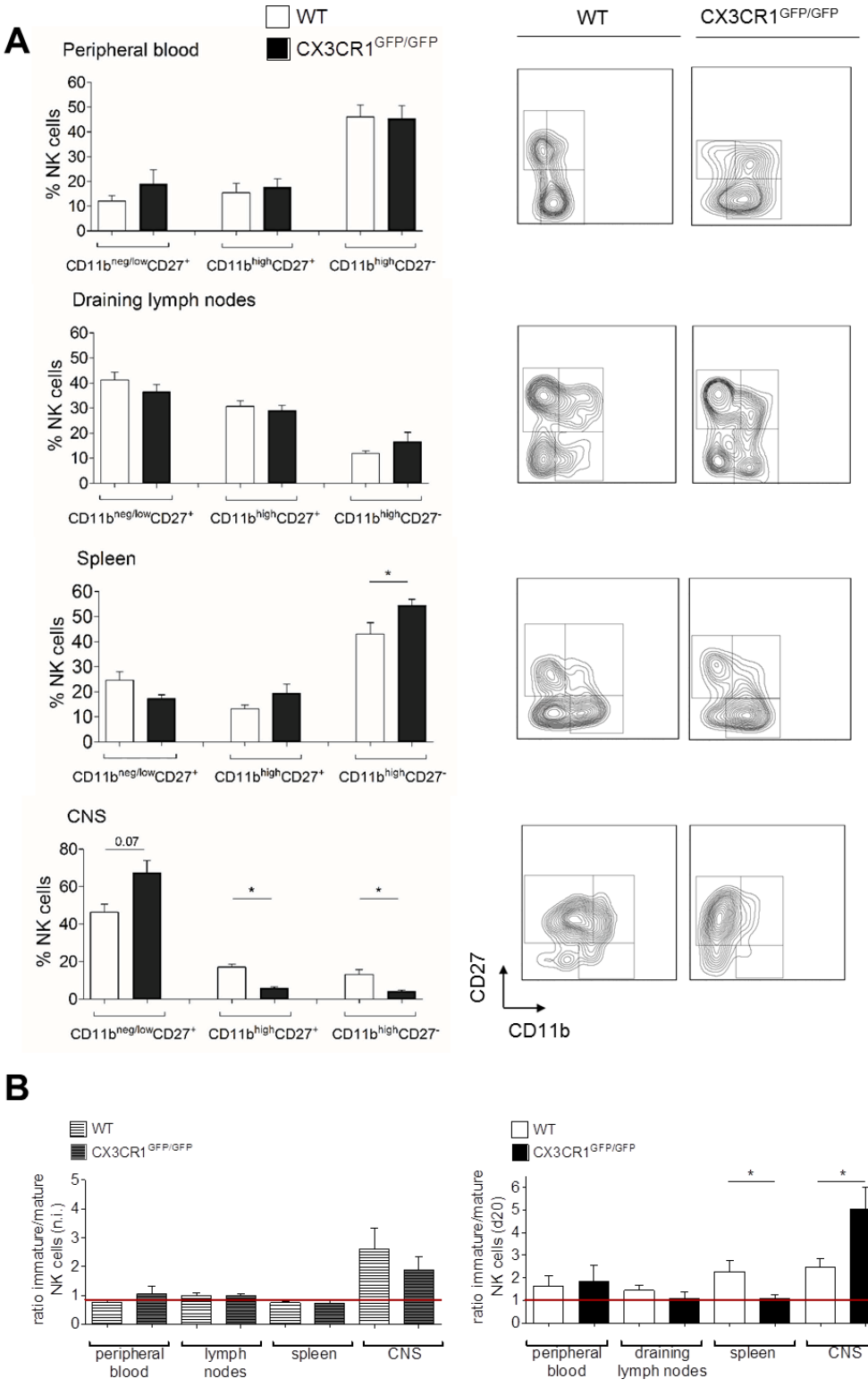

Figure 13. Proportioned distribution of NK cell subsets in WT and CX3CR1-deficient EAE mice. According to their maturation status, NK cell subsets were analysed by flow cytometry in MOG_{33-35} immunized WT and CX3CR1-deficient mice at day 20 (n = 10 and n = 8, respectively, per group) p.i. in A) peripheral blood, the draining lymph nodes, the spleen and the CNS. Representative contour plots are shown right beside. B) Ratios of immature to mature NK cells from n.i. mice (left graph) and mice at d20 after immunization (right graph) are shown. Graphs show mean ± SEM. * $P < 0.05$, ** $p < 0.01$, *** $p < 0.001$. (Hertwig et al., Eur J Immunol, in revision).

Due to these observations, the expression of another chemokine receptor – CCR7 – that could facilitate the migration of immature NK cells into the inflamed brain was aimed to be investigated. Contrary to CX3CR1 expression in circulating NK cells, CCR7 was found to be expressed primarily on the immature CD11b$^{neg/low}$ CD27^{+} fraction (Figure 14). However, CCR7 expression analysis on NK cells from WT and CX3CR1-deficient EAE mice did not revealed evaluable data so far.

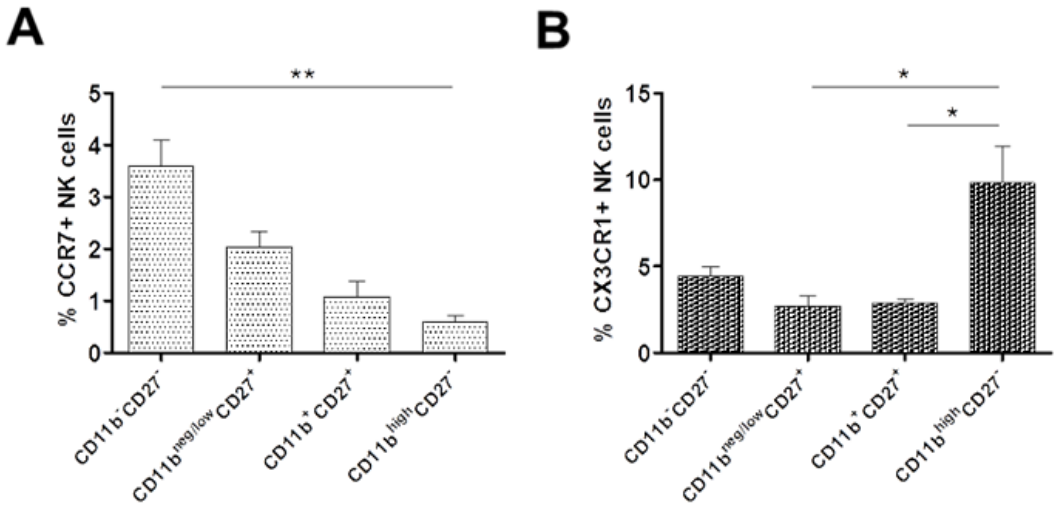

Figure 14. Chemokine receptor expressions on blood-derived NK cells. NK cells were isolated from peripheral blood of healthy WT mice (n = 5) and A) CCR7 and B) CX3CR1 expression on the NK cell subsets according to the maturation marker CD11b and CD27 were analyzed by flow cytometry. Data are shown as bars representing means ± SEM. * $P < 0.05$, ** $p < 0.01$, *** $p < 0.001$.

4.1.5 Disease-ameliorating effects of mature WT NK cells transferred prior to EAE induction into CX3CR1-deficient mice

As described above, it could be observed that the frequency of mature NK cells migrating into the CNS during EAE was reduced in CX3CR1-deficient mice compared to WT mice, although the total amounts of NK cells in the CNS were comparable (Figure 9B and 13A). Therewith associated deficient NK cell activity inside the CNS may contribute to the increased EAE severity observed in CX3CR1 deficient mice. To investigate whether mature spleen-derived NK cells from WT mice may restrict EAE development, splenic NK cells from WT and CX3CR1-deficient mice (or PBS as control) were transferred into CX3CR1-deficient recipient mice one day prior EAE induction.

Table 7. Clinical EAE disease parameter of CX3CR1-deficient mice transferred with NK cells or control PBS injection prior immunization.*

Genotype of transferred NK cells	N	Incidence	Mean disease onset ± SD	Mean maximum clinical score ± SD
$CX3CR1^{GFP/GFP}$	24	17 / 24	13.7 ± 1.6	1.7 ± 1.4
$CX3CR1^{+/+}$	24	15 / 24	13.9 ± 1.9	1.2 ± 1.3
PBS	24	21 / 24	11.6 ± 1.7	2.3 ± 1.1

* Hertwig et al., Eur J Immunol, in revision

In these experiments it could be observed that transfer of WT NK cells reduced EAE incidence (Table 7), ameliorated clinical severity (Figure 15A) and cumulative disease activity (12.9 ± 3.1% in CX3CR1-deficient mice receiving WT NK cells compared to 23.8 ± 2.9% in control mice) (Figure 15B), and delayed disease onset (Figure 15C and Table 7). Mice transferred with NK cells from CX3CR1-deficient donors also appeared to benefit from the transfer, although the effects were not statistically significant.

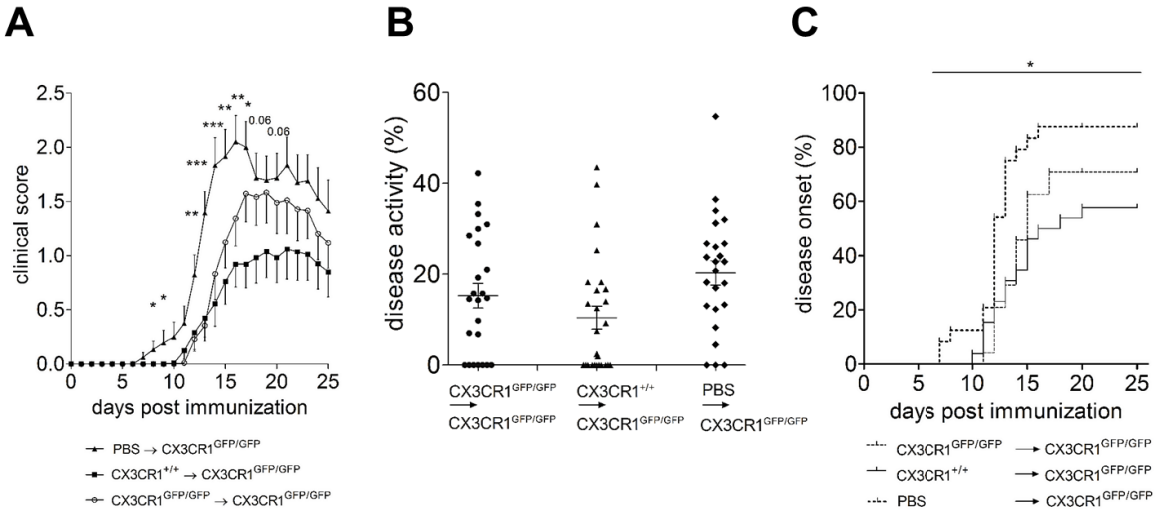

Figure 15. NK cell transfer into CX3CR1-deficient recipients prior to EAE induction. NK cells, isolated from WT and CX3CR1-deficient ($CX3CR1^{GFP/GFP}$) mice or PBS as control, were transferred intravenously into $CX3CR1^{GFP/GFP}$ mice one day before EAE induction. A) Daily clinical scores with mean ± SEM. B) Cumulative disease activity including mean values (horizontal bars) ± SEM. C) Percentual representation of disease onsets. * $P < 0.05$, ** $p < 0.01$, *** $p < 0.001$ (Hertwig et al., Eur J Immunol, in revision).

In six of the mice receiving WT $CX3CR1^{+/+}$ NK cells, it was next examined whether this single NK cell injection prior to immunization might affect NK cell distribution inside the CNS compared to the PBS control mice. Frequencies and absolute numbers of CNS NK cells were assessed at day 20 p.i., and the maturation phenotype was defined by the expression of CD27 and CD11b as described above. In mice receiving a transfer of WT-

NK cells an increased number of NK cells in the spleen and CNS (11714.0 ± 2271.0 cells/ Mio. compared to 9016.0 ± 1329.0 cells/ Mio. in spleen; 727.0 ± 134.2 cells/ Mio. compared to 300.6 ± 121.1 cells/ Mio. in the CNS) (Figure 16A), an enhanced proportion of early mature $CD11b^{+}$ $CD27^{+}$ NK cells inside the CNS (35.5 ± 10.4% compared to 20.2 ± 4.8%) (Figure 16B) and an overall smaller immature to mature NK cell ratio in this organ (2.0 ± 1.1 compared to 3.5 ± 1.1) (Figure 16C) could be detected.

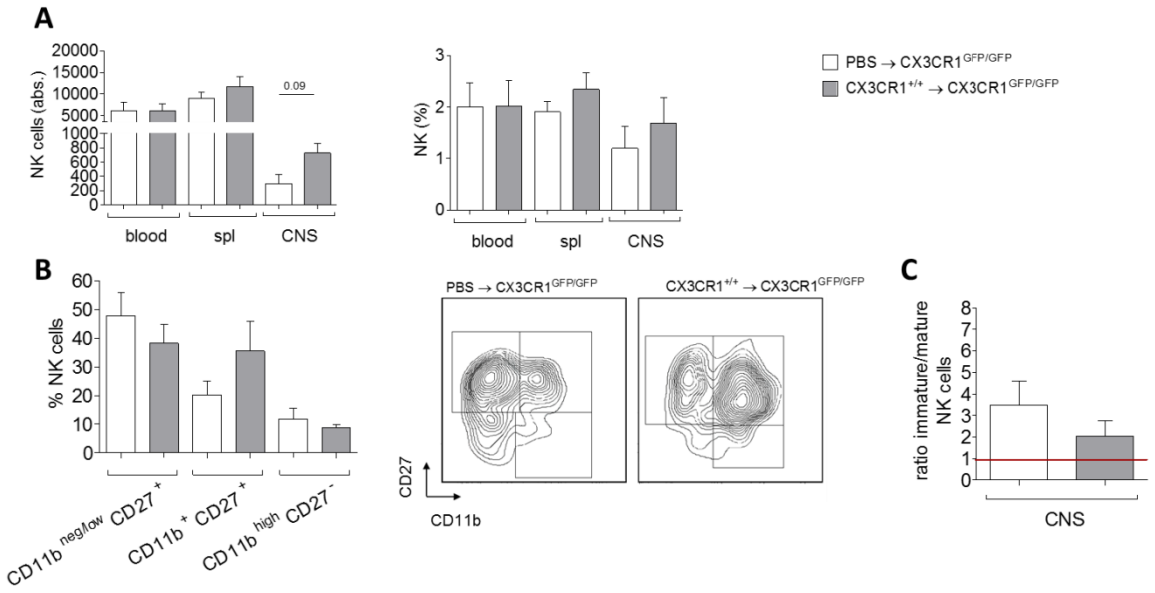

Figure 16. Effects of splenic $CX3CR1^{+/+}$ NK cells after transfer into CX3CR1-deficient recipients prior to EAE induction. To quantify and investigate the phenotype of NK cells in transferred EAE mice, a group of PBS-injected controls (n = 6) and WT (n = 6) NK cell transferred mice were sacrificed at day 20 p.i. A) Absolute numbers of NK cells (left graph) and NK cell frequencies (right graph) were determined in peripheral blood, spleen (spl) and the CNS. B) Frequencies of the different NK cell maturation subsets in the CNS of animals injected with PBS or WT NK cells prior immunization, and representative contour plots. D) Ratios of immature to mature NK cells in the CNS. * $P < 0.05$, ** $p < 0.01$, *** $p < 0.001$ (Hertwig et al., Eur J Immunol, in revision).

Frequencies and numbers of CD4 or CD8 T cells in peripheral blood, lymph nodes, spleen and the CNS remained unaltered in mice injected with WT NK cells with respect to the control mice injected with PBS (Figure 17).

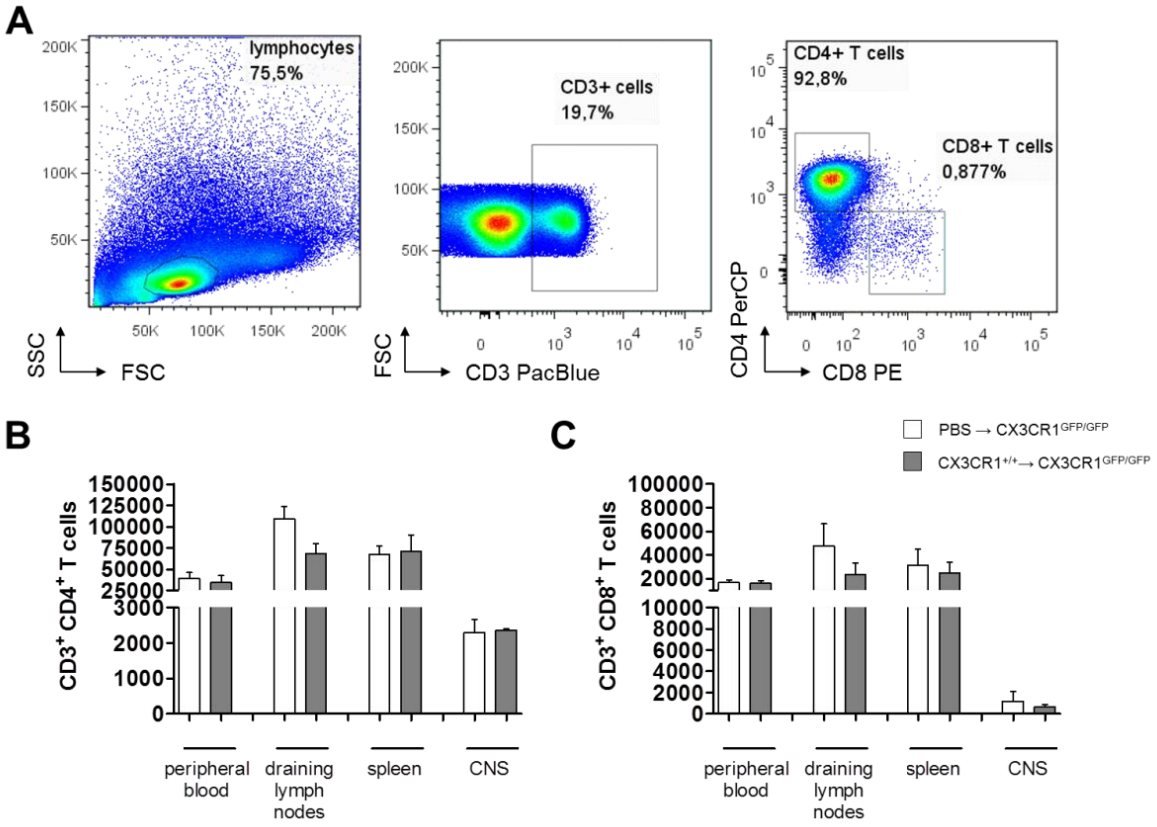

Figure 17: Distribution of T cells in NK cell transferred EAE mice. CX3CR1-deficient mice received a single injection of WT NK cells (n = 6) or PBS (n = 6) prior to immunization with MOG_{33-35}. At day 20 p.i., numbers of T cells were investigated by flow cytometry in various organs. A) Gating strategy for T cells (exemplarly shown for lymph node-derived T cells in n.i. mice). Numbers of B) $CD3^+$ $CD4^+$ and C) $CD3^+$ $CD8^+$ T cells in peripheral blood, lymph nodes, spleen and the CNS. Data are shown as bars indicating mean values ± SEM.

In parallel, peripheral blood, splenic and CNS NK cells of all three recipient groups were stained for GFP to differentiate between the $CX3CR1^{GFP/GFP}$ NK cells of the CX3CR1-deficient recipient mice and the transferred WT NK cells and therewith to investigate the exact migration pattern of the transferred NK cells and whether EAE disease amelioration of the $CX3CR1^{+/+} \rightarrow CX3CR1^{GFP/GFP}$ group (Figure 15) really was due to the migration of the transferred mature WT NK cells into the inflamed CNS.

Indeed, a higher proportion of GFP-negative NK cells could be detected in the CNS of mice receiving WT NK cells prior to immunization compared to the PBS control group and mice receiving CX3CR1-deficient NK cells (1384.0 ± 590.1 cells compared to 687.9 ± 309.7 and 318.7 ± 143.4 cells, respectively) (Figure 18). In contrast, no major differences could be observed in peripheral blood and spleen between the groups. Furthermore, the increased fraction of GFP-negative NK cells in the CNS of WT NK cell-

recipients displayed an highly mature phenotype consisting of CD11b^{high} CD27^{+} NK cells (57.1 ± 3.1% fully mature cells compared to 19.3 ± 5.4% in the control group and 21.9 ± 5.4% in the group receiving CX3CR1-deficient NK cells) (Figure 18).

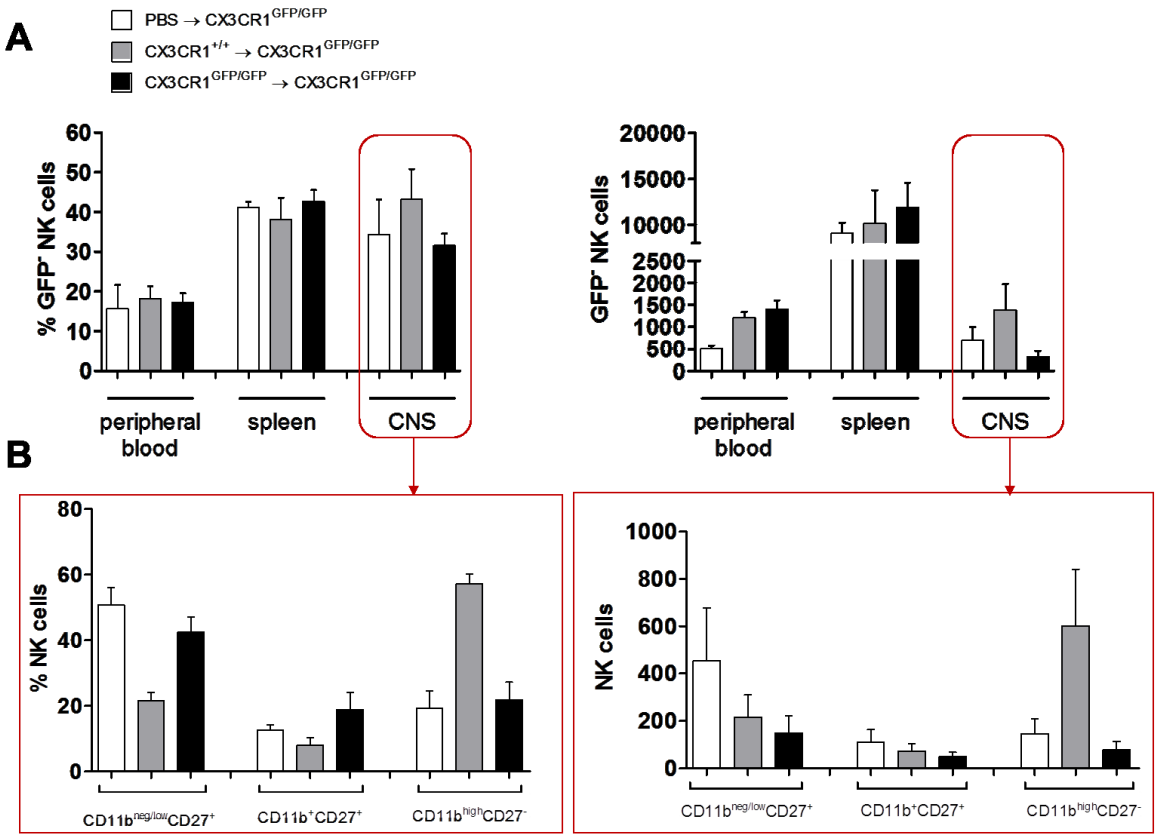

Figure 18. Tracking of NK cells 20 days after transfer into recipient mice. CX3CR1-deficient mice received a single injection of WT NK cells (n = 6), CX3CR1$^{GFP/GFP}$ NK cells (n = 6) or PBS (n = 6) one day prior to EAE immunization. When mice were sacrified 20 days p.i., tracking of the transferred NK cells was performed by GFP-staining for flow cytometry. A) Frequencies (left graph) and absolute numbers (right graph) of GFP-negative NK cells in peripheral blood, spleen and the CNS. B) Analysis of the GFP-negative NK cells in the CNS according to the maturation markers CD11b and CD27. Frequency-values are shown in the left graph, absolute numbers in the right graph. All data are shown as bars indicating mean values ± SEM.

Data from other markers for tracking the transferred NK cells (anti-CD45.1 in combination with anti-CD45.2 antibody, or anti-CX3CR1 antibody) were worked out to not be convenient or reliable.

4.2 Neutrophil characteristics in MS and NMO patients compared to healthy individuals

Although neutrophils represent a major feature of NMO lesions, and moreover are increased in patient's CSF during acute relapses [12-15], the implication of these cells in the pathogenesis of NMO is still unclear. Therefore, a basic phenotypic and functional examination of NMO neutrophils has been performed. Additionally, the same analyses were performed simultaneously on MS patients to evaluate putative differences in this cell type between the two diseases that could potentially be applied as diagnostic marker for discrimination.

To note, two independent cohorts of patients and HC were recruited for this study (see section 5.3.). After investigating the phenotypic and functional neutrophil characteristics in the first cohort, assays in which no differences between the groups were detected, were excluded in the following analysis of the second cohort. On this account, n-numbers vary between the performed assays.

4.2.1 Similar absolute numbers of peripheral blood neutrophils in MS, NMO and HC

Absolute numbers of circulating neutrophils were determined and compared in peripheral blood of MS, NMO and HC. Total counts lay within the reference range of 1.8 to 7.7 neutrophils per nanoliter (nl) without significant differences between the groups (Figure 19A). As well, concentrations of serum G-CSF as major regulator of neutrophil proliferation, maturation and survival [142] did not differ between HC, NMO and MS (Figure 19B).

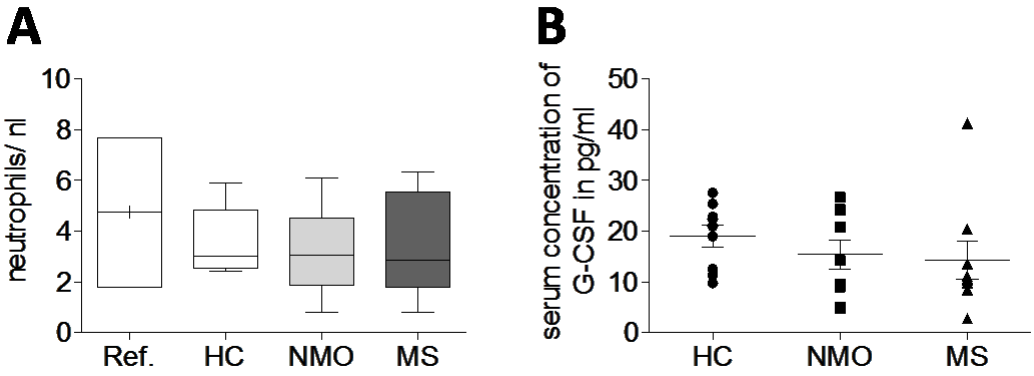

Figure 19. Neutrophil counts and G-CSF regulator concentrations. A) EDTA whole blood samples were analyzed for neutrophil absolute numbers in HC, NMO and MS (n = 9-11 in all groups). Results are shown as Tukey box and whiskers diagrams (mean ± SEM). B) Serum concentrations of the neutrophil regulator glycoprotein G-CSF in HC, NMO and MS are shown as aligned dot plots. Horizontal lines indicate means ± SEM.

4.2.2 Comparable expression of complement regulator proteins on neutrophils in MS, NMO and HC

Apart from granulocyte accumulations, complement deposits represent another major component of NMO lesions. Neutrophils possess the ability to directly activate the complement system, which itself can act as positive feedback for amplification of neutrophil activation. In peripheral blood, the activation of the complement system is kept under the control of several fluid phase and cell membrane regulators [179].

Therefore, the surface expression of the complement regulators CD46, CD55 and CD59 on neutrophils was monitored in HC, NMO and MS (Figure 20) by flow cytometry. No differences in the surface expression of these membrane regulators between the three groups were detected (Figure 20C).

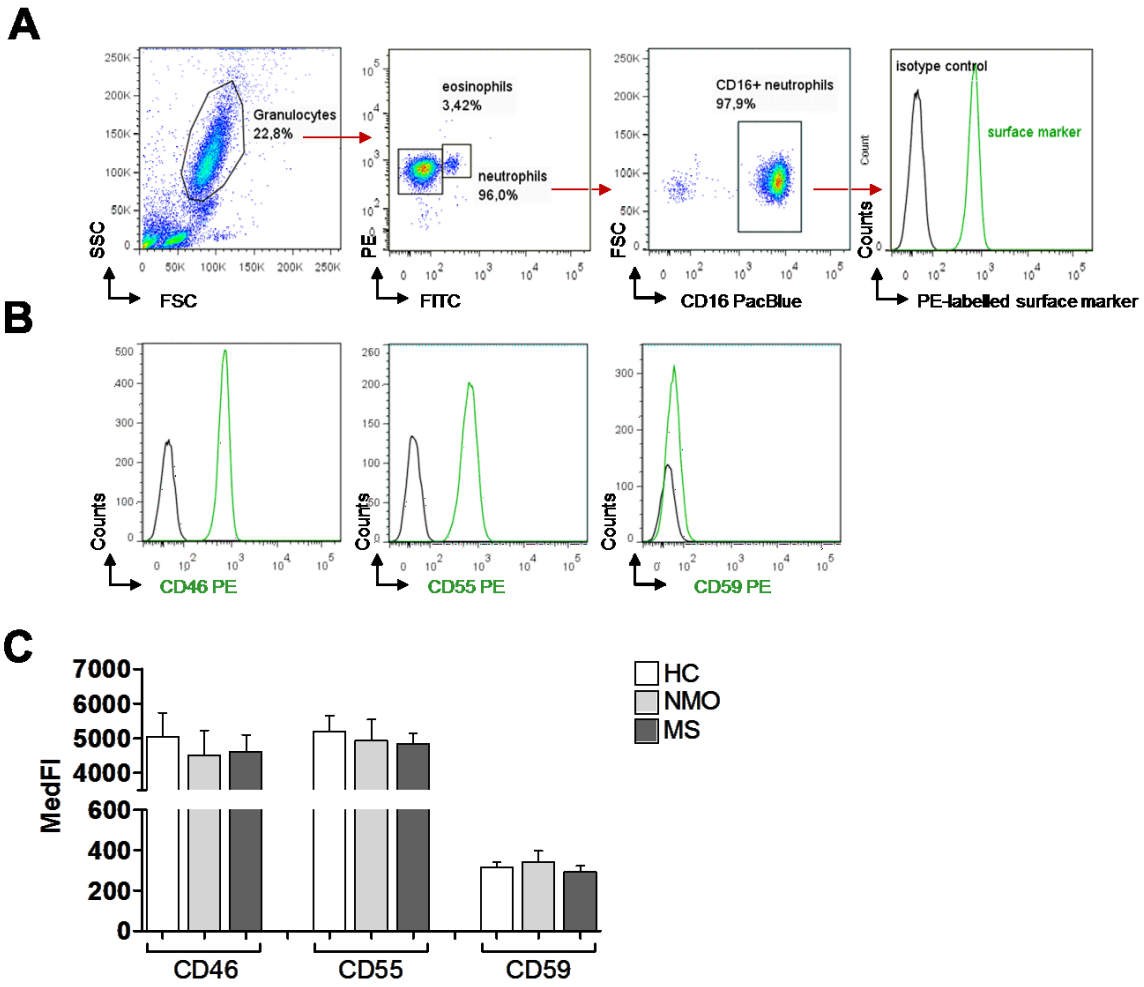

Figure 20. Expression of neutrophil complement regulator proteins. A) For all analyses of surface marker expression, granulocytes were identified by their characteristic size and granularity in the sideward to forward scatter graph. Neutrophils were distinguished from eosinophils by their lower autofluorescence in the FITC- and PE-channel and their expression of CD16b. Neutrophil PE median fluorescence (MedFl) was evaluated to assess expression of the respective surface marker and normalized to its isotype control value calculating MedFl (Marker) x 100 / MedFl (respective isotype control). B) Representative histograms for the complement regulators CD46, CD55 and CD59. C) Distinct surface expression of CD46, CD55 and CD59 in HC, NMO and MS patients (n = 9-11 in all groups). Mean values of each group are represented by bars ± SEM and Dunn's multiple comparison post-hoc-test p-values < 0.05 are considered significant ($p < 0.05$, ** $p < 0.01$, *** $p < 0.001$).

4.2.3 Activated neutrophil phenotype in MS and NMO patients

Priming of resting neutrophils in circulation takes place as soon as the cells encounter pathogenic stimuli. The latter trigger the up-regulation of surface receptors involved in neutrophil recruitment to sites of infection and inflammation, such as fMLPR, TLR2 and CXCR1.

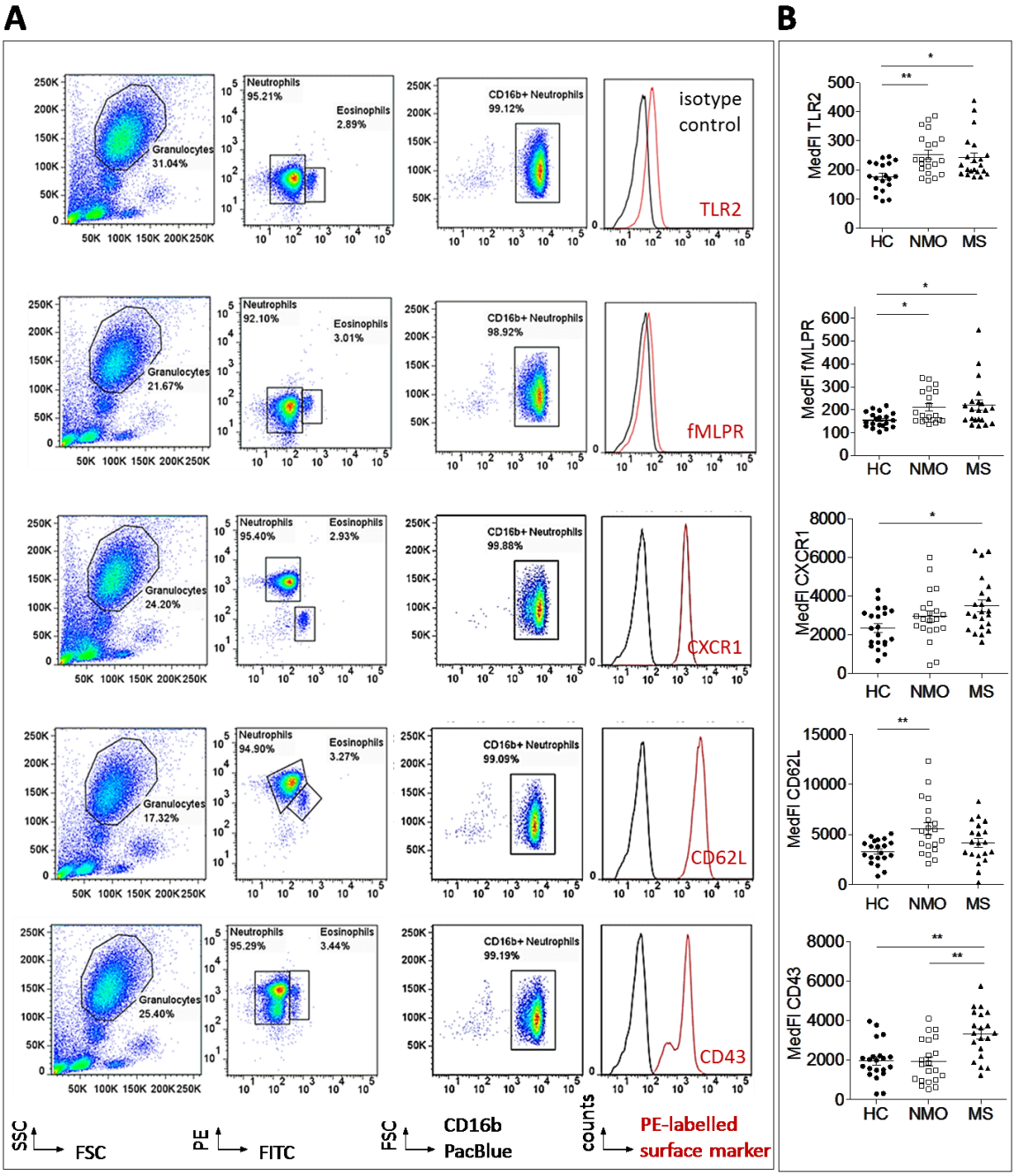

Figure 21. Expression of neutrophil marker for activation, immune response, chemotaxis and migration [171]. Analyses of surface marker expression were performed as described before. A) Representative dot plots and histograms for TLR2, fMLPR, as indicators for a response to pathogenic and bacterial agents, respectively, the chemokine receptor CXCR1 and the adhesion molecules CD62L and CD43 (from top to bottom). B) Distinct surface expression of TLR2, fMLPR, CXCR1, CD62L, CD43 (from top to bottom) in HC, NMO and MS patients. Mean values of each group are represented by horizontal bars ± SEM and Dunn's multiple comparison post-hoc-test p-values < 0.05 are considered significant ($p < 0.05$, ** $p < 0.01$, *** $p < 0.001$).

Expression analysis of these surface markers (Figure 21) by flow cytometry revealed a significant upregulation of TLR2 and fMLPR mean median fluorescence (MedFl) on

neutrophils in NMO (253.3 ± 15.3 and 210.8 ± 15.7 MedFl, respectively) and MS (242.2 ± 16.5 and 220.1 ± 22.5 MedFl, respectively) as compared to HC (176.7 ± 11.3 and 155.0 ± 7.3 MedFl, respectively) (Figure 21B).

The mean expression of the chemokine receptor CXCR1 was increased only in MS (3490.0 ± 297.2 MedFl) as compared to HC (2348.0 ± 221.2 MedFl) (Figure 21B). In this line, serum concentrations of IL-8, the ligand of CXCR1, showed a trend towards higher concentrations in MS compared to HC (Figure 22).

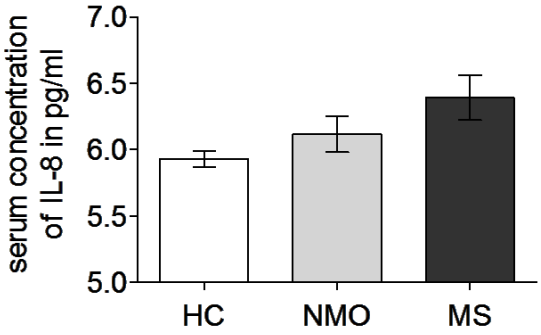

Figure 22. IL-8 serum concentration. Conventional ELISA was used to analyze IL-8 serum concentrations in HC, NMO and MS. Means values are shown as bars ± SEM.

4.2.4 Reduced neutrophil adhesion and migratory capacity in NMO compared to MS patients

In order to access sites of infection or inflammation, neutrophils undergo a selectin-mediated process called extravasation which includes the cell's adhesion, rolling, and transmigration through a respective endothelium [139]. To investigate the neutrophil extravasatory capacity in NMO and MS, the surface expression of CD62L (L-selectin) and CD43 (E-selectin ligand), which are both involved in leukocyte primary and firm adhesion to endothelium (Figure 21), was analyzed next by flow cytometry. Here, it could be observed that the mean expression of the homing receptor CD62L was significantly increased in NMO (5580.0 ± 607.1 MedFl) but not MS (4173.0 ± 452.1 MedFl) as compared to HC (3315.0 ± 265.6 MedFl). In contrast, the adhesion molecule CD43 was down-regulated in NMO (1936.0 ± 240.0 MedFl) when compared to MS (3331.0 ± 271.8 MedFl), but not when related to HC (1968.0 ± 211.3 MedFl) (Figure 21B).

In the last step of extravasation, neutrophils transmigrate through the endothelium and access the site of infection and inflammation, where they deploy their antimicrobial arsenal. To evaluate neutrophil transmigration in NMO, MS and HC, their migratory capacity towards a concentration gradient of the chemoattractant fMLP was assessed using the commercially available Migratest™ (Figure 23).

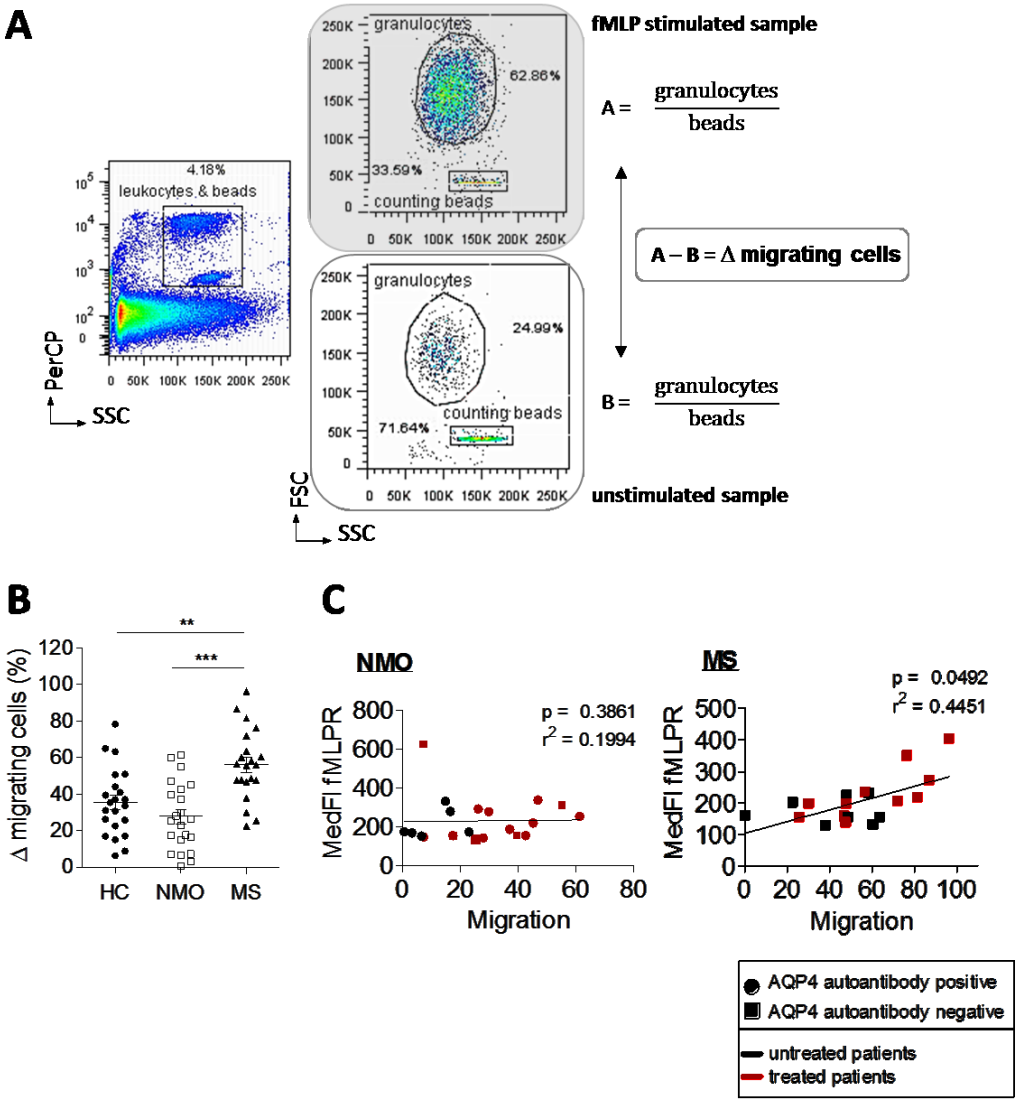

Figure 23. Neutrophil mirgation in response to fMLP [171]. A) Using Migratest™, the neutrophil migration capacity towards a concentration gradient of fMLP was evaluated. Granulocytes and counting beads were identified in the PerCP to SSC scatter, excluded from dead and other cells and depicted in the FSC to SSC scatter. The difference between migrated granulocytes with and without fMLP stimulation was calculated to assess the migratory capacity. B) Differences (Δ) in the mean migratory capacity of blood neutrophils stimulated with fMLP or left untreated in HC, NMO and MS patients. Mean values of each group are represented by horizontal bars ± SEM and Dunn's multiple comparison post-hoc-test p-values < 0.05 are considered significant ($p < 0.05$, ** $p < 0.01$, *** $p < 0.001$). C) Correlation between the neutrophil surface expression of fMLPR and their migratory capacity is shown. The non-parametric Spearman correlation test was used to calculate statistical significance. P-values < 0.05 are considered significant and r^2 indicates linear regression.

Here, NMO neutrophils displayed a trend towards decreased mean migratory capacity in response to fMLP (27.8 ± 3.9%) when compared to HC (35.3 ± 3.9%) and a diminished migration compared to MS (56.1 ± 4.2%) (Figure 23B). Contradictorily, NMO and MS neutrophils express comparable levels of fMLPR, which in both groups of patients was increased compared to HC (Figure 21B). This discrepancy was also reflected in the lack of correlation observed between migratory capacity and the expression of fMLPR in NMO. On the contrary, a positive correlation between the receptor and migration toward the ligand was detected in MS (Figure 23C).

4.2.5 Decreased production of ROS by NMO neutrophils compared to MS neutrophils

Reactive oxygen species (ROS) represent a major weapon of the neutrophil antimicrobial activity and are produced upon neutrophil activation in a reaction cascade initiated by the NADPH oxidase complex [139]. On this account, the capacity of NMO, MS and HC neutrophils to produce ROS upon stimulation with fMLP was investigated (Figure 24).

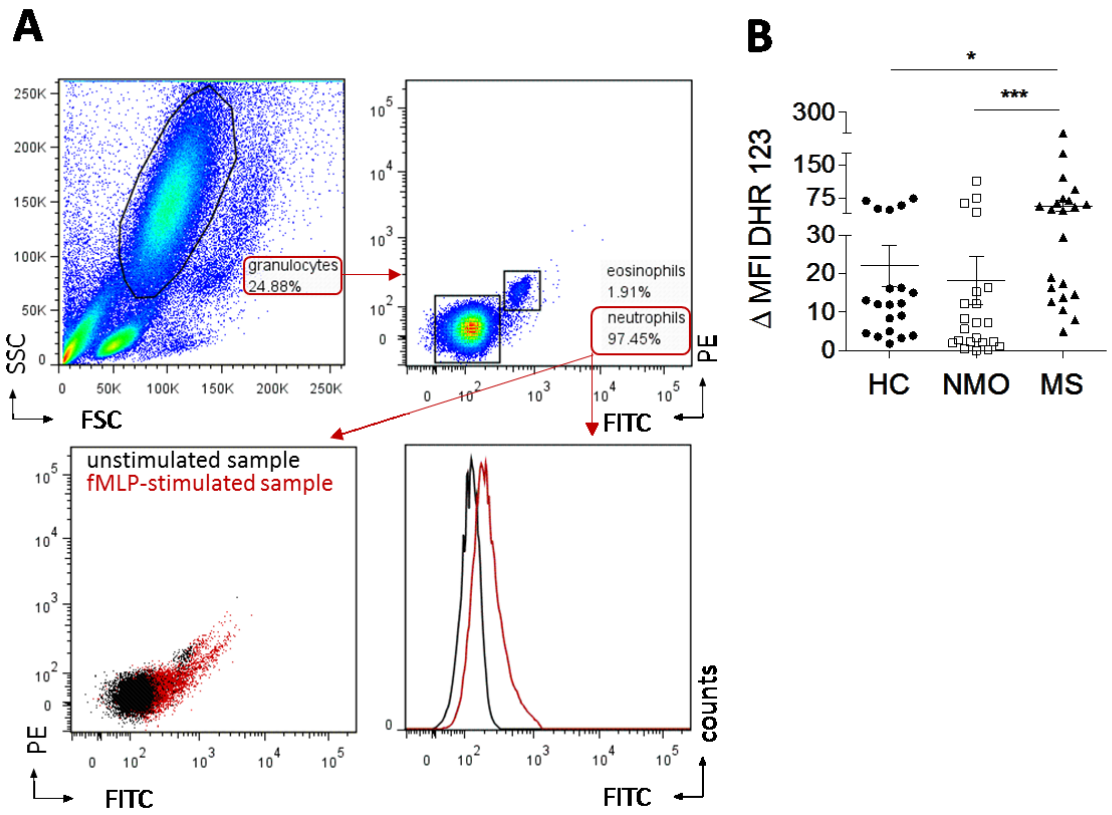

Abbildung 24: Neutrophil oxidative burst capacity [171]. A) The oxidative burst capacity of blood-derived neutrophils was evaluated by determining the difference in mean fluorescence intensity (MFI) of oxidized dihydrorhodamine 123 between fMLP-stimulated and unstimulated neutrophils. Neutrophils were identified as described before. B) Differences (Δ) in the MFI of the cell-permeable dye DHR 123 oxidized to rhodamine 123 by peripheral blood neutrophils in dependence of fMLP stimulation in HC, NMO and MS patients. Mean values of each group are represented by horizontal bars ± SEM and p-values < 0.05 are considered significant ($p < 0.05$, ** $p < 0.01$, *** $p < 0.001$).

In line with the data on migratory capacity, a trend towards decreased mean respiratory burst, i.e. mean fluorescent intensity (MFI) of DHR 123 oxidized by neutrophils, in response to the chemoattractant fMLP was observed in NMO neutrophils (18.9 ± 6.3 MFI) when compared to HC (21.9 ± 5.3 MFI), and a significant reduction when compared to MS (57.4 ± 12.7 MFI). As well, MS neutrophils displayed an enhanced respiratory burst compared to HC (Figure 24B), confirming a previous report by Naegele et al. (2012) [158].

4.2.6 Comparable neutrophil phagocytosis but decreased degranulation in NMO compared to MS patients

Apart from the production of ROS, phagocytosis and degranulation are additional crucial processes in the neutrophil spectrum of efficacy.

Data from Phagotest™ analysis to determine the mean percentage of phagocytic granulocytes and the number of ingested bacteria per granulocyte did not show differences between HC, NMO and MS (Figure 25B and C).

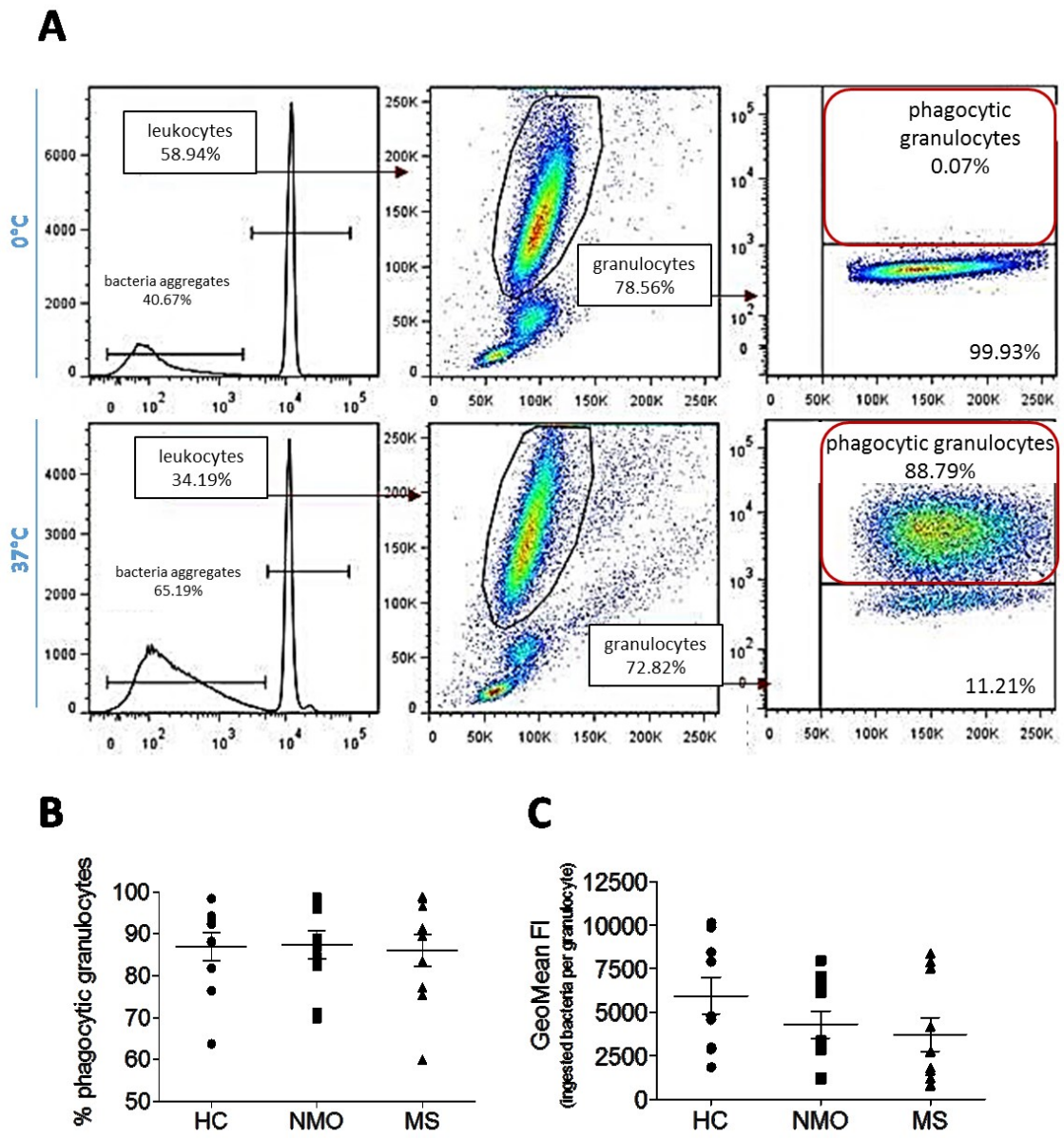

Figure 25. Neutrophil phagocytic capacity [171]. Using Phagotest™, the phagocytic capacity of peripheral blood neutrophils was determined in HC, NMO and MS patients evaluating the difference of phagocytized FITC-labelled, opsonized *E.coli*-bacteria at 0°C or 37°C. A) As indicated in the Phagotest™ manufacturer's instructions, bacteria aggregates were excluded from the leukocyte population in the PE-histogram and granulocytes were identified through their specific size and granularity in the SSC to FSC plot. The fraction of neutrophil phagocytized bacteria was thereafter depicted in the FITC to SSC plot. B) Difference (Δ) in the percentage of neutrophils phagocytizing FITC-labelled *E.coli*-bacteria at 0°C and 37°C in HC, NMO and MS patients. C) FITC Geometric Mean Fluorescence (GeoMean Fl) representing the number of ingested bacteria per granulocyte in HC, NMO and MS. Mean values of each group are represented by horizontal bars ± SEM and p-values < 0.05 are considered significant ($p < 0.05$, ** $p < 0.01$, *** $p < 0.001$).

In contrast, the flow cytometric assessment of the mean expression of the surface marker CD63 – due to exocytosis of azurophilic granules –, and ELISA determination of MPO serum concentrations revealed a significant decrease of these two degranulation markers in NMO (195.5 ± 10.9 MedFl and 10.6 ± 1.2 ng/ ml, respectively) compared to MS (284.8 ± 27.5 MedFl and 16.8 ± 1.2 ng/ ml, respectively) (Figure 26B and C). CD63 expression on NMO neutrophils and MPO levels in NMO serum were comparable to the values in HC (186.7 ± 11.1 MedFl and 8.7 ± 0.5 ng/ ml, respectively) (Figure 26B and C). Serum levels on the neutrophil polymorphonucler (PMN) elastase only showed trends toward higher concentrations in MS patients compared to NMO and were not different in NMO and MS as compared to HC (Figure 26D).

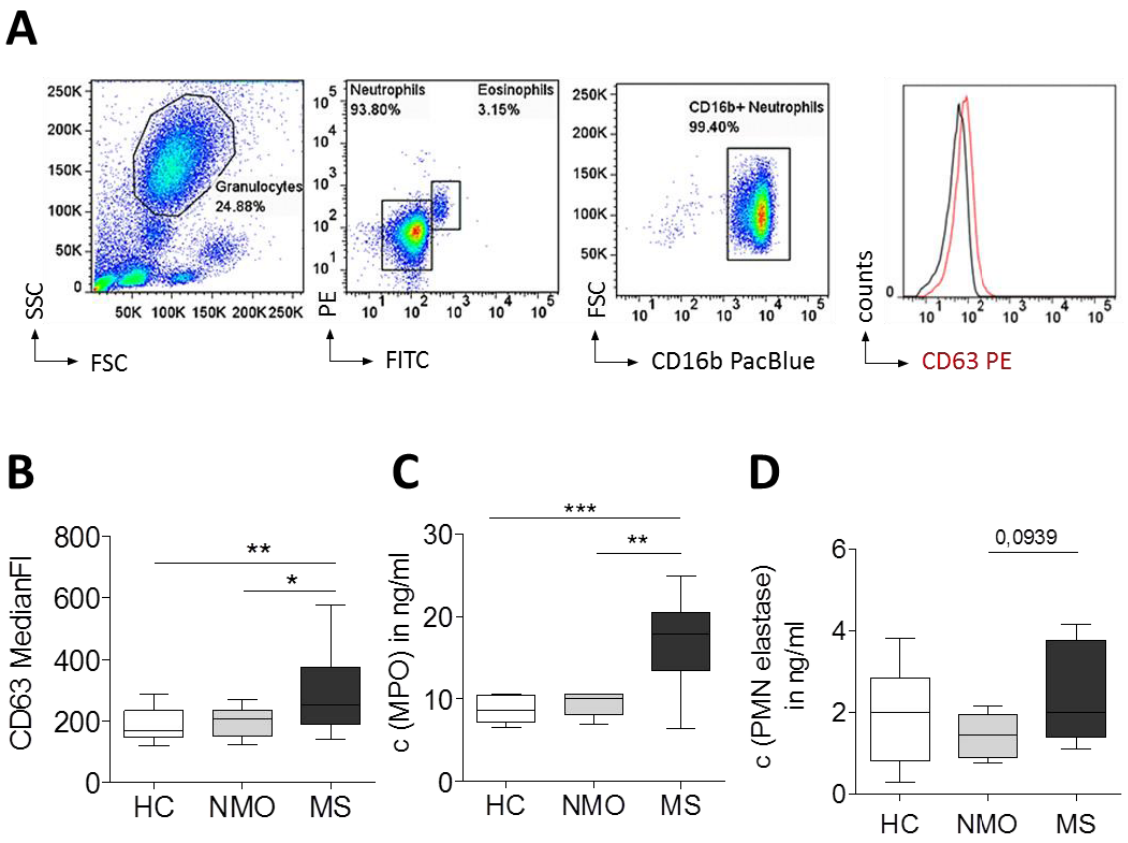

Figure 26. Neutrophil degranulation [171]. To compare neutrophil degranulation between HC, NMO and MS patients, CD63 surface expression and MPO levels were determined. A) Representative dot plots for CD63 expression on neutrophils. B) The expression of CD63 on the outer cell membrane due to azurophilic granule exocytosis was evaluated as described before. Serum levels of C) MPO and D) the PMN elastase were determined by conventional sandwich ELISA. Data are shown as Tukey box and whiskers diagrams (mean ± SEM). Dunn's multiple comparison post-hoc-test p-values < 0.05 are considered significant ($p < 0.05$, ** $p < 0.01$, *** $p < 0.001$).

4.2.7 No influence of the patients treatment status and neurological deficits on the neutrophil profile

In addition to the results described in sections 4.2.1-6, untreated NMO and MS patients included in the study were analyzed separately to examine potential effects of pharmacological treatment (Figure 27) on the neutrophil phenotype and functionality. Generally, it could be observed that these untreated patients showed the same neutrophil profile as the whole cohorts (Figures 21, 23-25). Although the number of patients was limited, group differences were identical in untreated cohorts, when data were analyzed using a two-group comparison test. However, due to the small sample size, differences were no longer significant after correction for multiple comparisons (Figure 27).

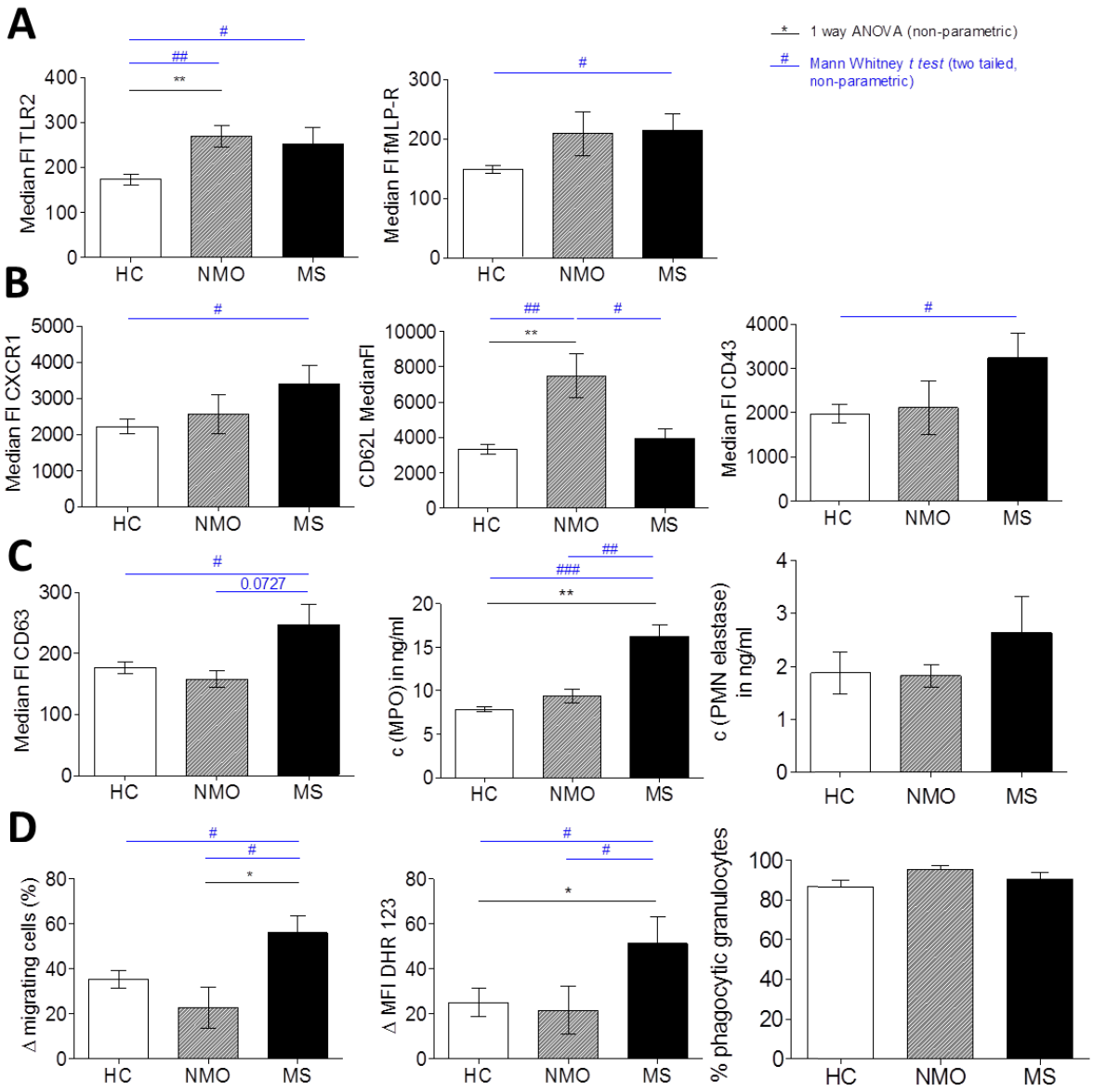

Figure 27. Treatment effects on the neutrophil phenotype and functionality [171]. To examine the influence of medical treatment on the results shown in figures 21-26 all data were validated on untreated NMO and MS patients. A) Neutrophil immune response (TLR2-, left graph and fMLPR expression, right graph). B) Expression of migratory and chemotactic molecules on neutrophils (CX3CR1, left graph; CD62L, middle graph; CD43, right graph). C) Neutrophil degranulation through CD63 surface expression (left graph), MPO serum (middle graph) and PMN elastase serum concentrations (right graph). D) Neutrophil migration (left graph), oxidative burst (middle graph) and phagocytic capacity (right graph). Bars indicate mean values ± SEM and p-values < 0.05 are considered significant ($p < 0.05$, ** $p < 0.01$, *** $p < 0.001$).

As well, all neutrophil data were analyzed for potential correlations with relevant clinical aspect of the patients. Analyses of individual EDSS with the phenotypic and functional neutrophil data did not reveal any significant correlations. Furthermore, no association between AQP4-IgG seropositivity and neutrophil profile were found (Figure 28).

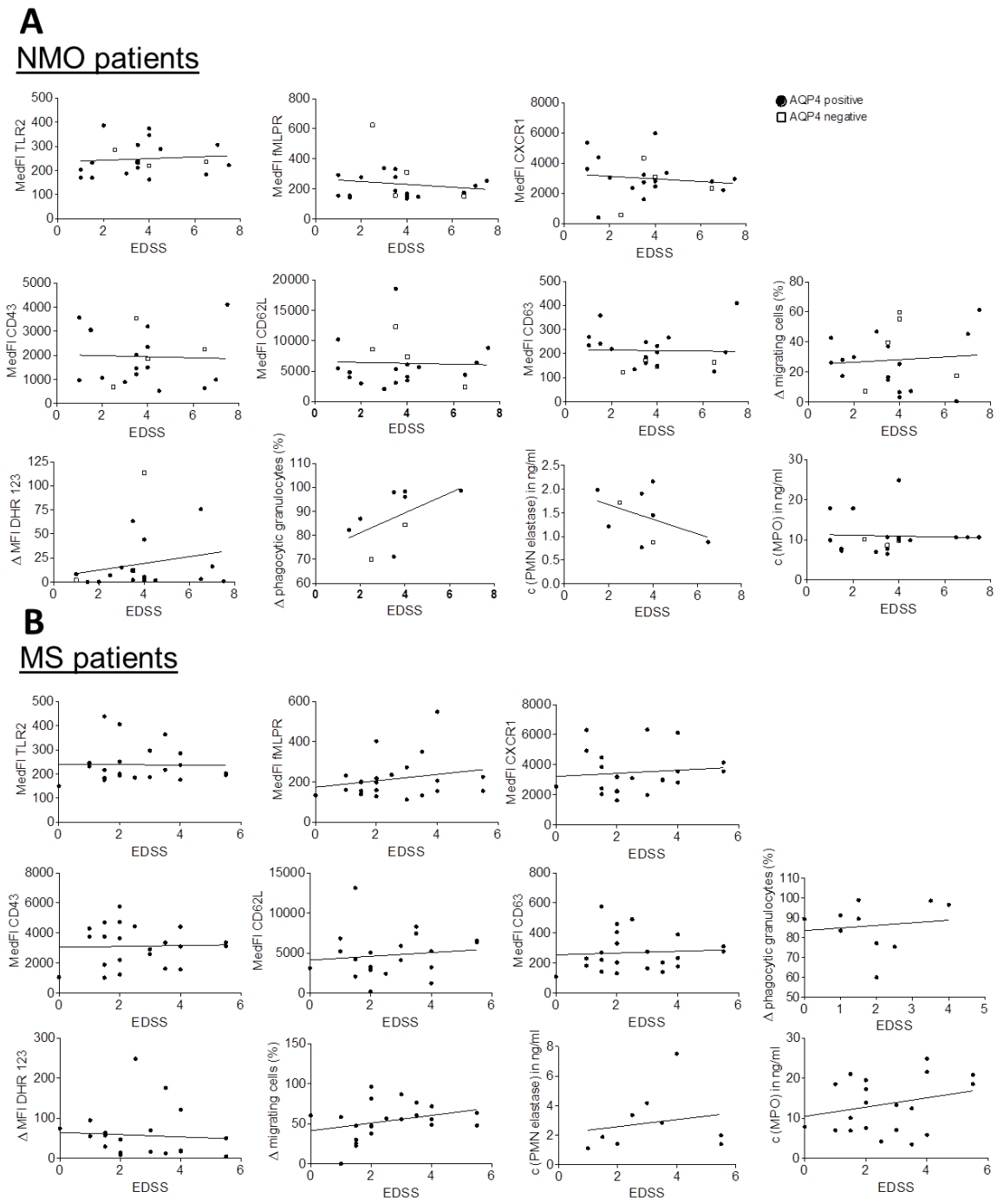

Figure 28. Correlation analyses between patient's EDSS and neutrophil characteristics. Correlation analyses of individual EDSS with neutrophil phenotypic and functional data were evaluated A) in NMO patients including consideration of AQP4-IgG seropositivity and B) in MS patients. Data are shown as dots representing single patients. Lines show linear regression.

The representation of the neutrophil data on a per patient basis further indicated that indeed the different neutrophil features exhibit an abnormal profile in single NMO individuals that differ from both HC and MS. As shown in table 8, 72.7% of NMO patients display a diminished neutrophil functionality with regards to both migratory and oxidative burst

capacity when compared to the respective average values of MS. 93.8% of these NMO patients additionally show reduced expression of the adhesion molecule CD43, 81.3% show reduced expression of the degranulation marker CD63 as well as reduced MPO serum levels (Table 8). Treatment effects were not identifiable.

Table 8. Comparison of neutrophil phenotypic and functional characteristics between NMO and MS on a per patient basis [171].

		Oxidative Burst	**Migration**	**CD43**	**CD62L**	**CD63**	**MPO**
		Δ DHR MFI 123	Δ migrating cells (%)	MedFl	MedFl	MedFl	c (ng/ ml)
	compared to average value for MS Patients	57.4	53.5	3123.7	4727.4	269,9	13.5
treated	**NMO 1**	↓	↑	↓	↑	↓	↓
	NMO 2	↓	↓	↓	↓	↓	↓
	NMO 3	↓	↓	↓	↓	↓	↓
	NMO 4	↓	↓	↓	↓	↓	↑
	NMO 5	↓	↓	↓	↓	↓	↓
	NMO 6	↓	↓	↓	↑	↓	↓
	NMO 7	↑	↓	↑	↑	↓	↓
	NMO 8	↓	↑	-	↑	↓	↓
	NMO 9	↓	↓	↓	↓	↑	↓
	NMO 10	↓	↓	↓	↑	↓	↓
	NMO 11	↑	↓	↓	↑	↓	-
	NMO 12	↓	↓	↓	↑	-	↓
	NMO 13	↓	↓	↓	↓	↓	-
	NMO 14	↓	↓	↓	↓	↓	↓
	NMO 15	↓	↓	↓	↓	↓	↓
	NMO 16	↓	↓	↑	-	↓	↓
untreated	**NMO 17**	↓	↓	↓	↑	↓	↓
	NMO 18	↓	↓	↓	↑	↓	↓
	NMO 19	↑	↓	↑	↑	↓	↓
	NMO 20	↓	↑	↑	↑	↑	↓
	NMO 21	↓	↓	↓	↓	↓	↑
	NMO 22	↓	↓	↓	↑	↓	↓

Comparing single NMO patients to HC similar observations could be made (Table 9.). Comparisons of single MS patients to HC revealed augmented oxidative burst and migration in 81.8%, of which around 72.7% additionally showed enhanced TLR2, fMLPR, CXCR1, CD43 and/ or CD63 surface expression and MPO serum levels (Table 10).

Table 9. Comparison of neutrophil phenotypic and functional characteristics between NMO and HC on a per patient basis.

		Oxidative Burst Δ DHR MFI 123	**Migration** Δ migrating cells (%)	**TLR2** MedFl	**fMLPR** MedFl	**CXCR1** MedFl	**CD43** MedFl	**CD62L** MedFl	**CD63** MedFl	**MPO** c (ng/ ml)	**PMN** c (ng/ ml)	**Phagocytosis** Δ phagocytic granulocytes (%)
	compared to average value for HC	13.7	35.2	179.6	155.7	2397.7	2062.1	3335.6	191.9	7.8	1.9	86.9
treated	**NMO 1**	↓	↑	↑	↑	↑	↓	↑	↓	↑	↓	↓
	NMO 2	↓	↓	↑	↑	↑	↓	↓	↑	↑	↓	↓
	NMO 3	↓	↓	↑	↑	↑	↓	↑	↑	↓	↓	↑
	NMO 4	↓	↓	↓	↓	↓	↓	↑	↑	↑	↓	-
	NMO 5	↓	↓	↑	↑	↓	↓	↑	↑	↑	↓	↓
	NMO 6	↓	↑	↓	↑	↑	↓	↑	↑	↑	-	↑
	NMO 7	↓	↓	↑	↑	↑	↑	↑	↑	↑		
	NMO 8	↓	↑	-	-	-	-	-	-	-		
	NMO 9	↓	↓	↓	↓	↓	↑	↑	↑	↑		
	NMO 10	↑	↑	↑	↑	↑	↓	↓	↓	↑		
	NMO 11	↓	↓	↑	↑	↑	↓	↓	↓	↑		
	NMO 12	↑	↑	↑	↑	↓	↓	↑	↑	↓		
	NMO 13	↑	↓	↑	↓	↑	↑	↓	↓	↓		
	NMO 14	↓	↓	↑	↑	↑	↑	↑	↑	↑		
	NMO 15	↓	↓	↑	↑	↑	↓	↑	↓	↓		
	NMO 16	↑	↓	↑	↑	↑	↑	↑	↑	-		
untreated	**NMO 17**	↓	↓	↑	↑	↓	↓	↑	↓	↑	↑	↑
	NMO 18	↓	↓	↑	↓	↑	↓	↑	↑	↓	↓	↑
	NMO 19	↑	↑	↑	↑	↑	↑	↑	↓	↑	↑	↑
	NMO 20	↓	↑	↑	↑	↑	↑	↑	↑	↑	↓	↑
	NMO 21	↑	↓	↑	↓	↑	↑	↑	↓	↑		
	NMO 22	↓	↓	↑	↑	↓	↓	↑	↓	↓		

Table 10. Comparison of neutrophil phenotypic and functional characteristics between MS and HC on a per patient basis.

		Oxidative Burst	**Migration**	**TLR2**	**fMLPR**	**CXCR1**	**CD43**	**CD62L**	**CD63**	**MPO**	**PMN**	**Phagocytosis**
		Δ DHR MFL 123	Δ migrating cells (%)	MedFl	MedFl	MedFl	MedFl	MedFl	MedFl	c (ng/ml)	c (ng/ml)	Δ phagocytic granulocytes
	compared to average value for HC	13.7	35.2	179.6	155.7	2397.7	2062.1	3335.6	191.9	7.8	1.9	86.9
treated	**MS 1**	↓	↑	↑	↑	↑	↑	↓	↑	↓	↑	↑
	MS 2	↓	↑	↑	↑	↑	↑	↑	↑	↑	↓	↓
	MS 3	↑	↑	↑	↓	↑	↑	↑	↑	↑	↑	↓
	MS 4	↑	↑	↑	↑	↑	↑	↑	↑	↑	↑	↑
	MS 5	↑	↑	↑	↑	↑	↑	↓	↑	↑	↓	↑
	MS 6	↑	↑	↑	↑	↓	↑	↓	↑	↑		
	MS 7	↑	↑	↑	↑	↑	↑	↓	↑	↓		
	MS 8	↑	↓	↑	↑	↑	↑	↑	↑	↑		
	MS 9	↑	-	↑	↑	↑	↑	↑	↓	-		
	MS 10	↓	↑	↑	↓	↑	↑	↑	↓	↑		
	MS 11	↑	↑	↑	↓	↑	↓	↓	↓	↓		
	MS 12	↑	↑	↓	↑	↑	↓	↓	↓	↑		
	MS 13	↑	↑	↑	↑	↓	↑	↑	↑	↓		
untreated	**MS 14**	↓	↑	↑	↑	↑	↓	↑	↑	↑	↑	↓
	MS 15	↑	↑	↓	↑	↑	↑	↑	↑	↓	↓	↑
	MS 16	↑	↑	↑	↑	↑	↑	↑	↑	↑	↑	↑
	MS 17	↑	↑	↑	↓	↑	↑	↑	↑	↑	↑	↑
	MS 18	↑	↑	↑	↑	↓	↑	↓	↑	↑		
	MS 19	↑	↑	↓	↓	↑	↓	↓	↓	↑		
	MS 20	↑	↓	↓	↑	↑	↓	↓	↓	↑		
	MS 21	↑	↑	↑	↓	↓	↑	↑	↓	↑		
	MS 22	↑	↓	↑	↑	↓	↓	↓	↑	↑		

4.2.8 Inter-assay variations

Finally, to exclude inter assay variations, 4 randomly selected HCs were tested twice for all the performed assays. Despite a large time interval of approximately 2 years between analyses, it could be observed that all parameters showed results which lay within the standard deviations of each respective assay (Figure 29).

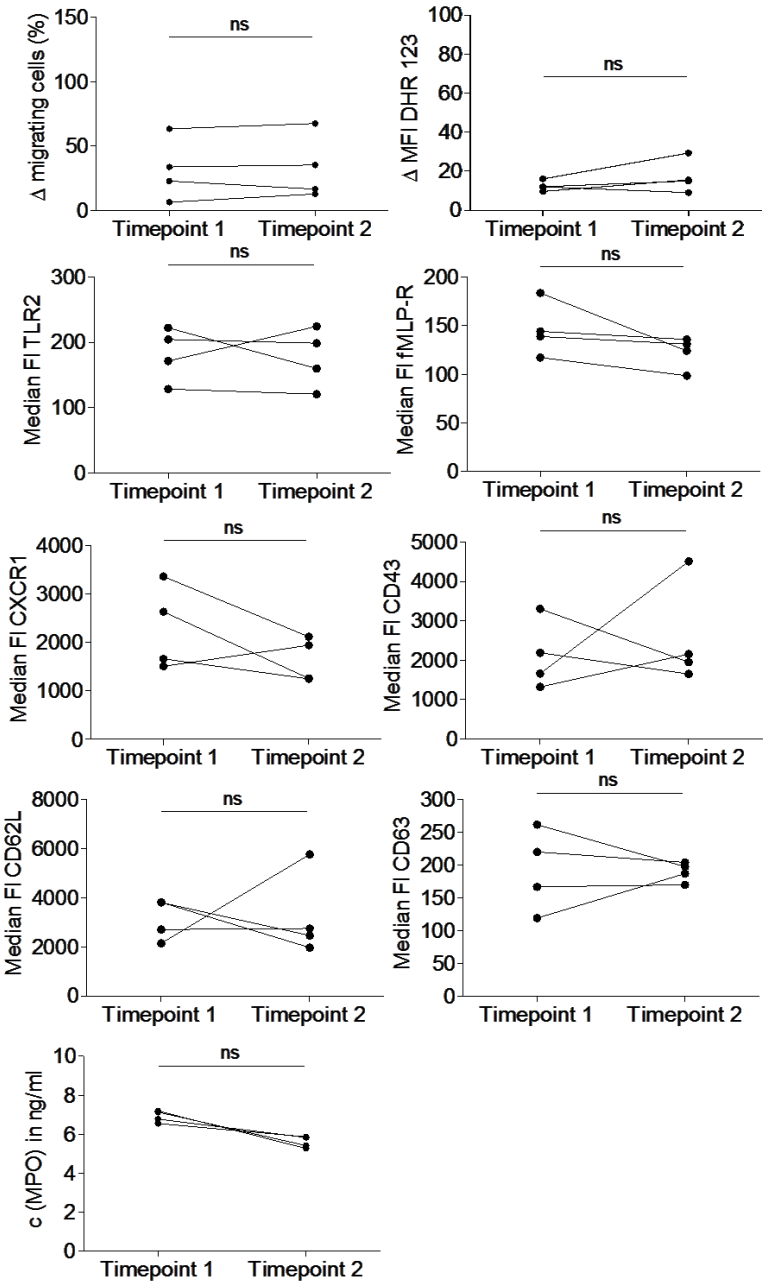

Figure 29. Inter-assay variations [171]**.** Four healthy donors were tested twice (with timepoint 2 two years after timepoint 1) for all parameters where significant differences between HC, NMO and MS could be detected. Left panel: oxidative burst capacity, TLRs, CXCR1 and CD62L surface expression and MPO serum concentration (top to bottom). Right panel: neutrophil migration capacity and expression of CD43 and CD63 (top to bottom). ns: no statistically significant difference between timepoint 1 and timepoint 2.

5. Discussion

Extensive research on autoimmune disorders of the CNS has been and is performed to better understand their etiopathogenic characteristics, whereby an emerging role of the innate immune system in CNS autoimmunity evolved in the last years. However, – and although enormous progress has been made – many innate cellular aspects are still elusive. Therefore, in the present thesis, the implication of innate immune cells – precisely NK cells and neutrophils – was investigated in the neuroinflammatory diseases MS and NMO. Here, the mouse model for MS, EAE, was used to investigate the role of natural killer cells and both, patients with MS and NMO were recruited to comparatively examine neutrophil characteristics in these disorders.

5.1 NK cell dynamics and the implication of the chemokine receptor CX3CR1 on NK cell migration and effector function during the course of EAE

NK cells belong the the group 1 of ILCs [85] and are involved in the immunological defense against viruses and tumor cells. Representing an interface between innate and adaptive immunity, NK cells possess immunomodulatory functionality in addition to their classical cytotoxic effector functions [86, 87].

In MS, decreased NK cell numbers and effector functions in the circulation correlating with the patients disease activity were shown [2-5, 129]. In this context, our group previously demonstrated that NK cell cytotoxicity can be associated with the expression of the chemokine receptor CX3CR1 [138] whose gene and protein expression are reduced in MS patients [6]. Moreover, patients in stable disease phase exhibit significantly low level of circulating $CX3CR1^{+}$ NK cells [6] and according to data from animal studies, CX3CR1-deficient NK cells do not adequately enter the inflamed CNS during EAE, resulting in disease exacerbation [7].

Based on these findings and therewith related open questions, in the present thesis work it was aimed to investigate the overall distribution of NK cells in the EAE mouse model compared to healthy mice, and the contibution of CX3CR1 to these dynamics. It should further be examined whether CX3CR1 is important for the NK cell recruitment into the inflamed CNS in general or rather involved in the migration of specific NK cell subtypes

to this organ during autoimmune inflammation. As well, it was of interest if NK cells exert a protective or rather detrimental effect in EAE and if different NK cells subsets are responsible for this protection or neuronal damage.

The obtained experimental data showed that NK cells are recruited from the periphery into the CNS during neuroinflammation and further that CX3CR1-mediated migration of mature CD11b^{high} NK cells contributes to limit EAE.

The investigation of NK cell dynamics im WT EAE mice revealed that during the course of EAE disease, more precisely from the day of immunization until EAE was established by reaching the peak of disease, the frequency and absolute numbers of NK cells decreased in peripheral blood, lymph nodes and spleen, but increased inside the CNS, pointing towards a selective NK cell migration from the periphery into the CNS during inflammation (Figure 7).

In association with alterations in numbers and function of circulating NK cells, NK cell mobilization to specific target organs has been reported in the course of autoimmune [180, 181] and CNS pathology [137]. Here, it is assumed that the targeted migration of NK cells may either contribute to, or restrict the pathologic process. For example, NK cells appear to have a disease controlling role in patients with SLE in which primary regulatory CD56^{bright} NK cell migrate and accumulate into the synovial fluid. In contrast, NK cells were shown to be disease enhancing in patients with type 1 diabetes by being involved in the destruction of pancreatic β-cells [181]. In MS patients, previous reports from our group on NK cells suggested that abnormal NK cell differentiation and activity may support chronic inflammation [6, 178, 182, 183]. Specifically, disease activity-associated expression of the chemokine receptor CX3CR1 on NK cells appeared to contibute to an altered function and migration of NK cells displaying an immature phenotype with bright expression of CD56 in the CSF [6, 178] as hypothetical intermediary compartment for NK cell trafficking into the inflamed CNS. Therefore, it was speculated that CX3CR1^{+} NK cell might have a protective, disease-restricting impact in MS and, with regard to the EAE mouse as model for MS, that migration of this NK cell subset into the CNS after peak of disease could contribute to EAE amelioration.

To test this hypothesis the well-described CX3CR1-deficient (CX3CR1$^{GFP/GFP}$) mouse was used in comparison to WT mice. CX3CR1-deficient mice were shown to develop severe

EAE, with deficient NK cell migration into the CNS. Importantly, CX3CR1-deficiency was shown to not affect the migration of T cells, NKT cells and monocytes/ macrophages [7].

Here, it could be confirmed that CX3CR1-deficient mice are more susceptible to EAE than WT mice, showing a more severe disease course, a higher disease activity and an earlier onset of the disease, although EAE disease was generally rather mildly pronounced in both mice types (Figure 8). In addition, in previous experiments performed in the group (Dr. Isabell Hamann) it could be confirmed that this increased susceptibility relies on the lack of the CX3CR1 receptor on peripheral immune cells rather than CNS-cells as demonstrated in bone marrow chimeric experiments, which complemented the recent proofs reported by Garcia et al. [184]. The transversal analysis of NK cell migration patterns in the CX3CR1-deficient EAE mice showed a NK cell mobilization similar to the WT counterparts (Figure 9). With the exception of peripheral blood, NK cell numbers decreased in the spleen and showed smaller reductions in the draining lymph nodes. However, in contrast to the previous report from Huang et al. (2006) [7], a mobilization of NK cells into the inflamed CNS in the CX3CR1-deficient EAE mice was observed. Precisely, the direct comparison of healthy WT and CX3CR1-deficient mice (Figure 9) revealed a generally lower number and frequency of NK cells in the CX3CR1-deficient mice in the periphery as well as significantly less NK cells in the CNS. In contrast, the latter observation is abrogated in CX3CR1-deficient mice with established EAE showing similar level of CNS infiltrated NK cells. This discrepancy in the migration of NK cells into the inflamed CNS in CX3CR1-deficient EAE mice may result from differences in the experimental approaches used in the two studies. In the present study, CNS infiltrating NK cells were assessed during the earlier EAE phases, i.e. from the day of immunization until disease peak/ established EAE. In contrast, Huang et al. (2006) [7] analyzed NK cells at the time of remission, approximately 60 days after immunization. Consistently, transient alterations in NK cell frequencies and cytotoxic activity have been described in MS patients during periods of disease activity [6].

In EAE, the dynamics of NK cells and disease activity may also be interrelated. Moreover, taking into account that the magnitude of CX3CR1 expression discriminates between different NK cell subsets in human [138], Huang et al. (2006) only analyzed the NK.1.1^{+} GFP^{+} NK cells, i.e. only the proportion of NK cells expressing CX3CR1 without

consideration of the CX3CR1$^-$ NK cell subpopulations, whereas the whole CD3$^-$ NK1.1$^+$ NK cell population was investigated here [7].

Together, these data suggest that CX3CR1 is not involved in the overall migration of NK cell under inflammatory conditions, but rather related to the recruitment of a specific NK cell subtype.

In human, CX3CR1 has been shown to influence NK cell functionality with regard to cytokine expression, activation status, proliferation and cytotoxicity [138]. Therefore, CX3CR1$^+$ versus CX3CR1$^-$ NK cells were investigated in view of their cytokine production, cytotoxicity and maturational status. These *ex vivo* experiments did not show evidence of intrinsic alteration in NK cell phenotype or function in CX3CR1-deficient mice that could possibly influence the experimental EAE data. Peripheral blood and splenic CX3CR1-deficient NK cells were found to display the same distinct maturation stages as WT cells (Figure 11). As well, the comparison of CX3CR1-deficient and WT NK cells revealed similar cytotoxic capacities and cytokine productions (Figure 10). However, the obtained data on the cytolytic capacity of CX3CR1-deficient and WT cells are in disagreement with a report by Ponzetta et al. (2013), which showed an enhanced cytotoxicity of splenic NK cells from CX3CR1-deficient mice [185]. While Ponzetta et al. (2013) used whole splenocytes activated with IL-15 for their cytotoxic assay [185], sorted NK cells were utilized in the present study to avoid contamination of cytotoxic CD8$^+$ T cells. Moreover, the sorted NK cells were not pre-activate with IL-15. In this context, other studies reported minimal deficits in cytotoxic activity of CX3CR1-deficient NK cells as compared to CX3CR1$^+$ NK cells after pretreatment with polyinosinic–polycytidylic acid [186], and anti-CX3CR1 antibody was shown to neutralize the cytotoxicity of NK cells against human K562 tumor cells [187]. Thus, experimental differences may explain divergent results on NK cell effector functionality. Altogether, these data indicate that CX3CR1-signalling is not essential for NK cell activation or differentiation in the here used mice and experimental settings and strengthen the hypothesis that CX3CR1 may rather be involved in the recruitment of a particular NK cell subtype into the inflamed CNS, as it has been postulated for human NK cells as well [137, 178].

According to the expression of surface CD11b and CD27, NK cell maturation is conventionally defined as a 4-stage developemental pathway in mouse, differentiating premature NK cells as CD3$^-$ NK1.1$^+$ CD11b$^-$ CD27$^-$, immature NK cells as

$CD3^-$ $NK1.1^+$ $CD11b^{neg/low}$ $CD27^+$, mature NK cells as $CD3^-$ $NK1.1^+$ $CD11b^+$ $CD27^+$ and fully differentiated NK cells as $CD3^-$ $NK1.1^+$ $CD11b^{high}$ $CD27^-$ [188]. As shown for human NK cells [138], CX3CR1 was found to be predominantly expressed on fully differentiated $CD11b^{high}$ $CD27^-$ NK cells (Figure 12), confirming a previous report on CX3CR1 expression within the late differentiated fraction of $CD11b^+$ $KLRG1^+$ NK cells [185]. Fractalkine (CX3CL1), the ligand of CX3CR1 which occurs as membrane-anchored and soluble form functioning as adhesion molecule and chemokine, respectively, has been reported to be expressed by many cell types including epithelial cells or lymphocytes and abundantly by neurons in the CNS [189]. In the latter, CX3CL1 controls and regulates the activity and communication between neurons, glia and microglia cells under physiological conditions and respectively appears to direct the activity of CX3CR1-expressing microglia in various pathological scenarios in the brain [190-196]. For instance, CX3CL1 has been shown to reduce neurotoxicity and microglial activation in a rat model of Parkinson's disease [193] while CX3CR1-deficiency was reported to result in the reduction of microglial activity and neurotoxic Aβ accumulations in a mouse model for Alzheimer's disease [196].

Based on this background and the experimental evaluation of CX3CR1 expression on maturational NK cell subsets (Figure 12), increased neuron-derived fractalkine may contribute to the recruitment of mature NK cells to inflamed sites during EAE. Accordingly, it could be observed that at day 20 p.i., the CX3CR1-deficient mice displayed a diminished frequency of mature $CD11b^{high}$ $CD27^+$ and cells, and an elevated frequency of immature $CD11b^{neg/low}$ $CD27^+$ NK cells in the CNS, whereas the proportion of $CD11b^{high}$ $CD27^-$ NK cells was elevated in spleen, compared to WT animals (Figure 13). Interestingly, in non-immunized CX3CR1-deficient mice the proportion of mature fully differentiated $CD11b^{high}$ $CD27^-$ NK cells was generally higher in peripheral blood and spleen compared to WT mice, while the proportions of immature $CD11b^{neg/low}$ $CD27^+$ and mature $CD11b^{high}$ $CD27^+$ were diminished (Figure 11). As well, previously described data of Poli et al. (2013) showing a predominant presence of immature NK cells in the brains of healthy mice [137] could be confirmed (Figure 13B). Thus, these data suggest a specific involvement of CX3CL1/ CX3CR1 in the recruitment of mature NK cells into CNS during inflammation and moreover indicate that the distinct maturational NK cell subsets are recruited through different chemotactic signals during EAE-mediated neuroinflammation.

Recently, our group showed that NK cells in the human CSF display an immature phenotype ($CD56^{bright}$ $CD27^{+}$ $CX3CR1^{low}$), suggesting that CSF may represent an intermediary compartment for NK cell trafficking and differentiation before entering the CNS parenchyma as postulated for $CCR7^{+}$ central memory T cells [197]. While human $CD56^{bright}$ NK cells express high levels of the chemokine receptor CCR7 [198], it could be verified that only a small fraction of circulating mouse NK cells express CCR7 [199] and that its expression is diametrically opposite to the expression of CX3CR1 in peripheral blood of healthy WT mice (Figure 14). Consequently, CCR7 may contribute to the recruitment of immature NK cells into the CNS during EAE. In human, CCR7 has been shown to be expressed in MS lesions and the CCR7 ligands CCL19 and CCL21 are expresses at the choroid plexus and meninges [197, 200]. In mouse, however, the ligands are also expressed in cerebral venules surrounded by inflammatory cuffs [201, 202] and their expression has been shown to be upregulatd during experimental neuroinflammation, while CCR7 expression on blood mononuclear cells was reduced [203]. Interestingly, murine CCL21 is also a ligand for CXCR3, a homing receptor of NK cells [204] that is expressed primarily on immature NK cells [199]. This could be confirmed in preliminary data from our goup showing that CXCR3 is expressed inversely to CX3CR1 suggesting this receptor a potential candidate for the recruitment of immature NK cells into the inflamed CNS (S. Romero-Suarez, unpublished data). However, further experiments are needed to delineate the chemotactic tools and route of entry of immature NK cells into the CNS during inflammation.

So far, the increased EAE severity observed in CX3CR1 deficient mice appears to be associated with an impaired recruitment of mature $CD11b^{+}$ NK cells into the CNS suggesting a protective, disease-limiting role of this NK cell population. Therefore, splenic NK cells from WT and CX3CR1-deficient mice (or PBS as control) were transferred into CX3CR1-deficient recipient mice one day prior EAE induction to investigate whether mature NK cells from WT mice may restrict EAE development. Indeed, it could be demonstrated that transfer of $CX3CR1^{+/+}$ NK cells, but not of CX3CR1-deficient NK cells prior to EAE induction, led to a significant disease amelioration, delayed disease onset and reduced EAE incidence in CX3CR1-deficient mice when compared to the PBS control group (Figure 15). A small number of mice from the PBS control group and mice receiving an injection of $CX3CR1^{+/+}$ NK cells was investigated with regard to NK cell and T cell distribution and organ-specific NK cell maturation profiles. Hereby, numbers and frequencies of $CD4^{+}$ and $CD8^{+}$ T cells remained unaffected in the periphery as well as in

the CNS and did not show differences between the groups according to the injection received, although cell functionalities were not validated at this point (Figure 17). In contrast, while numbers and frequencies of NK cells were similar in the periphery of both mice groups, enhanced NK cell numbers were detected in mice after transfer of CX3CR1$^{+/+}$ NK cells. In addition, this transfer of WT NK cells appeared to restore the balance of immature and mature NK cell in the CNS during EAE (Figure 16) and analysis of GFP expression further revealed a increased number GFP^{-} NK cells of a predominantly fully differentiated CD11b^{high} CD27^{-} phenotype in the CNS of the recipient mice (Figure 18).

Together, these data point to a protective role of mature CD11b^{+} NK cells into the EAE. However, also the transfer of CX3CR1$^{GFP/GFP}$ NK cells showed minor disease-ameliorating effects supporting the idea that not a single NK cell subset confers neuroprotection but rather the balance between the different and well functionning NK cells subsets. In this line, it was reported in MS patients that the susceptibility for the development of active lesions on magnetic resonance imaging (MRI) and clinical attacks result from valleys/ transient deficits in NK cell killing activity that are associated with a NK phenotype being unable to deliver a “lethal” hit to targets [129], while other studies supported the existence of an immunoregulatory pathway wherein expansion of regulatory CD16^{-} CD56^{bright} NK cells inhibits T cell survival through disease-modifying therapies such as IFN-β [205] or daclizumab [130]. Therefore, to use single sorted NK cell subsets in the here performed transfer experiments, to perform these transfers at distinct EAE disease stages and simultaneously to accurately track the transferred NK cells may help to better understand their precise implication in, and contribution to EAE/ MS disease pathogenesis, and to answer open questions as for example why mature CX3CR1^{+} CD11b^{+} NK cells limit EAE while in an experimental stroke model they seem to contribute to exacerbation of brain infarction through increased cytotoxicity that resulted in enhanced neuronal death [206].

Deficient CX3CR1 expression on NK cells might further influence NK cell-mediated immuregulation as for instance interactions of NK cells with other immune cells, such as DCs. Although with the here performed experiments it cannot be ruled out so far whether the beneficial effects of transferred, mature NK cells were exerted in the periphery, preliminary *in vitro* experiments using bone marrow derived DCs co-cultured with either CX3CR1-deficient or WT NK cells did not show evidence of different effects of these NK

cells on DC differentiation and activation. Thus, the present data rather point to modulatory effects inside the CNS, as postulated by Hao et al. (2010) who showed that CNS-resident but not peripheral NK cells surpress T_h17 cell responses and CNS pathology in the EAE mouse model by modulating the cytokine microinvironement in the CNS as well as microglial activity [134].

Cardona et al. (2006) reported that CX3CR1 deficiency dysregulates microglial responses, resulting in enhanced neurotoxicity [191]. Moreover, Garcia et al. (2013) recently provided evidence that CX3CR1 deficiency resulted in an enhanced recruitment of $CD115^+$ $Ly6C^-$ $CD11c^+$ DCs into the inflamed EAE brain, correlating with increased severity of CNS pathology, i.e. enhanced demyelination and neuronal damage. As well, peripheral DCs in these mice were shown to induce T cell proliferation to a higher extent during the initial phases of EAE disease corresponding with increased IFN-γ and IL-17 producing T cells in lymphoid tissues [184]. In this line, the present data showed that NK cells also contribute to disease aggravation in the CX3CR1-deficient mice. Therfore, it could be speculated that in CX3CR1-deficent mice, the presence of CX3CR1-negative, immature NK cells may lead to an altered immunomodulatory interactions between NK cells and myeloid cells, such as DCs [184] and/ or microglia [134, 207], contributing to an enhanced pathogenic T cell response, and hence increased EAE disease severity in CX3CR1-deficient mice.

In summary, the present study revealed that NK cells are recruited from the periphery into the CNS during neuroinflammation and that CX3CR1 deficiency results in an impaired migration of mature $CD11b^+$ NK cells into the CNS during EAE. This demonstrates for the first time that mature and immature NK cells are recruited into the CNS by distinct chemotactic signals and further suggests that recruitment of fully matured $CX3CR1^+$ $CD11b^+$ NK cells may contribute to limit neuroinflammation. Control of the EAE severity was recovered by transfer of mature NK cells suggesting an interesting therapeutic option.

5.1.1 Outlook 1

The contradictory functions of NK cells are reflected in the pathology of CNS diseases by being implicated in either neuroprotection [134] or neurotoxicity [135]. The here presented experimental data indicate that in the EAE mouse as model for MS, NK cells limit CNS inflammation, more precisely the CX3CR1^{+} CD11b^{+} NK cell subset appears to confer this neuroprotection, and therewith may represent a valuable target/ tool in NK-cell based therapeutical approaches for MS. However, many questions remain to be addressed and further investigations are essential to delineate the mechanisms of NK cell involvement in autoimmune neuroinflammation.

With regard to the obtained data and since the pleiotropic functions of NK cells are likely to be related to their phenotypic heterogeneity, an analysis in more depth of mouse NK cell subsets and their so far understudied organ-specific phenotype and function in health compared to EAE disease is indispensable. A very simple panel of surface markers was used in the present study, only permitting to differentiate between immature, mature and fully differentiated CD3^{-} NK1.1^{+} NK cells according to the expression of CD11b and CD27 [188]. Considering the latest classification of NK cells into the group 1 of innate lymphoid cells [85], the analysis should include the transcription factors Eomes and T-Bet [95]. Moreover, the expression of activating and inhibitory receptors as well as of a range of chemokine receptors known to be expressed at different stages of NK cell differentiation needs to be integrated. In this line and in order to investigate the precise routes of entry into the inflamed CNS, CCR7 and CXCR3 [199] may represent potential candidate chemokine receptors for the mobilization of immature and early mature NK cells in comparison to the here analyzed fractalkine receptor CX3CR1, which is primary expressed on mature NK cells in both mouse and human [138].

The cytotoxic activity of circulating NK cell has been shown to be decreased during acute relapses in MS while restored during remission phases. These transient deficits in NK cell killing activity were related to phenotypic alterations [129]. In contrast, rare NKp46^{+} NK cells were detected in MS lesions of *post morten* brain tissues [208] and, although CX3CR1 is emphasized in NK cell homing into the CNS [7], NK cells were shown to display an immature CD56^{bright} phenotype with negative/ low CX3CR1 expression and associated with primary regulatory functions in the CSF of MS patients [178]. These CX3CR1^{-} CD56^{bright} NK cells have further been demonstrated to be expanded after

medical treatment with IFN-β [205] or daclizumab [130] in association with diminished disease flares. Since frequencies of circulating CX3CR1^{+} NK cells were also shown to correlate with MS disease activity [6], it could be of interest how CX3CR1 expression is modulated by IFN-β or daclizumab treatment. Moreover, to investigate the influence of the inflammatory CNS microenvironment on systemic NK cell phenotypic and functional alterations as well as the characterization of CNS-resident NK cells needs to be performed in order to better understand the presence and contribution of specific NK cell subtypes in the CNS and CSF during neuroinflammation.

In this line, the here performed transfer EAE experiments need to be optimized and extended. After precise evaluation of the distinct NK cell subsets, they should be separately transferred into respective mice strains (such as CX3CR1-, CXCR3- or CCR7-deficient compared to WT mice) before EAE induction and at distinct stages of EAE disease to address several open questions. First, what are the NK cell routes of entry into the CNS? Do distinct NK cell subsets use different trafficking routes? The BBB has been considered the obvious place of entry for peripheral immune cells into the CNS. However, the choroid plexus evolved as an alternative entry site for circulating lymphocytes [209] and distinct molecular requirements have been identified for the entry of T cell subsets, suggesting that the choroid plexus is involved in the immune surveillance of the CNS [210]. Accordingly, is has to be clarified if the CSF may represent an intermediary compartment for trafficking and differentiation of distinct NK cell subsets before entering the CNS parenchyma as it has been shown for T cells [197]. In a second approach, these transfer experiments could be used to evaluate if all NK cell subsets exert a neuroprotective role, and moreover to investigate how/ by which mechanisms distinct NK cell subsets control/ limit EAE neuroinflammation. Are they involved in the killing of autoreactive or pro-inflammatory microglia? Do and how do they contribute to the modulation of DC and/ or encephalitogenic T cells?

5.2 Contribution of neutrophils to MS and NMO disease pathogenesis

As part of the innate immune system, neutrophil granulocytes represent the most abundant type of white blood cells and participate in the first line of host defense and inflammation, and further in shaping the adaptive immune response [155]. However, neutrophils were not only shown to be involved in physiological but also pathological processes and many studies revealed evidence for detrimental effects of neutrophils in the pathogeneses of various diseases and autoimmune disorders [156, 157].

In MS, patients exhibit activated neutrophils in circulation and increased levels of NETs in serum [158]. Moreover, findings from animal studies indicate a disease-promoting involvement of neutrophils during all phases of the disease, e.g. by contributing to the disruption of the BBB and formation of inflammatory lesions in preclinical phases or by stimulation and promotion of innate and adaptive immune responses in the effector phases [160-162]. Although increased neutrophil numbers were detected in the acute EAE mouse brain [159], neutrophils were not found to be a (major) component of cellular deposits in MS/ EAE inflammatory lesions. In contrast, lesions of NMO patients contain accumulated numbers of neutrophils [12, 70, 76, 165]. Furthermore, these patients display increased neutrophil counts and levels of neutrophil-related cytokines in the CSF [14, 15] and depletion of neutrophils in the NMO mouse model was associated with a reduction in neuroinflammation, myelin and AQP4 loss [163, 167].

To better understand the potential contribution of neutrophils to the NMO and MS pathology, a detailed analysis of the neutrophil phenotype and function in both conditions compared to HC was performed. The main aspects of this study were to, first, analyse the surface expression of peripheral blood neutrophils in patients and HC taking into consideration markers which are involved in the neutrophilic immune response, complement regulation, chemotaxis, adhesion and migration processes. Second, to evaluate neutrophil effector functions with respect to migration, ROS production, degranulation and phagocytosis. Third, to correlate the neutrophil phenotypic and functional data with clinical parameters of the NMO and MS patients. And fourth, to examine the influence of the patient's medical treatment on the neutrophil phenotype and functionality.

The resulting data showed that, independently of the patient's medical treatment or influence of clinical parameters, neutrophils exhibited a primed phenotype in both NMO

and MS when compared to HC. However, neutrophil functionality was compromised in NMO as compared to MS with respect to adhesion and (trans-) migration, oxidative burst and degranulation.

No differences in the neutrophil absolute counts between the patient groups and also when compared to HC were observed. Naegele et al. (2012) found increased neutrophil counts in their RRMS patient cohort compared to HC, associating it with delayed neutrophil apoptosis what they verified *in vitro* [158]. In contrast – but in line with the data presented here (Figure 19B) – they did not find higher serum concentrations of G-CSF, a major regulator of neutrophil granulopoiesis that further is known to delay apoptosis when present in elevated concentrations [147]. These discrepancies might be due to the clinical and demographic characteristics (specifically with regard to gender and medical treatment) between the patients recruited for the present study and the one's investigated by Naegele et al. (2012) [158]. Moreover, the here observed similar neutrophils counts and serum G-CSF levels were determined in a cohort including as few as 12 NMO, 12 MS and 10 HC (see section 3.3).

In view of the fact that NMO is a rare disease and patient recruitment is highly limited, neutrophil phenotype and function was first investigated in this preliminary cohort of 10 HC, 12 NMO and 12 MS patients, and subsequently extended by analyzing a second cohort of 12 HC, 10 NMO and 10 MS patients. Similar results were obtained in both cohorts. However, due to limited sample size, the multiple comparison testing showed only a trend for some of the parameters when each cohort was analyzed separately, although the two-group comparisons did reach statistical significance. Therefore, the final data analysis was performed in the combined cohort of 22 HC, 22 MS and 22 NMO.

As well, four randomly selected HC were tested twice for all experimental protocols to monitor the precision of results in the combined analysis of the two cohorts showing that the applied methodology was reliable and inter-assay variations for the repeated measurements were acceptable (Figure 29).

Under systemic stress or inflammation, circulating neutrophils are primed by classical or bacterial/ fungal-derived pro-inflammatory mediators to be subsequently recruited to the sites of infection or inflammation [139]. Therefore, the neutrophil surface markers essential for efficient response to infectious agents (fMLP receptor, TLR2), chemotaxis (CXCR1)

and extravasation (CD62L, CD43) as well as complement regulation (CD46, CD55, CD59) were investigated for the purposes of comparative phenotypical characterization in NMO, MS and HC.

NMO is thought to be primary driven by humoral processes. In this line, inflammatory feedback-loops between neutrophils and the complement system might promote and sustain NMO disease progression since intense complement deposits associated with granulocyte infiltrations were found in *post mortem* NMO brains [12, 70, 76, 165] and neutrophil-derived components were shown to activate the complement system in other autoimmune disease and vice versa [14, 15]. In contrast, MS is considered a T cell-mediated disease and the roles of the classical and terminal complement pathways are less clear. However, the complement alternative pathway has been shown to be involved in the pathogenesis in MS [211]. Therefore, the investigation of the neutrophil ability to regulate complement activation was included in the present study. Here, it could be observed that the complement regulator proteins CD46, CD55 and CD59 were expressed at similar levels on neutrophils from HC, NMO and MS patients (Figure 20) indicating that no major alterations in the regulation of complement activation via these regulators during the remission phase in NMO and MS patients contribute to the disease pathogenesis.

As part of activation and recruitment to sites of infection and inflammation, the neutrophil surface receptors TLR2 and fMLPR, which are involved in the response to infection, and the chemokine receptor CXCR1 are up-regulated by respective priming agents [212, 213]. In accordance, the analysis of these markers showed an increase in the MedFl of fMLPR and TLR2 in both, NMO and MS compared to HC (Figure 21), presumably due to the chronic inflammatory milieu characteristic for the two disease conditions. CXCR1, whose expression can enhance the neutrophil adhesive and migratory capacities as well as effector functionality [214, 215], was significantly up-regulated in MS compared to HC and showed slightly enhanced expression in NMO (Figure 21). These findings resonate with previously published data on RRMS patients [158]. In contrast, while Naegele et al. (2012) observed increased serum IL-8, the ligand of CXCR1 [158], only a trend towards higher concentrations in MS could be detected in the present study participants (Figure 22), though stimulated neutrophils themselves produce IL-8 in an autocrine mechanism through TLR2 signaling [213]. As for the G-CSF serum concentrations, IL-8 levels were determined in only 12 NMO and 12 MS patients. To verify whether these apparently inconsistent data result

from the limited number of patients or rather are due to clinical or demographic patient characteristics or neutrophil functional deficits needs to be investigated.

Primed neutrophils enter the sites of infection or inflammation by migrating from the circulation through endothelium. This extravasation process is mediated by a range of selectins and integrins on the neutrophil and endothelial cell surface [139]. Therefore, the neutrophil surface expression of the L-selectin CD62L and the E-selectin ligand CD43 were analyzed. The expression of CD62L was significantly increased in NMO compared to HC and enhanced compared to MS. In contrast, the adhesion molecule CD43 expression was significantly down-regulated on NMO neutrophils compared to MS (Figure 21). The initial adhesion of circulating neutrophils to the endothelium takes place through CD62L mediating the interaction with other endothelial cell ligands important for transendothelial migration to the target tissue. After binding, CD62L is rapidly shed from the neutrophil surface releasing an extracellular, functionally active fragment which – in respective amounts – can inhibit further leukocyte attachment to the endothelium [216]. CD43 has been shown to have dual-adhesive/ anti-adhesive functions, depending on the cell type, cell developmental stage, glycosylation and sialylation of CD43 and importantly also depending on the presence or absence of E-selectin [217, 218]. Since CD62L has been reported to mediate E-selectin binding in human [219], neutrophils may have a pro-adhesive function of CD43 in the context of neutrophil extravasation. In consideration of these findings, the here obtained CD62L and CD43 expression data might point towards a dysfunctional ability of NMO neutrophils to effectively adhere to endothelium compared to HC and MS. In fact, such a failure of neutrophil extravasation has already been described for other systemic and chronic inflammatory conditions such as sepsis or RA [216, 220-222]. In septic patients, it has been shown that over-activation of the TLR2-signalling is involved in the neutrophil migration defects resulting in the down-regulation of chemotactic receptors [221] and the production of high amounts of nitric oxides (NO) which in turn lead to inhibited expression of adhesion molecules on endothelial cells [221, 223]. In this line, significantly higher TLR2 expression on NMO neutrophils compared to HC were also detected in the present study (Figure 21) further supporting an impaired extravasation of NMO neutrophils. Moreover, a decreased migration of NMO, but not MS neutrophils towards a gradient of fMLP was observed (Figure 23B). Here, a positive correlation between the neutrophil migratory capacity and the surface expression of fMLPR could be evaluated only in MS and, unexpectedly, not in NMO (Figure 23C), although both NMO and MS

patients displayed increased fMLPR expression (Figure 21). Thus, it could be speculated that adhesion failure through disequilibrated expression of molecules such as CD62L or CD43, and neutrophil exhaustion (e.g. through enhanced signaling via TLR2) may contribute to an impaired migration of neutrophils in NMO. However, further investigations are needed to prove this conjecture.

As neutrophil migration, the oxidative burst capacity of peripheral blood neutrophils was analyzed in response to fMLP stimulation (Figure 24A). Here, an increased mean oxidative burst capacity was detected in MS patients compared to HC and NMO, whereas NMO neutrophils further showed a trend towards lower oxidative activity when compared to HC (Figure 24B). Alterations in the oxidative burst metabolism were previously described in other autoimmune disorders. For example, inappropriate release of ROS was found in RA joints and also the synovial fluid of SLE patients. However, data are controversial and reduced as well as increased oxidative burst activities were described [224-226]. As a result from the obtained data on MS and NMO patients, altered oxidative burst metabolism in these disease conditions can be hypothesized. As well, an involvement of ROS in the formation of inflammatory lesions and/ or promoting disease chronicity appears reasonable in both MS and NMO but even more in the latter with regard to histological findings [12, 70, 76, 165]. However, the presented data result from neutrophils after *in vitro* stimulation with fMLP while oxidative burst can be induced intra- and extracellularly involving signaling through various receptors (e.g. FcγR, TLRs or complement receptors) [227]. Thus, the data indicate increased oxidative burst in MS via fMLP/ fMLPR-mediated NADPH oxidase activation what is in line with the increased expression of fMLPR detected on MS neutrophils (Figure 21). In NMO, on the other hand, the received data do not indicate a generally impaired ROS metabolism but rather support a speculation of an altered fMLP signaling since fMLP-mediated migration of NMO neutrophils was reduced as well (Figure 23B), although fMLPR expression was increased (Figure 21). Therefore, patient serum level could further be investigated for ROS components and derivates, and other stimuli inducing oxidative burst should be tested on NMO neutrophils.

Neutrophils have previously been shown to incur functional exhaustion displaying inhibited chemotaxis and migration [220-223, 228], reduced oxidative burst activity, but a phagocytic activity comparable to HC [229-232]. In this line, similar proportions of phagocytic neutrophils and comparable phagocytic activities were found in NMO as compared to HC

and also MS (Figure 25). As one of the final effector mechanisms in the neutrophil life-cycle, phagocytosis is induced after neutrophil extravasation into infected/ inflamed tissue while oxidative burst or degranulation already can occur directly after priming. Since phagocytic activity of peripheral blood neutrophils was tested *in vitro* using opsonized *E.coli* bacteria, the obtained data show that neutrophils in NMO and MS are generally able to exert phagocytic activity through complement receptor-mediated internalization. However, if and how phagocytosis might be affected by the diminished adhesion and migratory capacities observed in NMO patients remains to be evaluated.

Another effector function of neutrophils is represented by the process of degranulation, which is induced in part through fMLP signaling [233]. Neutrophil degranulation was investigated by evaluating the expression level of CD63 due to exocytosis of azurophilic granules and assessing serum concentrations of the azurophilic granule-derived enzymes MPO and PMN elastase. The mean expression of CD63 as well as MPO level were significantly reduced in NMO compared to MS. PMN serum concentration was diminished in NMO compared to MS as well (Figure 26). However, no differences between NMO and HC were observed although a higher degranulation of NMO neutrophils is likely due to the inflammatory environment and the fact that circulating NMO neutrophils were found to be primed (Figure 21). Considering the results obtained from the migration and oxidative burst assays discussed above, it appears that functional processes mediated by the fMLPR are defective in NMO. Whether an overall dysfunction in fMLP-fMLPR-signaling underlies these effects remains unknown and it has to be clarified if such a potential dysfunction in fMLP-fMLPR-signaling or in other signaling cascades important for the neutrophil functionality possibly contributes to the increased neutrophil accumulation in inflammatory lesions reported for NMO but not observed in MS. Assuming a leaky BBB mediated by autoantibodies such as AQP4 and/ or complement components, primed NMO neutrophils could immigrate into the CNS even though showing reduced migratory capacities (Figure 21 and 23). It could further be speculated that – once neutrophils have entered the CNS – altered signaling mechanisms promote a prolonged neutrophil survival by inhibiting spontaneous apoptosis and therewith promoting neutrophil accumulation at the sites of inflammation, as it has already been described for other diseases such as chronic obstructive pulmonary disease (COPD) or sepsis [234, 235].

In summary, the phenotypical and functional analyses showed that MS neutrophils are primed and display significantly enhanced effector activities when compared to HC. These findings are in agreement with a study performed by Naegele et al. (2012) [158]. In contrast, although the disease-related inflammatory environment resulted in their priming, NMO neutrophils showed a compromised functionality with regard to migration, oxidative burst and degranulation as compared to MS. However, these neutrophils have been found to be accumulated in the CSF [14, 15] and inflammatory lesions [12, 70, 76, 165] of NMO patients and, interestingly, have been shown also in another common autoimmune disorder, RA, to intensely accumulate in the target organ, i.e. the synovial fluid of the disease-affected joints [236]. These neutrophils show a primed phenotype releasing inflammatory mediators such as IL-1β or IL-8 [237]. In addition, functional abnormalities in neutrophil phagocytosis and the production of ROS have been demonstrated in RA [238, 239] and further that these neutrophils are more prone to form NETs [240]. Accordingly, anti-neutrophil cytoplasmic and anti-granulocyte antibodies have been described in RA patients and it has been suggested that inflammatory feedback-loops initiated by NET-components may be key in arthritis development [241].

Finally, all data generated on the neutrophil profile in NMO and MS were validated for potential influences of clinical parameters and medical treatments.

Correlation analyses excluded that the phenotypical and functional characteristics of neutrophils are influenced by the patient's EDSS in MS and NMO. Presence or absence of the AQP4 autoantibody also appears to not directly influence the neutrophil hallmarks in NMO (Figure 28).

Analysis of potential effects of immunosuppressive or immunomodulatory medications on the neutrophil phenotype and functionality (Figure 27) revealed that medical treatment does not seem to influence the specific properties of neutrophils observed in MS and NMO patients. However, due to the limited number of untreated patients, results between groups were only significant when applying a two-group test (non-parametric Mann-Whitney U-test). In line with this, a previous report showed similar data in an extended cohort of untreated MS patients [158] suggesting that the results presented here may truly reflect the limitations of a small sample size of untreated patients. In addition, the analysis based on individual patient responses showed that 89% of untreated MS patients displayed increased neutrophil oxidative burst capacity and MPO serum levels, 75-78% showed increased

migration capacity and PMN serum concentrations, 67% exhibited increased surface expression of TLR2, fMLPR and CXCR1 and 56% increased CD43 as compared to HC (Table 10). Similarly, 67-100% of untreated NMO patients showed increased TLR2, fMLPR, CXCR1 and CD62L expression whereby around 67% showed decreased CD63, CD43, oxidative burst and migration compared to HC (Table 9). As well, monitoring neutrophil alterations on a per patient basis independently of treatment revealed an NMO neutrophil profile that differs from MS. In 93% of the untreated NMO patients neutrophils showed decreased migratory and oxidative burst abilities compared to MS and 67-93% showed reduced CD43, CD63 despite similar levels of TLR2 and fMLPR expression (Table 8).

In conclusion, the present study shows that peripheral blood neutrophils are primed in NMO and MS but, point to functional differences between these two conditions. Importantly, these findings were independent of the patient's clinical data and medication. Thus, neutrophil functionality with respect to neutrophil adhesion, migration, oxidative burst and degranulation in response to fMLP may represent a tool – in addition to the AQP4 autoantibody – to discriminate between NMO and MS.

5.2.1 Outlook 2

The present study provides the first comparative, basic analysis of the neutrophil phenotype and functionality after *in vitro* stimulation in NMO and MS patients in remission. It revealed several interesting aspects highlighting not only the involvement of these cells in the pathogenesis of both disease conditions, but further presenting them as a potential marker for discrimination what could be of interest especially for the differentiation between MS and the up to 20% of AQP4 seronegative NMO patients. In this line, a more extended investigation of neutrophilic characteristics, including a major range of phenotypic markers and also genetic analyses, in both conditions needs to be performed. Importantly, a larger number of patients has to be recruited taking into account clinical and demographic characteristics although they were not found to influence the neutrophil profile in the small cohorts investigated here. Furthermore, it needs to be clarified if and how neutrophils and neutrophil-related factors in the peripheral blood differ from those in the CSF, as representative for the CNS, from which only few data on the neutrophil phenotype, activation status and neutrophil-derived cytokines and products are available so far [14, 15, 166, 242].

Supported by EAE animal studies [159-163], it seems likely that in MS neutrophils occur as a secondary phenomenon, become primed and highly activated by the inflammatory environment and primary contribute to the disease pathogenesis by damaging tissues (e.g. damage of the BBB through azurophilic granules or demyelination of neurons through ROS components) and/ or modulating the encephalitogenic T cell responses. Thus, targeting neutrophil priming, activation and functionality could reveal interesting approaches of therapeutic strategies for MS.

In contrast to MS, neutrophils are accumulated in the CSF [14, 15] and inflammatory lesions [12, 70, 76, 165] of NMO patients, presumably contributing to the disease pathogenesis in a more prominent way and by pathways distinct from those in MS. Based on the experimental data presented in this thesis work [171] and in context of the current knowledge of neutrophils in other inflammatory diseases [151, 234, 235, 243, 244], it could be hypothesized that neutrophils might display functional dysregulations in NMO such as altered signaling pathways (e.g. the fMLP/ fMLPR-signaling pathway) resulting in apoptosis abnormalities, and finally leading to the observed accumulation in inflammatory lesions. Furthermore, these accumulated neutrophils might sustain disease chronicity and severity by influencing

the CNS immune response and environment. In this line, defective neutrophil apoptosis accompanied by neutrophil deposits have been shown for several inflammatory diseases such as sepsis or chronic obstructive pulmonary disease [234, 235]. Similarly, in patients with chronic granulomatous disease impaired neutrophil apoptosis has been reported *in vitro* resulting from neutrophil hypoxia due to a defective NADPH oxidase activity [243]. Accordingly, examination of neutrophil apoptosis in NMO, e.g. by determining the gene expression of NADPH oxidase, fMLP receptor and TNFR1, molecules that are all involved in the signaling process of reactive oxygen species (ROS) production [245], would further illuminate the implication of neutrophils in NMO.

Another form of neutrophil cell death is the recently discovered NETosis [150], i. e formation of neutrophil extracellular traps composed of decondensed chromatin DNA in association with histones, granular proteins, and a few cytoplasmic proteins [151, 152, 246]. NETosis seems to depend on the generation of ROS by the NADPH oxidase complex. Moreover, neutrophils from patients with chronic granulomatous disease, who have mutations in NADPH oxidase, fail to make NETs [154]. These patients are severely immunodeficient, suffer from recurrent infections and have poor prognosis. Moreover, Villanueva et al. (2011) showed that tissue NETosis is associated with increased anti-dsDNA in sera of lupus erythematosus (SLE) patients, suggesting that dysregulation of NET formation and its subsequent responses may play a prominent deleterious role in SLE [244]. It has further been reported that NETs, which are not degraded in SLE, activate the complement and plasmacytoid dendritic cells leading to disease exacerbation [247-249]. In this line, complement activation and intense complement deposits associated with granulocyte infiltrations found in *post mortem* NMO brains [12, 70, 76, 165] might suggest a role of NETs in NMO as well. However, no precise data on NETosis and NETs are available in NMO so far and it remains to investigate whether NETosis is dysregulated in NMO and if this dysregulation of neutrophil extracellular trap (NET) formation contributes to disease progression in NMO.

6. References

1. Sospedra M, Martin R. Immunology of multiple sclerosis. Annual review of immunology 2005;23:683-747.
2. Benczur M, Petranyl GG, Palffy G, et al. Dysfunction of natural killer cells in multiple sclerosis: a possible pathogenetic factor. Clinical and experimental immunology 1980;39:657-662.
3. Merrill J, Jondal M, Seeley J, Ullberg M, Siden A. Decreased NK killing in patients with multiple sclerosis: an analysis on the level of the single effector cell in peripheral blood and cerebrospinal fluid in relation to the activity in the disease. Clinical and experimental immunology 1982;47:419-430.
4. Kastrukoff LF, Morgan NG, Aziz TM, Zecchini D, Berkowitz J, Paty DW. Natural killer (NK) cells in chronic progressive multiple sclerosis patients treated with lymphoblastoid interferon. Journal of neuroimmunology 1988;20:15-23.
5. Neighbour PA, Grayzel AI, Miller AE. Endogenous and interferon-augmented natural killer cell activity of human peripheral blood mononuclear cells in vitro. Studies of patients with multiple sclerosis, systemic lupus erythematosus or rheumatoid arthritis. Clinical and experimental immunology 1982;49:11-21.
6. Infante-Duarte C, Weber A, Kratzschmar J, et al. Frequency of blood CX3CR1-positive natural killer cells correlates with disease activity in multiple sclerosis patients. FASEB journal : official publication of the Federation of American Societies for Experimental Biology 2005;19:1902-1904.
7. Huang D, Shi FD, Jung S, et al. The neuronal chemokine CX3CL1/fractalkine selectively recruits NK cells that modify experimental autoimmune encephalomyelitis within the central nervous system. FASEB journal : official publication of the Federation of American Societies for Experimental Biology 2006;20:896-905.
8. Jarius S, Wildemann B, Paul F. Neuromyelitis optica: clinical features, immunopathogenesis and treatment. Clinical and experimental immunology 2014;176:149-164.
9. Pfueller CF, Paul F. Imaging the visual pathway in neuromyelitis optica. Multiple sclerosis international 2011;2011:869814.
10. Lennon VA, Wingerchuk DM, Kryzer TJ, et al. A serum autoantibody marker of neuromyelitis optica: distinction from multiple sclerosis. Lancet 2004;364:2106-2112.
11. Jarius S, Ruprecht K, Wildemann B, et al. Contrasting disease patterns in seropositive and seronegative neuromyelitis optica: A multicentre study of 175 patients. Journal of neuroinflammation 2012;9:14.
12. Lucchinetti CF, Mandler RN, McGavern D, et al. A role for humoral mechanisms in the pathogenesis of Devic's neuromyelitis optica. Brain 2002;125:1450-1461.
13. Saadoun S, Waters P, MacDonald C, et al. Neutrophil protease inhibition reduces neuromyelitis optica-immunoglobulin G-induced damage in mouse brain. Annals of neurology 2012;71:323-333.
14. Uzawa A, Mori M, Arai K, et al. Cytokine and chemokine profiles in neuromyelitis optica: significance of interleukin-6. Multiple sclerosis 2010;16:1443-1452.
15. Matsushita T, Tateishi T, Isobe N, et al. Characteristic cerebrospinal fluid cytokine/chemokine profiles in neuromyelitis optica, relapsing remitting or primary progressive multiple sclerosis. PloS one 2013;8:e61835.
16. Dendrou CA, Fugger L, Friese MA. Immunopathology of multiple sclerosis. Nat Rev Immunol 2015;15:545-558.
17. Compston A, Coles A. Multiple sclerosis. Lancet 2002;359:1221-1231.
18. Marrie RA, Gryba C. The incidence and prevalence of neuromyelitis optica: a systematic review. International journal of MS care 2013;15:113-118.
19. Clanet M. Jean-Martin Charcot. 1825 to 1893. International MS journal / MS Forum 2008;15:59-61.
20. Hoer A, Schiffhorst G, Zimmermann A, et al. Multiple sclerosis in Germany: data analysis of administrative prevalence and healthcare delivery in the statutory health system. BMC Health Serv Res 2014;14:381.
21. Milo R, Kahana E. Multiple sclerosis: geoepidemiology, genetics and the environment. Autoimmun Rev 2010;9:A387-394.
22. Alonso A, Hernan MA. Temporal trends in the incidence of multiple sclerosis: a systematic review. Neurology 2008;71:129-135.
23. Nicholas J, Morgan-Followell B, Pitt D, Racke MK, Boster A. New and Emerging Disease-Modifying Therapies for Relapsing-Remitting Multiple Sclerosis: What is New and What is to Come. J Cent Nerv Syst Dis 2012;4:81-103.
24. Naito S, Namerow N, Mickey MR, Terasaki PI. Multiple sclerosis: association with HL-A3. Tissue Antigens 1972;2:1-4.
25. Jersild C, Svejgaard A, Fog T. HL-A antigens and multiple sclerosis. Lancet 1972;1:1240-1241.

26. Ascherio A, Munger KL, Simon KC. Vitamin D and multiple sclerosis. The Lancet Neurology 2010;9:599-612.
27. Pawate S, Sriram S. The role of infections in the pathogenesis and course of multiple sclerosis. Annals of Indian Academy of Neurology 2010;13:80-86.
28. Olson JK, Croxford JL, Calenoff MA, Dal Canto MC, Miller SD. A virus-induced molecular mimicry model of multiple sclerosis. The Journal of clinical investigation 2001;108:311-318.
29. Munz C, Lunemann JD, Getts MT, Miller SD. Antiviral immune responses: triggers of or triggered by autoimmunity? Nat Rev Immunol 2009;9:246-258.
30. Mielcarz DW, Kasper LH. The gut microbiome in multiple sclerosis. Current treatment options in neurology 2015;17:344.
31. Bhargava P, Mowry EM. Gut microbiome and multiple sclerosis. Current neurology and neuroscience reports 2014;14:492.
32. Lublin FD, Reingold SC, Cohen JA, et al. Defining the clinical course of multiple sclerosis: the 2013 revisions. Neurology 2014;83:278-286.
33. Hellings N, Baree M, Verhoeven C, et al. T-cell reactivity to multiple myelin antigens in multiple sclerosis patients and healthy controls. Journal of neuroscience research 2001;63:290-302.
34. Lassmann H, Bruck W, Lucchinetti CF. The immunopathology of multiple sclerosis: an overview. Brain pathology 2007;17:210-218.
35. Grigoriadis N, van Pesch V. A basic overview of multiple sclerosis immunopathology. European journal of neurology 2015;22 Suppl 2:3-13.
36. Nuyts AH, Lee WP, Bashir-Dar R, Berneman ZN, Cools N. Dendritic cells in multiple sclerosis: key players in the immunopathogenesis, key players for new cellular immunotherapies? Multiple sclerosis 2013;19:995-1002.
37. Huppert J, Closhen D, Croxford A, et al. Cellular mechanisms of IL-17-induced blood-brain barrier disruption. FASEB journal : official publication of the Federation of American Societies for Experimental Biology 2010;24:1023-1034.
38. Larochelle C, Alvarez JI, Prat A. How do immune cells overcome the blood-brain barrier in multiple sclerosis? FEBS letters 2011;585:3770-3780.
39. Peters A, Pitcher LA, Sullivan JM, et al. Th17 cells induce ectopic lymphoid follicles in central nervous system tissue inflammation. Immunity 2011;35:986-996.
40. von Budingen HC, Palanichamy A, Lehmann-Horn K, Michel BA, Zamvil SS. Update on the autoimmune pathology of multiple sclerosis: B-cells as disease-drivers and therapeutic targets. Eur Neurol 2015;73:238-246.
41. Babbe H, Roers A, Waisman A, et al. Clonal expansions of CD8(+) T cells dominate the T cell infiltrate in active multiple sclerosis lesions as shown by micromanipulation and single cell polymerase chain reaction. The Journal of experimental medicine 2000;192:393-404.
42. Saxena A, Martin-Blondel G, Mars LT, Liblau RS. Role of CD8 T cell subsets in the pathogenesis of multiple sclerosis. FEBS letters 2011;585:3758-3763.
43. Bitsch A, Schuchardt J, Bunkowski S, Kuhlmann T, Bruck W. Acute axonal injury in multiple sclerosis. Correlation with demyelination and inflammation. Brain 2000;123 (Pt 6):1174-1183.
44. Cunnusamy K, Baughman EJ, Franco J, et al. Disease exacerbation of multiple sclerosis is characterized by loss of terminally differentiated autoregulatory CD8+ T cells. Clinical immunology 2014;152:115-126.
45. Rao P, Segal BM. Experimental autoimmune encephalomyelitis. Methods in molecular biology 2012;900:363-380.
46. Baker D, Amor S. Experimental autoimmune encephalomyelitis is a good model of multiple sclerosis if used wisely. Multiple sclerosis and related disorders 2014;3:555-564.
47. Rivers TM, Sprunt DH, Berry GP. Observations on Attempts to Produce Acute Disseminated Encephalomyelitis in Monkeys. The Journal of experimental medicine 1933;58:39-53.
48. Ransohoff RM. Animal models of multiple sclerosis: the good, the bad and the bottom line. Nature neuroscience 2012;15:1074-1077.
49. Constantinescu CS, Farooqi N, O'Brien K, Gran B. Experimental autoimmune encephalomyelitis (EAE) as a model for multiple sclerosis (MS). British journal of pharmacology 2011;164:1079-1106.
50. Tabira T. Autoimmune demyelination in the central nervous system. Ann N Y Acad Sci 1988;540:187-201.
51. Sriram S, Steiner I. Experimental allergic encephalomyelitis: a misleading model of multiple sclerosis. Annals of neurology 2005;58:939-945.
52. Ransohoff RM. A mighty mouse: building a better model of multiple sclerosis. The Journal of clinical investigation 2006;116:2313-2316.

53. Stromnes IM, Goverman JM. Active induction of experimental allergic encephalomyelitis. Nature protocols 2006;1:1810-1819.
54. Stromnes IM, Goverman JM. Passive induction of experimental allergic encephalomyelitis. Nature protocols 2006;1:1952-1960.
55. Wingerchuk DM, Banwell B, Bennett JL, et al. International consensus diagnostic criteria for neuromyelitis optica spectrum disorders. Neurology 2015;85:177-189.
56. Uzawa A, Mori M, Kuwabara S. Neuromyelitis optica: concept, immunology and treatment. J Clin Neurosci 2014;21:12-21.
57. Wingerchuk DM, Weinshenker BG. Neuromyelitis optica (Devic's syndrome). Handbook of clinical neurology 2014;122:581-599.
58. Wingerchuk DM, Lennon VA, Pittock SJ, Lucchinetti CF, Weinshenker BG. Revised diagnostic criteria for neuromyelitis optica. Neurology 2006;66:1485-1489.
59. Lennon VA, Kryzer TJ, Pittock SJ, Verkman AS, Hinson SR. IgG marker of optic-spinal multiple sclerosis binds to the aquaporin-4 water channel. The Journal of experimental medicine 2005;202:473-477.
60. Vincent T, Saikali P, Cayrol R, et al. Functional consequences of neuromyelitis optica-IgG astrocyte interactions on blood-brain barrier permeability and granulocyte recruitment. Journal of immunology 2008;181:5730-5737.
61. Mealy MA, Wingerchuk DM, Greenberg BM, Levy M. Epidemiology of neuromyelitis optica in the United States: a multicenter analysis. Archives of neurology 2012;69:1176-1180.
62. Wingerchuk DM, Lennon VA, Lucchinetti CF, Pittock SJ, Weinshenker BG. The spectrum of neuromyelitis optica. The Lancet Neurology 2007;6:805-815.
63. Wingerchuk DM. Neuromyelitis optica: effect of gender. Journal of the neurological sciences 2009;286:18-23.
64. Papadopoulos MC, Bennett JL, Verkman AS. Treatment of neuromyelitis optica: state-of-the-art and emerging therapies. Nature reviews Neurology 2014;10:493-506.
65. Jarius S, Paul F, Franciotta D, et al. Mechanisms of disease: aquaporin-4 antibodies in neuromyelitis optica. Nature clinical practice Neurology 2008;4:202-214.
66. Jarius S, Wildemann B. AQP4 antibodies in neuromyelitis optica: diagnostic and pathogenetic relevance. Nature reviews Neurology 2010;6:383-392.
67. Kim SH, Kim W, Huh SY, Lee KY, Jung IJ, Kim HJ. Clinical efficacy of plasmapheresis in patients with neuromyelitis optica spectrum disorder and effects on circulating anti-aquaporin-4 antibody levels. Journal of clinical neurology 2013;9:36-42.
68. Ayzenberg I, Kleiter I, Schroder A, et al. Interleukin 6 receptor blockade in patients with neuromyelitis optica nonresponsive to anti-CD20 therapy. JAMA neurology 2013;70:394-397.
69. Matiello M, Schaefer-Klein J, Sun D, Weinshenker BG. Aquaporin 4 expression and tissue susceptibility to neuromyelitis optica. JAMA neurology 2013;70:1118-1125.
70. Misu T, Fujihara K, Kakita A, et al. Loss of aquaporin 4 in lesions of neuromyelitis optica: distinction from multiple sclerosis. Brain 2007;130:1224-1234.
71. Roemer SF, Parisi JE, Lennon VA, et al. Pattern-specific loss of aquaporin-4 immunoreactivity distinguishes neuromyelitis optica from multiple sclerosis. Brain 2007;130:1194-1205.
72. Jarius S, Jacob S, Leite MI, Waters P, Vincent A. NMO-IgG/Aqp4-Ab belongs to the IgG1 subclass and activates complement in vitro. Mult Scler J 2007;13:S159-S159.
73. Varrin-Doyer M, Spencer CM, Schulze-Topphoff U, et al. Aquaporin 4-specific T cells in neuromyelitis optica exhibit a Th17 bias and recognize Clostridium ABC transporter. Annals of neurology 2012;72:53-64.
74. Shimizu F, Sano Y, Takahashi T, et al. Sera from neuromyelitis optica patients disrupt the blood-brain barrier. Journal of neurology, neurosurgery, and psychiatry 2012;83:288-297.
75. Chihara N, Aranami T, Oki S, et al. Plasmablasts as migratory IgG-producing cells in the pathogenesis of neuromyelitis optica. PloS one 2013;8:e83036.
76. Saadoun S, Bridges LR, Verkman AS, Papadopoulos MC. Paucity of natural killer and cytotoxic T cells in human neuromyelitis optica lesions. Neuroreport 2012;23:1044-1047.
77. Uzawa A, Mori M, Ito M, et al. Markedly increased CSF interleukin-6 levels in neuromyelitis optica, but not in multiple sclerosis. Journal of neurology 2009;256:2082-2084.
78. Icoz S, Tuzun E, Kurtuncu M, et al. Enhanced IL-6 production in aquaporin-4 antibody positive neuromyelitis optica patients. The International journal of neuroscience 2010;120:71-75.
79. Wang H, Wang K, Zhong X, et al. Cerebrospinal fluid BAFF and APRIL levels in neuromyelitis optica and multiple sclerosis patients during relapse. Journal of clinical immunology 2012;32:1007-1011.
80. Chihara N, Aranami T, Sato W, et al. Interleukin 6 signaling promotes anti-aquaporin 4 autoantibody production from plasmablasts in neuromyelitis optica. Proceedings of the National Academy of Sciences of the United States of America 2011;108:3701-3706.

81. Korn T, Mitsdoerffer M, Croxford AL, et al. IL-6 controls Th17 immunity in vivo by inhibiting the conversion of conventional T cells into Foxp3+ regulatory T cells. Proceedings of the National Academy of Sciences of the United States of America 2008;105:18460-18465.
82. Kiessling R, Klein E, Wigzell H. "Natural" killer cells in the mouse. I. Cytotoxic cells with specificity for mouse Moloney leukemia cells. Specificity and distribution according to genotype. European journal of immunology 1975;5:112-117.
83. Kiessling R, Klein E, Pross H, Wigzell H. "Natural" killer cells in the mouse. II. Cytotoxic cells with specificity for mouse Moloney leukemia cells. Characteristics of the killer cell. European journal of immunology 1975;5:117-121.
84. McCoy JL, Herberman RB, Rosenberg EB, Donnelly FC, Levine PH, Alford C. 51 Chromium-release assay for cell-mediated cytotoxicity of human leukemia and lymphoid tissue-culture cells. National Cancer Institute monograph 1973;37:59-67.
85. Gasteiger G, Rudensky AY. Interactions between innate and adaptive lymphocytes. Nat Rev Immunol 2014;14:631-639.
86. Moretta L, Ferlazzo G, Mingari MC, Melioli G, Moretta A. Human natural killer cell function and their interactions with dendritic cells. Vaccine 2003;21 Suppl 2:S38-42.
87. Vivier E, Raulet DH, Moretta A, et al. Innate or adaptive immunity? The example of natural killer cells. Science 2011;331:44-49.
88. Paust S, Senman B, von Andrian UH. Adaptive immune responses mediated by natural killer cells. Immunological reviews 2010;235:286-296.
89. Sun JC, Beilke JN, Lanier LL. Adaptive immune features of natural killer cells. Nature 2009;457:557-561.
90. Mandal A, Viswanathan C. Natural killer cells: In health and disease. Hematology/oncology and stem cell therapy 2015;8:47-55.
91. Barton K, Muthusamy N, Fischer C, et al. The Ets-1 transcription factor is required for the development of natural killer cells in mice. Immunity 1998;9:555-563.
92. Boggs SS, Trevisan M, Patrene K, Geogopoulos K. Lack of natural killer cell precursors in fetal liver of Ikaros knockout mutant mice. Natural immunity 1998;16:137-145.
93. Ma A, Koka R, Burkett P. Diverse functions of IL-2, IL-15, and IL-7 in lymphoid homeostasis. Annual review of immunology 2006;24:657-679.
94. Sun JC, Lanier LL. NK cell development, homeostasis and function: parallels with CD8(+) T cells. Nat Rev Immunol 2011;11:645-657.
95. Gordon SM, Chaix J, Rupp LJ, et al. The transcription factors T-bet and Eomes control key checkpoints of natural killer cell maturation. Immunity 2012;36:55-67.
96. Boos MD, Ramirez K, Kee BL. Extrinsic and intrinsic regulation of early natural killer cell development. Immunologic research 2008;40:193-207.
97. Bernardini G, Gismondi A, Santoni A. Chemokines and NK cells: regulators of development, trafficking and functions. Immunology letters 2012;145:39-46.
98. Walzer T, Chiossone L, Chaix J, et al. Natural killer cell trafficking in vivo requires a dedicated sphingosine 1-phosphate receptor. Nature immunology 2007;8:1337-1344.
99. Cooper MA, Fehniger TA, Caligiuri MA. The biology of human natural killer-cell subsets. Trends in immunology 2001;22:633-640.
100. Gregoire C, Chasson L, Luci C, et al. The trafficking of natural killer cells. Immunological reviews 2007;220:169-182.
101. Shi FD, Ljunggren HG, La Cava A, Van Kaer L. Organ-specific features of natural killer cells. Nat Rev Immunol 2011;11:658-671.
102. Bekiaris V, Timoshenko O, Hou TZ, et al. Ly49H+ NK cells migrate to and protect splenic white pulp stroma from murine cytomegalovirus infection. Journal of immunology 2008;180:6768-6776.
103. Salazar-Mather TP, Lewis CA, Biron CA. Type I interferons regulate inflammatory cell trafficking and macrophage inflammatory protein 1alpha delivery to the liver. The Journal of clinical investigation 2002;110:321-330.
104. Lanier LL. NK cell recognition. Annual review of immunology 2005;23:225-274.
105. Vivier E, Ugolini S, Blaise D, Chabannon C, Brossay L. Targeting natural killer cells and natural killer T cells in cancer. Nat Rev Immunol 2012;12:239-252.
106. Thomas LM. Current perspectives on natural killer cell education and tolerance: emerging roles for inhibitory receptors. ImmunoTargets & Therapy 2015;4.
107. Campbell KS, Hasegawa J. Natural killer cell biology: an update and future directions. The Journal of allergy and clinical immunology 2013;132:536-544.
108. Shifrin N, Raulet DH, Ardolino M. NK cell self tolerance, responsiveness and missing self recognition. Seminars in immunology 2014;26:138-144.

109. Smyth MJ, Cretney E, Kelly JM, et al. Activation of NK cell cytotoxicity. Molecular immunology 2005;42:501-510.
110. Seidel UJ, Schlegel P, Lang P. Natural killer cell mediated antibody-dependent cellular cytotoxicity in tumor immunotherapy with therapeutic antibodies. Frontiers in immunology 2013;4:76.
111. Sharma R, Das A. Organ-specific phenotypic and functional features of NK cells in humans. Immunologic research 2014;58:125-131.
112. Lunemann A, Lunemann JD, Munz C. Regulatory NK-cell functions in inflammation and autoimmunity. Molecular medicine 2009;15:352-358.
113. Carson WE, Giri JG, Lindemann MJ, et al. Interleukin (IL) 15 is a novel cytokine that activates human natural killer cells via components of the IL-2 receptor. The Journal of experimental medicine 1994;180:1395-1403.
114. Carson WE, Lindemann MJ, Baiocchi R, et al. The functional characterization of interleukin-10 receptor expression on human natural killer cells. Blood 1995;85:3577-3585.
115. Wang KS, Frank DA, Ritz J. Interleukin-2 enhances the response of natural killer cells to interleukin-12 through up-regulation of the interleukin-12 receptor and STAT4. Blood 2000;95:3183-3190.
116. Fehniger TA, Shah MH, Turner MJ, et al. Differential cytokine and chemokine gene expression by human NK cells following activation with IL-18 or IL-15 in combination with IL-12: implications for the innate immune response. Journal of immunology 1999;162:4511-4520.
117. Inngjerdingen M, Damaj B, Maghazachi AA. Expression and regulation of chemokine receptors in human natural killer cells. Blood 2001;97:367-375.
118. Caligiuri MA, Zmuidzinas A, Manley TJ, Levine H, Smith KA, Ritz J. Functional consequences of interleukin 2 receptor expression on resting human lymphocytes. Identification of a novel natural killer cell subset with high affinity receptors. The Journal of experimental medicine 1990;171:1509-1526.
119. Lanier LL, Le AM, Civin CI, Loken MR, Phillips JH. The relationship of CD16 (Leu-11) and Leu-19 (NKH-1) antigen expression on human peripheral blood NK cells and cytotoxic T lymphocytes. Journal of immunology 1986;136:4480-4486.
120. Jacobs R, Hintzen G, Kemper A, et al. CD56bright cells differ in their KIR repertoire and cytotoxic features from CD56dim NK cells. European journal of immunology 2001;31:3121-3127.
121. Montaldo E, Del Zotto G, Della Chiesa M, et al. Human NK cell receptors/markers: a tool to analyze NK cell development, subsets and function. Cytometry Part A : the journal of the International Society for Analytical Cytology 2013;83:702-713.
122. Hayakawa Y, Huntington ND, Nutt SL, Smyth MJ. Functional subsets of mouse natural killer cells. Immunological reviews 2006;214:47-55.
123. Hayakawa Y, Andrews DM, Smyth MJ. Subset analysis of human and mouse mature NK cells. Methods in molecular biology 2010;612:27-38.
124. Gregoire C, Cognet C, Chasson L, et al. Intrasplenic trafficking of natural killer cells is redirected by chemokines upon inflammation. European journal of immunology 2008;38:2076-2084.
125. French AR, Yokoyama WM. Natural killer cells and autoimmunity. Arthritis research & therapy 2004;6:8-14.
126. Verbsky JW, Grossman WJ. Hemophagocytic lymphohistiocytosis: diagnosis, pathophysiology, treatment, and future perspectives. Annals of medicine 2006;38:20-31.
127. Fogel LA, Yokoyama WM, French AR. Natural killer cells in human autoimmune disorders. Arthritis research & therapy 2013;15:216.
128. Lo CK, Lam QL, Sun L, et al. Natural killer cell degeneration exacerbates experimental arthritis in mice via enhanced interleukin-17 production. Arthritis and rheumatism 2008;58:2700-2711.
129. Kastrukoff LF, Lau A, Wee R, Zecchini D, White R, Paty DW. Clinical relapses of multiple sclerosis are associated with 'novel' valleys in natural killer cell functional activity. Journal of neuroimmunology 2003;145:103-114.
130. Bielekova B, Catalfamo M, Reichert-Scrivner S, et al. Regulatory CD56(bright) natural killer cells mediate immunomodulatory effects of IL-2Ralpha-targeted therapy (daclizumab) in multiple sclerosis. Proceedings of the National Academy of Sciences of the United States of America 2006;103:5941-5946.
131. Airas L, Saraste M, Rinta S, et al. Immunoregulatory factors in multiple sclerosis patients during and after pregnancy: relevance of natural killer cells. Clinical and experimental immunology 2008;151:235-243.
132. Hirsch RL, Johnson KP. Natural killer cell activity in multiple sclerosis patients treated with recombinant interferon-alpha 2. Clinical immunology and immunopathology 1985;37:236-244.
133. Uchida A, Maida EM, Lenzhofer R, Micksche M. Natural killer cell activity in patients with multiple sclerosis: interferon and plasmapheresis. Immunobiology 1982;160:392-402.

134. Hao J, Liu R, Piao W, et al. Central nervous system (CNS)-resident natural killer cells suppress Th17 responses and CNS autoimmune pathology. The Journal of experimental medicine 2010;207:1907-1921.
135. Winkler-Pickett R, Young HA, Cherry JM, et al. In vivo regulation of experimental autoimmune encephalomyelitis by NK cells: alteration of primary adaptive responses. Journal of immunology 2008;180:4495-4506.
136. Huntington ND, Vosshenrich CA, Di Santo JP. Developmental pathways that generate natural-killer-cell diversity in mice and humans. Nat Rev Immunol 2007;7:703-714.
137. Poli A, Kmiecik J, Domingues O, et al. NK cells in central nervous system disorders. Journal of immunology 2013;190:5355-5362.
138. Hamann I, Unterwalder N, Cardona AE, et al. Analyses of phenotypic and functional characteristics of CX3CR1-expressing natural killer cells. Immunology 2011;133:62-73.
139. Amulic B, Cazalet C, Hayes GL, Metzler KD, Zychlinsky A. Neutrophil function: from mechanisms to disease. Annual review of immunology 2012;30:459-489.
140. Summers C, Rankin SM, Condliffe AM, Singh N, Peters AM, Chilvers ER. Neutrophil kinetics in health and disease. Trends in immunology 2010;31:318-324.
141. Borregaard N. Neutrophils, from marrow to microbes. Immunity 2010;33:657-670.
142. Roberts AW. G-CSF: a key regulator of neutrophil production, but that's not all! Growth Factors 2005;23:33-41.
143. Ma Q, Jones D, Springer TA. The chemokine receptor CXCR4 is required for the retention of B lineage and granulocytic precursors within the bone marrow microenvironment. Immunity 1999;10:463-471.
144. Petty JM, Lenox CC, Weiss DJ, Poynter ME, Suratt BT. Crosstalk between CXCR4/stromal derived factor-1 and VLA-4/VCAM-1 pathways regulates neutrophil retention in the bone marrow. Journal of immunology 2009;182:604-612.
145. Kolaczkowska E, Kubes P. Neutrophil recruitment and function in health and inflammation. Nat Rev Immunol 2013;13:159-175.
146. Mayadas TN, Cullere X, Lowell CA. The multifaceted functions of neutrophils. Annu Rev Pathol 2014;9:181-218.
147. Eyles JL, Roberts AW, Metcalf D, Wicks IP. Granulocyte colony-stimulating factor and neutrophils--forgotten mediators of inflammatory disease. Nat Clin Pract Rheumatol 2006;2:500-510.
148. Vethanayagam RR, Almyroudis NG, Grimm MJ, et al. Role of NADPH oxidase versus neutrophil proteases in antimicrobial host defense. PloS one 2011;6:e28149.
149. Lee WL, Harrison RE, Grinstein S. Phagocytosis by neutrophils. Microbes Infect 2003;5:1299-1306.
150. Brinkmann V, Reichard U, Goosmann C, et al. Neutrophil extracellular traps kill bacteria. Science 2004;303:1532-1535.
151. Fuchs TA, Abed U, Goosmann C, et al. Novel cell death program leads to neutrophil extracellular traps. J Cell Biol 2007;176:231-241.
152. Urban CF, Ermert D, Schmid M, et al. Neutrophil extracellular traps contain calprotectin, a cytosolic protein complex involved in host defense against Candida albicans. PLoS Pathog 2009;5:e1000639.
153. Papayannopoulos V, Zychlinsky A. NETs: a new strategy for using old weapons. Trends in immunology 2009;30:513-521.
154. Heyworth PG, Cross AR, Curnutte JT. Chronic granulomatous disease. Curr Opin Immunol 2003;15:578-584.
155. Mocsai A. Diverse novel functions of neutrophils in immunity, inflammation, and beyond. The Journal of experimental medicine 2013;210:1283-1299.
156. Kaplan MJ. Role of neutrophils in systemic autoimmune diseases. Arthritis research & therapy 2013;15:219.
157. Nemeth T, Mocsai A. The role of neutrophils in autoimmune diseases. Immunology letters 2012;143:9-19.
158. Naegele M, Tillack K, Reinhardt S, Schippling S, Martin R, Sospedra M. Neutrophils in multiple sclerosis are characterized by a primed phenotype. Journal of neuroimmunology 2012;242:60-71.
159. Wu F, Cao W, Yang Y, Liu A. Extensive infiltration of neutrophils in the acute phase of experimental autoimmune encephalomyelitis in C57BL/6 mice. Histochem Cell Biol 2010;133:313-322.
160. Wojkowska DW, Szpakowski P, Ksiazek-Winiarek D, Leszczynski M, Glabinski A. Interactions between neutrophils, Th17 cells, and chemokines during the initiation of experimental model of multiple sclerosis. Mediators Inflamm 2014;2014:590409.
161. Simmons SB, Liggitt D, Goverman JM. Cytokine-regulated neutrophil recruitment is required for brain but not spinal cord inflammation during experimental autoimmune encephalomyelitis. Journal of immunology 2014;193:555-563.

162. Steinbach K, Piedavent M, Bauer S, Neumann JT, Friese MA. Neutrophils amplify autoimmune central nervous system infiltrates by maturing local APCs. Journal of immunology 2013;191:4531-4539.
163. McColl SR, Staykova MA, Wozniak A, Fordham S, Bruce J, Willenborg DO. Treatment with anti-granulocyte antibodies inhibits the effector phase of experimental autoimmune encephalomyelitis. Journal of immunology 1998;161:6421-6426.
164. Misu T, Hoftberger R, Fujihara K, et al. Presence of six different lesion types suggests diverse mechanisms of tissue injury in neuromyelitis optica. Acta Neuropathol 2013;125:815-827.
165. Bruck W, Popescu B, Lucchinetti CF, et al. Neuromyelitis optica lesions may inform multiple sclerosis heterogeneity debate. Annals of neurology 2012;72:385-394.
166. Ishizu T, Osoegawa M, Mei FJ, et al. Intrathecal activation of the IL-17/IL-8 axis in opticospinal multiple sclerosis. Brain 2005;128:988-1002.
167. Saadoun S, Waters P, Bell BA, Vincent A, Verkman AS, Papadopoulos MC. Intra-cerebral injection of neuromyelitis optica immunoglobulin G and human complement produces neuromyelitis optica lesions in mice. Brain 2010;133:349-361.
168. Jarius S, Paul F, Franciotta D, et al. Revised diagnostic criteria for neuromyelitis optica--incorporation of NMO-IgG status. Nature clinical practice Neurology 2007;3:E1.
169. Polman CH, Reingold SC, Banwell B, et al. Diagnostic criteria for multiple sclerosis: 2010 revisions to the McDonald criteria. Annals of neurology 2011;69:292-302.
170. Kurtzke JF. Rating neurologic impairment in multiple sclerosis: an expanded disability status scale (EDSS). Neurology 1983;33:1444-1452.
171. Hertwig L, Pache F, Romero-Suarez S, et al. Distinct functionality of neutrophils in multiple sclerosis and neuromyelitis optica. Multiple sclerosis 2015.
172. Heid CA, Stevens J, Livak KJ, Williams PM. Real time quantitative PCR. Genome Res 1996;6:986-994.
173. Jozefczuk J, Adjaye J. Quantitative real-time PCR-based analysis of gene expression. Methods Enzymol 2011;500:99-109.
174. Livak KJ, Schmittgen TD. Analysis of relative gene expression data using real-time quantitative PCR and the 2(-Delta Delta C(T)) Method. Methods 2001;25:402-408.
175. Ibrahim SF, van den Engh G. Flow cytometry and cell sorting. Adv Biochem Eng Biotechnol 2007;106:19-39.
176. Rieseberg M, Kasper C, Reardon KF, Scheper T. Flow cytometry in biotechnology. Applied microbiology and biotechnology 2001;56:350-360.
177. Pols MS, Klumperman J. Trafficking and function of the tetraspanin CD63. Exp Cell Res 2009;315:1584-1592.
178. Hamann I, Dorr J, Glumm R, et al. Characterization of natural killer cells in paired CSF and blood samples during neuroinflammation. Journal of neuroimmunology 2013;254:165-169.
179. Camous L, Roumenina L, Bigot S, et al. Complement alternative pathway acts as a positive feedback amplification of neutrophil activation. Blood 2011;117:1340-1349.
180. Flodstrom-Tullberg M, Bryceson YT, Shi FD, Hoglund P, Ljunggren HG. Natural killer cells in human autoimmunity. Curr Opin Immunol 2009;21:634-640.
181. Mandal A, Viswanathan C. Natural killer cells: In health and disease. Hematology/oncology and stem cell therapy 2014.
182. Chanvillard C, Jacolik RF, Infante-Duarte C, Nayak RC. The role of natural killer cells in multiple sclerosis and their therapeutic implications. Frontiers in immunology 2013;4:63.
183. Chanvillard C, Millward JM, Lozano M, et al. Mitoxantrone induces natural killer cell maturation in patients with secondary progressive multiple sclerosis. PloS one 2012;7:e39625.
184. Garcia JA, Pino PA, Mizutani M, et al. Regulation of adaptive immunity by the fractalkine receptor during autoimmune inflammation. Journal of immunology 2013;191:1063-1072.
185. Ponzetta A, Sciume G, Benigni G, et al. CX3CR1 regulates the maintenance of KLRG1+ NK cells into the bone marrow by promoting their entry into circulation. Journal of immunology 2013;191:5684-5694.
186. Yu YR, Fong AM, Combadiere C, Gao JL, Murphy PM, Patel DD. Defective antitumor responses in CX3CR1-deficient mice. Int J Cancer 2007;121:316-322.
187. Zhang X, Wei H, Wang H, Tian Z. Involvement of interaction between Fractalkine and CX3CR1 in cytotoxicity of natural killer cells against tumor cells. Oncol Rep 2006;15:485-488.
188. Chiossone L, Chaix J, Fuseri N, Roth C, Vivier E, Walzer T. Maturation of mouse NK cells is a 4-stage developmental program. Blood 2009;113:5488-5496.
189. Ferretti E, Pistoia V, Corcione A. Role of fractalkine/CX3CL1 and its receptor in the pathogenesis of inflammatory and malignant diseases with emphasis on B cell malignancies. Mediators Inflamm 2014;2014:480941.

190. Limatola C, Ransohoff RM. Modulating neurotoxicity through CX3CL1/CX3CR1 signaling. Frontiers in cellular neuroscience 2014;8:229.
191. Cardona AE, Pioro EP, Sasse ME, et al. Control of microglial neurotoxicity by the fractalkine receptor. Nature neuroscience 2006;9:917-924.
192. Garcia JA, Cardona SM, Cardona AE. Analyses of microglia effector function using CX3CR1-GFP knock-in mice. Methods in molecular biology 2013;1041:307-317.
193. Pabon MM, Bachstetter AD, Hudson CE, Gemma C, Bickford PC. CX3CL1 reduces neurotoxicity and microglial activation in a rat model of Parkinson's disease. Journal of neuroinflammation 2011;8:9.
194. Zujovic V, Benavides J, Vige X, Carter C, Taupin V. Fractalkine modulates TNF-alpha secretion and neurotoxicity induced by microglial activation. Glia 2000;29:305-315.
195. Nash KR, Lee DC, Hunt JB, Jr., et al. Fractalkine overexpression suppresses tau pathology in a mouse model of tauopathy. Neurobiology of aging 2013;34:1540-1548.
196. Lee S, Varvel NH, Konerth ME, et al. CX3CR1 deficiency alters microglial activation and reduces beta-amyloid deposition in two Alzheimer's disease mouse models. The American journal of pathology 2010;177:2549-2562.
197. Kivisakk P, Mahad DJ, Callahan MK, et al. Expression of CCR7 in multiple sclerosis: implications for CNS immunity. Annals of neurology 2004;55:627-638.
198. Berahovich RD, Lai NL, Wei Z, Lanier LL, Schall TJ. Evidence for NK cell subsets based on chemokine receptor expression. Journal of immunology 2006;177:7833-7840.
199. Bernardini G, Benigni G, Antonangeli F, Ponzetta A, Santoni A. Multiple levels of chemokine receptor regulation in the control of mouse natural killer cell development. Frontiers in immunology 2014;5:44.
200. Williams JL, Holman DW, Klein RS. Chemokines in the balance: maintenance of homeostasis and protection at CNS barriers. Frontiers in cellular neuroscience 2014;8:154.
201. Alt C, Laschinger M, Engelhardt B. Functional expression of the lymphoid chemokines CCL19 (ELC) and CCL 21 (SLC) at the blood-brain barrier suggests their involvement in G-protein-dependent lymphocyte recruitment into the central nervous system during experimental autoimmune encephalomyelitis. European journal of immunology 2002;32:2133-2144.
202. Columba-Cabezas S, Serafini B, Ambrosini E, Aloisi F. Lymphoid chemokines CCL19 and CCL21 are expressed in the central nervous system during experimental autoimmune encephalomyelitis: implications for the maintenance of chronic neuroinflammation. Brain pathology 2003;13:38-51.
203. Bielecki B, Jatczak-Pawlik I, Wolinski P, Bednarek A, Glabinski A. Central Nervous System and Peripheral Expression of CCL19, CCL21 and Their Receptor CCR7 in Experimental Model of Multiple Sclerosis. Archivum immunologiae et therapiae experimentalis 2015.
204. Martin-Fontecha A, Thomsen LL, Brett S, et al. Induced recruitment of NK cells to lymph nodes provides IFN-gamma for T(H)1 priming. Nature immunology 2004;5:1260-1265.
205. Saraste M, Irjala H, Airas L. Expansion of CD56Bright natural killer cells in the peripheral blood of multiple sclerosis patients treated with interferon-beta. Neurol Sci 2007;28:121-126.
206. Gan Y, Liu Q, Wu W, et al. Ischemic neurons recruit natural killer cells that accelerate brain infarction. Proceedings of the National Academy of Sciences of the United States of America 2014;111:2704-2709.
207. Lunemann A, Lunemann JD, Roberts S, et al. Human NK cells kill resting but not activated microglia via NKG2D- and NKp46-mediated recognition. Journal of immunology 2008;181:6170-6177.
208. Durrenberger PF, Ettorre A, Kamel F, et al. Innate immunity in multiple sclerosis white matter lesions: expression of natural cytotoxicity triggering receptor 1 (NCR1). Journal of neuroinflammation 2012;9:1.
209. Engelhardt B, Wolburg-Buchholz K, Wolburg H. Involvement of the choroid plexus in central nervous system inflammation. Microsc Res Tech 2001;52:112-129.
210. Reboldi A, Coisne C, Baumjohann D, et al. C-C chemokine receptor 6-regulated entry of TH-17 cells into the CNS through the choroid plexus is required for the initiation of EAE. Nature immunology 2009;10:514-523.
211. Ingram G, Hakobyan S, Robertson NP, Morgan BP. Complement in multiple sclerosis: its role in disease and potential as a biomarker. Clinical and experimental immunology 2009;155:128-139.
212. Kurt-Jones EA, Mandell L, Whitney C, et al. Role of toll-like receptor 2 (TLR2) in neutrophil activation: GM-CSF enhances TLR2 expression and TLR2-mediated interleukin 8 responses in neutrophils. Blood 2002;100:1860-1868.
213. Hayashi F, Means TK, Luster AD. Toll-like receptors stimulate human neutrophil function. Blood 2003;102:2660-2669.
214. Brandolini L, Bertini R, Bizzarri C, et al. IL-1 beta primes IL-8-activated human neutrophils for elastase release, phospholipase D activity, and calcium flux. J Leukoc Biol 1996;59:427-434.

215. Green SP, Chuntharapai A, Curnutte JT. Interleukin-8 (IL-8), melanoma growth-stimulatory activity, and neutrophil-activating peptide selectively mediate priming of the neutrophil NADPH oxidase through the type A or type B IL-8 receptor. J Biol Chem 1996;271:25400-25405.
216. Meddows-Taylor S, Kuhn L, Meyers TM, Tiemessen CT. Altered expression of L-selectin (CD62L) on polymorphonuclear neutrophils of children vertically infected with human immunodeficiency virus type 1. Journal of clinical immunology 2001;21:286-292.
217. Ostberg JR, Barth RK, Frelinger JG. The Roman god Janus: a paradigm for the function of CD43. Immunol Today 1998;19:546-550.
218. Matsumoto M, Shigeta A, Miyasaka M, Hirata T. CD43 plays both antiadhesive and proadhesive roles in neutrophil rolling in a context-dependent manner. Journal of immunology 2008;181:3628-3635.
219. Zarbock A, Ley K, McEver RP, Hidalgo A. Leukocyte ligands for endothelial selectins: specialized glycoconjugates that mediate rolling and signaling under flow. Blood 2011;118:6743-6751.
220. Bostan M, Constantin MC, Nicolau A, et al. Study of chemotactic activity developed by neutrophils from rheumatoid arthritis patients. Roum Arch Microbiol Immunol 2002;61:243-258.
221. Alves-Filho JC, Freitas A, Souto FO, et al. Regulation of chemokine receptor by Toll-like receptor 2 is critical to neutrophil migration and resistance to polymicrobial sepsis. Proceedings of the National Academy of Sciences of the United States of America 2009;106:4018-4023.
222. Tavares-Murta BM, Zaparoli M, Ferreira RB, et al. Failure of neutrophil chemotactic function in septic patients. Crit Care Med 2002;30:1056-1061.
223. Benjamim CF, Silva JS, Fortes ZB, Oliveira MA, Ferreira SH, Cunha FQ. Inhibition of leukocyte rolling by nitric oxide during sepsis leads to reduced migration of active microbicidal neutrophils. Infect Immun 2002;70:3602-3610.
224. Cedergren J, Forslund T, Sundqvist T, Skogh T. Intracellular oxidative activation in synovial fluid neutrophils from patients with rheumatoid arthritis but not from other arthritis patients. J Rheumatol 2007;34:2162-2170.
225. Alves CM, Marzocchi-Machado CM, Louzada-Junior P, et al. Superoxide anion production by neutrophils is associated with prevalent clinical manifestations in systemic lupus erythematosus. Clin Rheumatol 2008;27:701-708.
226. Bengtsson AA, Pettersson A, Wichert S, et al. Low production of reactive oxygen species in granulocytes is associated with organ damage in systemic lupus erythematosus. Arthritis research & therapy 2014;16:R120.
227. Petry A, Weitnauer M, Gorlach A. Receptor activation of NADPH oxidases. Antioxid Redox Signal 2010;13:467-487.
228. Alves-Filho JC, de Freitas A, Spiller F, Souto FO, Cunha FQ. The role of neutrophils in severe sepsis. Shock 2008;30 Suppl 1:3-9.
229. Panasiuk A, Wysocka J, Maciorkowska E, et al. Phagocytic and oxidative burst activity of neutrophils in the end stage of liver cirrhosis. World J Gastroenterol 2005;11:7661-7665.
230. Eksioglu-Demiralp E, Direskeneli H, Kibaroglu A, Yavuz S, Ergun T, Akoglu T. Neutrophil activation in Behcet's disease. Clin Exp Rheumatol 2001;19:S19-24.
231. Houston N, Stewart N, Smith DS, Bell SC, Champion AC, Reid DW. Sputum neutrophils in cystic fibrosis patients display a reduced respiratory burst. J Cyst Fibros 2013;12:352-362.
232. Guarnieri C, Melandri G, Caldarera I, et al. Reduced oxidative activity of circulating neutrophils in patients after myocardial infarction. Cell Biochem Funct 1990;8:157-162.
233. Vines CM, Xue M, Maestas DC, Cimino DF, Prossnitz ER. Regulation of N-formyl peptide-mediated degranulation by receptor phosphorylation. Journal of immunology 2002;169:6760-6766.
234. Pletz MW, Ioanas M, de Roux A, Burkhardt O, Lode H. Reduced spontaneous apoptosis in peripheral blood neutrophils during exacerbation of COPD. Eur Respir J 2004;23:532-537.
235. Harter L, Mica L, Stocker R, Trentz O, Keel M. Mcl-1 correlates with reduced apoptosis in neutrophils from patients with sepsis. J Am Coll Surg 2003;197:964-973.
236. Kitsis E, Weissmann G. The role of the neutrophil in rheumatoid arthritis. Clin Orthop Relat Res 1991:63-72.
237. Edwards SW, Hallett MB. Seeing the wood for the trees: the forgotten role of neutrophils in rheumatoid arthritis. Immunol Today 1997;18:320-324.
238. Caccavo D, Garzia P, Sebastiani GD, et al. Expression of lactoferrin on neutrophil granulocytes from synovial fluid and peripheral blood of patients with rheumatoid arthritis. J Rheumatol 2003;30:220-224.
239. Corberand J, Amigues H, de Larrard B, Pradere J. Neutrophil function in rheumatoid arthritis. Scand J Rheumatol 1977;6:49-52.
240. Khandpur R, Carmona-Rivera C, Vivekanandan-Giri A, et al. NETs are a source of citrullinated autoantigens and stimulate inflammatory responses in rheumatoid arthritis. Sci Transl Med 2013;5:178ra140.

241. Cesaro A, Anceriz N, Plante A, Page N, Tardif MR, Tessier PA. An inflammation loop orchestrated by S100A9 and calprotectin is critical for development of arthritis. PloS one 2012;7:e45478.
242. Michael BD, Elsone L, Griffiths MJ, et al. Post-acute serum eosinophil and neutrophil-associated cytokine/chemokine profile can distinguish between patients with neuromyelitis optica and multiple sclerosis; and identifies potential pathophysiological mechanisms - a pilot study. Cytokine 2013;64:90-96.
243. Kasahara Y, Iwai K, Yachie A, et al. Involvement of reactive oxygen intermediates in spontaneous and CD95 (Fas/APO-1)-mediated apoptosis of neutrophils. Blood 1997;89:1748-1753.
244. Villanueva E, Yalavarthi S, Berthier CC, et al. Netting neutrophils induce endothelial damage, infiltrate tissues, and expose immunostimulatory molecules in systemic lupus erythematosus. Journal of immunology 2011;187:538-552.
245. Rommel C, Camps M, Ji H. PI3K delta and PI3K gamma: partners in crime in inflammation in rheumatoid arthritis and beyond? Nat Rev Immunol 2007;7:191-201.
246. Steinberg BE, Grinstein S. Unconventional roles of the NADPH oxidase: signaling, ion homeostasis, and cell death. Sci STKE 2007;2007:pe11.
247. Leffler J, Martin M, Gullstrand B, et al. Neutrophil extracellular traps that are not degraded in systemic lupus erythematosus activate complement exacerbating the disease. Journal of immunology 2012;188:3522-3531.
248. Hakkim A, Furnrohr BG, Amann K, et al. Impairment of neutrophil extracellular trap degradation is associated with lupus nephritis. Proceedings of the National Academy of Sciences of the United States of America 2010;107:9813-9818.
249. Lande R, Ganguly D, Facchinetti V, et al. Neutrophils activate plasmacytoid dendritic cells by releasing self-DNA-peptide complexes in systemic lupus erythematosus. Sci Transl Med 2011;3:73ra19.

7. List of publications

Original papers

Wicklund L, Marutle A, **Hertwig L,** Hovatta O,Nordberg A, Darreh-Shori T, *The influence of beta-amyloid 1-42 on inflammatory processes and regenerative mechanisms in Alzheimer's disease* Alzheimer's & Dementia: The Journal of the Alzheimer's Association (July 2011), 7 (4)

Hedskog L, Pinho CM, Filadi R, Rönnbäck A, **Hertwig L**, Wiehager B, Larssen P, Gellhaar S, Sandebring A, Westerlund M, Graff C, Winblad B, Galter D,Behbahani H, Pizzo P, Glaser E, Ankarcrona M., *Modulation of the endoplasmic reticulum-mitochondria interface in Alzheimer's disease and related models.* Proc Natl Acad Sci U S A. 2013 May 7;110(19):7916-21.

Hertwig L, Pache F, Romero-Suarez S, Stürner KH, Borisow N, Behrens J, Bellmann-Strobl J, Seeger B, Asselborn N, Ruprecht K, Millward JM, Infante-Duarte C, Paul F. *Distinct functionality of neutrophils in multiple sclerosis and neuromyelitis optica.* Mult Scler. 2016 Feb;22(2):160-73. doi: 10.1177/1352458515586084. Epub 2015 Jun 25.

Janssen A, Fiebiger S, Bros H, **Hertwig L**, Romero-Suarez S, Hamann I, Chanvillard C, Bellmann-Strobl J, Paul F, Millward JM, Infante-Duarte C. *Treatment of Chronic Experimental Autoimmune Encephalomyelitis with Epigallocatechin-3-Gallate and Glatiramer Acetate Alters Expression of Heme-Oxygenase-1.* PLoS One. 2015 Jun 26;10(6):e0130251. doi: 10.1371/journal.pone.0130251. eCollection 2015.

Hertwig L, Hamann I, Romero-Suarez S, Millward J. M., Pietrek R, Pollok K, Ransohoff R. M., Cardona A. E., Infante-Duarte C., *CX3CR1-dependent recruitment of mature NK cells into the CNS contributes to control CNS autoimmunity.* Eur J Immunol. In revision.

Poster contributions

Hertwig L, Borisow N, Stürner K.H, Seeger B, Infante-Duarte C and Paul F, *Neutrophils as potential biomarkers in the differentiation of multiple sclerosis and neuromyelitis optica*, 15th International Congress of Immunology (ICI 2013), 22.08-27.08.2013, Milan, Italy.

- supported by a travel grant from the German Society for Immunology, DGfI

Hertwig L, Romero-Suarez S, Stürner K.H., Borisow N, Pache F, Behrens J, Millward J.M., Ruprecht K, Infante-Duarte C and Paul F, *Neutrophil profile in Multiple Sclerosis and Neuromyelitis Optica.*12th International Congress of Neuroimmunology (ISNI 2014), 09.11.-13.11.2014, Mainz, Germany

Hertwig L, Romero-Suarez S, Millward J.M., Stuis H, Ransohoff R.M., Cardona A.E., Infante-Duarte C, *CX3CR1-dependent recruitment of mature NK cells into the CNS contributes to the control of CNS autoimmunity*, 4th European Congress of Immunology (ECI 2015), 06.09.-09.09.2015, Vienna, Austria

- supported by a travel grant from the German Society for Immunology, DGfI

Hertwig L, Romero-Suarez S, Millward J.M., Stuis H, Ransohoff R.M., Cardona A.E., Infante-Duarte C, *Recruitment of CD11b^{high} NK cells into the inflamed CNS depends on CX3CR1 and contributes to control autoimmune neuroinflammation*, accepted for poster presentation at the Natural Killer Cell Symposium, 07.10.-09.10.2015, Göttingen, Germany

- supported by a EFIS-ECI travel grant from the European Federation of Immunological Societies

8. Statutory declaration

I declare that I have authored this thesis independently, that I have not used other than the declared sources/resources, and that I have explicitly marked all materials which have been quoted either literally or by content from the used sources.

In addition, I declare that all texts, figures and tables included in the following manuscripts

- **Hertwig L**, Pache F, Romero Suarez S, Stürner K.H., Borisow N, Behrens J, Bellmann-Strobl J, Seeger B, Asselborn N, Ruprecht C, Millward J.M., Infante Duarte C and Paul F, *Distinct neutrophil functionality in multiple sclerosis and neuromyelitis optica,* Mult Scler. 2016 Feb;22(2):160-73. doi: 10.1177/1352458515586084. Epub 2015 Jun 25.

- **Hertwig L**, Hamann I, Romero-Suarez S, Millward J. M., Pietrek R, Pollok K, Ransohoff R. M., Cardona A. E., Infante-Duarte C., *CX3CR1-dependent recruitment of mature NK cells into the CNS contributes to control CNS autoimmunity.* Eur J Immunol. In revision.

were generated by myself. PD Dr. Carmen Infante Duarte and Prof. Dr. Friedemann Paul primary supervised the PhD project work. Listed co-authors were involved in experimental support or proofreading of the manuscripts. On this account, excerpts and text passages, figures and figure legends as well as tables from both manuscripts were used partly or modified in the present thesis work. Permission to use the manuscript material was further asked and obtained from Multiple Sclerosis Journal and the European Journal of Immunology.

Berlin, 30.08.2016 Laura Hertwig

9. Acknowledgements

First, I would like to thank my supervisors and reviewers of the PhD thesis PD Dr. Carmen Infante Duarte, Prof. Dr. med. Friedemann Paul, Prof. Dr. Hans-Dieter Volk and PD Dr. med. Olaf Hoffmann.

Thank you Carmen for giving me the opportunity to work on this really interesting and challenging project – about the impact of innate immune cells in MS – in your research group, for your guidance during my doctoral thesis, for the intellectual support and continual encouragement through the project. Moreover, thank you for being not only a good superior dedicated to a professional and pleasant working atmosphere but also a person always honestly interested in her staff beyond the work creating a friendly and even familiar basis in the group. Muchas gracias de corazón.

Thank you to Friedemann who promptly invited me for an interview after I sent my CV and introduced me to Carmen and her group. Many thanks for your intellectual and financial support and your commitment as well as your belief and patience in the neutrophil project.

Thank you also to Prof. Dr. Hans-Dieter Volk, the head of the Institute for Medical Immunology at the Charité Berlin, who kindly agreed in undertaking supervision and review of my PhD thesis. Especially, thank you for organizing the Wednesday seminars at the institute which were/ are always inspiring, motivating and invite to discuss and reflect various immunological topics also apart from the own projects.

Thank you to Prof. Dr. med. Olaf Hoffmann who kindly and very short notice contracted into reviewing this thesis work. I further wish to thank Prof. Dr. Kai Matuschewski and Dr. Michal Or-Guil who kindly agreed on taking part – as committee members – on the oral defense of this thesis work.

I thank all my present and former colleagues from the Experimental Immunology lab of PD Dr. Carmen Infante Duarte and the Institute for Medical Immunology at the Charité Berlin. Especially, I would like to thank Dr. Jason Millward who was always very dedicated to help with statistical and experimental issues as well as proofreading of manuscripts and applications, and giving intellectual input supporting critical discussions

on obtained project data. Thank you to Dr. Isabell Hamann for extensively introducing me to the NK cell project. Thank you Natascha Asselborn and Bibiane Seeger for technical and experimental support as well as Silvina Romero-Suarez and Hanna Stuis who were very ambitious in investigating aspects of neutrophils and NK cells during neuroinflammtion within the framework of their master theses, respectively.

My very special gratitude goes to my Mom and my Sister. Thank you both so much for all the moral and emotional support, for your patience and love. Even though our family had to incur many backstrokes and painful losses during the last years, we always stuck together and were always there for one another. You are the greatest and most precious persons to me. Thank you Andreas and Max for enriching our little family and being marvellous partners for my Mom and my Sister. A very big thank you also to all my friends and dearest who accompanied me not only through the years of the PhD but also every other condition of life, especially Benni and Franzi. Thank you both for enriching my life with your colorful, caring and unique personalities, for your love and friendship.

Not least, I would like to thank the Humboldt University of Berlin, Institute for Biology, which acceded my promotion request allowing me to perform my PhD work, and the Charité – University Medicine Berlin for supporting my thesis projects with a doctoral stipend.